

DEVELOPMENT OF A SMARTPHONE APPLICATION TO MEASURE PAVEMENT
ROUGHNESS AND TO IDENTIFY SURFACE IRREGULARITIES

BY

MD SHAHIDUL ISLAM

DISSERTATION

Submitted in partial fulfillment of the requirements
for the degree of Doctor of Philosophy in Civil Engineering
in the Graduate College of the
University of Illinois at Urbana-Champaign, 2015

Urbana, Illinois

Doctoral Committee:

Professor William G. Buttlar, Chair
Professor Jeffery R. Roesler
Professor Daniel B. Work
Dr. William Vavrik, Applied Research Associates, Inc.

ABSTRACT

Pavement roughness is an expression of the unevenness or disturbance in a pavement surface that adversely affects the ride quality of a vehicle. Roughness also affects user delay costs, fuel consumption, tire, and maintenance costs. Roughness is predominantly characterized in terms of International Roughness Index (IRI), which is often measured using inertial profilers. Inertial profilers are equipped with sensitive accelerometers, a height measuring laser, a distance measuring instrument, etc., to measure pavement profile. Modern smartphones are equipped with a number of sensors including a three-axis accelerometer, which has been utilized in this project to collect vehicle acceleration data using an android-based smartphone application. Two data analysis schemes have been developed to determine pavement profile from vehicle vertical acceleration data: a double integration and an inverse state space model. Acceleration data was double-integrated numerically to obtain a surrogate estimate of pavement profile based on the calculated vertical position of the vehicle cab. After noting a fairly significant underprediction of IRI for rough pavement sections with the double integration method, due in part to the dampening effects of the vehicle suspension, an inverse state space model was developed. This model enhances the double integration procedure by considering the physics of the mass-spring-damper system of the vehicle sprung mass as part of the back-estimation of road profile from vehicle cab acceleration. In addition, MATLAB and C# scripts were developed to estimate IRI from the pavement profile, using the procedure specified by ASTM.

For initial validation, three test sites were selected to collect pavement profile using an inertial profiler along with acceleration collected using the smartphone application. These results demonstrated the potential for smartphone-measure IRI, as good correspondence to the inertial profiler was found for all but the roughest pavement investigated. The state space model was shown to provide significantly better estimates of IRI for rough pavement sections. Good repeatability between measurement replications was also noted, particularly when the space state model was used. For further validation, pavement roughness data was also collected using six smartphones and four vehicles. It was found that both the smartphone model and the vehicle used for data collection will affect the IRI measurement. However, averaged IRI values measured across all smartphones and vehicles were found to be in good agreement with the inertial profiler measured IRI for most of the pavement sections.

The final phase of the study involved preliminary work in using the smartphone application for the purpose of pavement feature identification (bumps and potholes). Acceleration data collected using the smartphone application was filtered using an experimentally determined threshold value of 4 m/s^2 to identify occurrences of significant localized distresses, and a MATLAB script has been developed to locate those distresses on a digital map. Finally, the smartphone application was used to collect roughness data over about 60 miles of roadway located in Champaign and Piatt County, IL, and measured IRI data has been integrated into a roadway network map using ArcGIS. In the roadway network map, every 0.1-mile pavement section has been highlighted with different colors based on measured roughness. It is hoped that the approach can be used to help reduce the cost of acquiring pavement roughness data for agencies and to reduce user costs for the traveling public by providing more robust feedback regarding route choice and its effect on estimated vehicle maintenance cost and fuel efficiency.

To my parents

ACKNOWLEDGMENTS

I would like to express my sincere appreciation to my advisor Prof. William G. Buttlar for all of his infinite support, insightful guidance, invaluable suggestions and feedback, and encouragement throughout the course of this study. His excellent knowledge, dedication to research, and great enthusiasm have always been continuous source of motivation during my study. I have thoroughly enjoyed working with him and feel that I have learned a lot. I would also like to show my sincere thanks to my thesis committee members, Prof. Jeffery R. Roesler, Prof. Daniel B. Work, and Dr. William Vavrik, for their time, helpful discussions, and valuable inputs to my dissertation.

I would like to thank the NexTrans – USDOT Region V Regional University Transportation Center, and Department of Civil and Environmental Engineering of University of Illinois for providing financial support to complete this research.

I would like to acknowledge Applied Research Associates, Inc. (ARA), and Vice-President Dr. William Vavrik for providing the inertial profiler to collect pavement roughness data for last three years. I also acknowledge the help of ARA employees including Mr. Gregg Larson, Mr. Mark Stanely, Ms. Rachel Baker, Mr. Brett Polling, and many others.

I would like to thank my colleagues: Mr. Brian Hill, Mr. Matheus Chagas, Ms. Colleen M. Madden, Ms. Hermione Wang, Dr. Eshan Dave, Dr. Salman Hakimzadeh, Mr. Nathan Abay Kebede, and Mr. Adam Beach who always encouraged and helped me during the course of this study. I would like to thank Dr. Sharmin Sultana, Ms. Tanjila Jesmin, Ms. Romin Tamanna, Ms. Samira Masoom, Ms. Priyanka Sarker, Dr. Mohammad Ilias, Mr. Hasan Kazmee, Dr. Hasib Uddin, Dr. Kallol Das, Dr. Md. Sarwar Siddiqui, Mr. ASM Jonayat, Mr. Piyas Bal, Dr. Shakil Kashem, Dr. Md. Liakat Ali, and members of the Bangladeshi community here for being such fantastic friends, and their company made my study here at the UIUC memorable.

I finally would like to express my profound appreciation to my dear family, specially my parents, for all their endless love and support throughout my life.

TABLE OF CONTENTS

CHAPTER 1	1
INTRODUCTION	1
1.1 BACKGROUND AND MOTIVATION	1
1.2 PROBLEM STATEMENT	1
1.3 RESEARCH OBJECTIVES AND OUTLINE	2
1.4 ORGANIZATION OF THIS DISSERTATION	4
CHAPTER 2	6
EFFECT OF PAVEMENT ROUGHNESS ON USER COSTS	6
2.1 BACKGROUND	6
2.2 PAVEMENT COSTS	8
2.3 AGENCY COSTS	9
2.4 PAVEMENT USER COSTS	9
2.5 ROUGHNESS PREDICTION.....	14
2.6 ESTIMATION OF COST DUE TO PAVEMENT ROUGHNESS	16
2.7 CONCLUSIONS.....	25
CHAPTER 3	27
ENVIRONMENTAL ASSESSMENT OF CONSTRUCTION ACTIVITIES TO REDUCE ROUGHNESS	27
3.1 INTRODUCTION	27
3.2 MODELING APPROACH.....	29
3.3 SYSTEM DEFINITION	30
3.4 ROUGHNESS RELATED USER COSTS.....	32
3.5 POLLUTION DAMAGE COST RATES.....	32
3.6 ENVIRONMENTAL COSTS	33
3.7 SENSITIVITY OF EMISSION COST TO ROUGHNESS AND TRAFFIC VOLUME	41
3.8 AGENCY INVESTMENT, USERS, AND EMISSIONS COSTS.....	42
3.9 CONCLUSION.....	43
CHAPTER 4	45
PAVEMENT ROUGHNESS	45
4.1 PAVEMENT ROUGHNESS.....	45
4.2 QUARTER-CAR MODEL TO IRI CALCULATION.....	46
4.3 HALF-CAR MODEL	47

4.4 LIMITATIONS OF IRI	48
4.5 EXISTING ROUGHNESS MEASUREMENT SYSTEMS.....	49
4.6 APPLICATION OF SMARTPHONE TO MEASURE PAVEMENT ROUGHNESS	56
CHAPTER 5.....	58
ACCELERATION DATA ANALYSIS METHOD	58
5.1 INTRODUCTION	58
5.2 VEHICLE DYNAMIC MODEL	58
5.3 ESTIMATION OF PAVEMENT PROFILE	64
5.4 DETERMINATION OF PAVEMENT ROUGHNESS	71
5.5 PROJECT APPROACH	72
5.6 COMPARISON OF IRI ESTIMATED BY APP AND DATA COLLECTION VEHICLE	76
5.7 CALIBRATION AND VALIDATION OF ROUGHNESS CAPTURE APP	95
5.8 EFFECT OF DIFFERENT SMARTPHONES ON IRI MEASUREMENT	100
5.9 EFFECT OF DIFFERENT VEHICLES ON IRI	106
5.10 STATISTICAL ANALYSIS OF IRI DATA	112
5.11 MAP-21 ROUGHNESS DATA COLLECTION	116
5.12 SUMMARY AND CONCLUSIONS	120
CHAPTER 6.....	123
SURFACE IRREGULARITY DETECTION AND VISUALIZATION OF IRI IN ArcGIS	123
6.1 INTRODUCTION	123
6.2 DETECTION METHOD	123
6.3 DATA COLLECTION	124
6.4 DATA ANALYSIS.....	126
6.5 LOCALIZED DISTRESS FROM SELECTED PAVEMENT SECTIONS	130
6.6 APPLICATION OF ArcGIS TO VISUALIZE IRI DATA	131
CHAPTER 7.....	133
CONCLUSION AND RECOMMENDATIONS.....	133
7.1 SUMMARY AND FINDINGS.....	133
7.2 CONCLUSIONS.....	136
7.3 FUTURE EXTENSIONS	136
REFERENCES.....	138
APPENDIX A.....	147

CHAPTER 1

INTRODUCTION

1.1 BACKGROUND AND MOTIVATION

With shrinking maintenance budgets and the need to ‘do more with less,’ the need for accurate, robust asset management data and tools is greatly needed for the transportation engineering community. There are about 2.6 million paved public roads in the United States roadway network, and many transportation agencies such as state DOTs, tollways, and counties utilize pavement management system (PMS) to manage their pavement network in an efficient and cost-effective manner [1]. PMSs, particularly in national highway system, require pavement roughness information along with other distress data. Pavement roughness is the deviation of pavement surface profile from planarity, which affects overall ride quality. Pavement roughness also slightly increases fuel consumption and therefore emission levels. Fuel consumption can be increased as much as 4-5 percent for very rough pavements [2]. Most transportation agencies use measures of the International Roughness Index (IRI) in planning maintenance and rehabilitation operations. Decades ago, roughness measurements were generally performed using manual equipment, such as a sliding straightedge. Technological advances have led to highly automated pavement condition assessments using sophisticated data collection vehicles equipped with sensitive inertial profilers.

1.2 PROBLEM STATEMENT

According to NCHRP Report 334, transportation agencies such as state DOTs, tollways, and counties now collect pavement roughness data using automated systems for at least part of their roadway network. Although very little has been reported in the literature on the cost of conducting IRI measurements, one study found reported pavement profile data collection and analysis involve agency costs in the range of \$2.23 - \$10.00/mile with an average cost of \$6.12/mile [3]. Considering the 139,577 miles of roadways of the state of Illinois, this would involve an expenditure of approximately \$1.4 million per pavement network system assessment. This is consistent with a report by the Mid-Atlantic universities transportation center which found that the Virginia Department of Transportation (VDOT), “a contractor is employed to

gather roughness data at an annual cost of \$1.8 million” [4], and data are collected once every five years for secondary roads. Many transportation agencies do not collect pavement condition data on an annual basis for large portions of their road network because of these high costs. For small transportation agencies such as counties and cities with low operating budgets, it is difficult to find sufficient funding to collect network-wide pavement condition data surveys even annually. Thus, maintenance and rehabilitation decisions are oftentimes performed using outdated roughness and distress data. In addition, infrequent roughness measurements preclude the identification of rapidly developing distress features on pavements such as potholes developing during spring thaw or dangerous blow ups in Portland cement concrete pavements, which is a missed opportunity for the enhancement of roadway safety and therefore increases tort liability.

Modern smartphones have built-in, 3-axis accelerometers and global positioning systems, which were investigated in this study as an efficient means for collecting and mapping vehicle vertical acceleration data and estimated pavement roughness (IRI). If successful, a crowd-sourcing based system has the potential to save agencies millions of dollars, while also providing the traveling public useful feedback on route choice and its effect on user costs, sustainability, and eventually perhaps even a measure of safety (through real-time tracking of high-acceleration events caused by severe potholes, blowups, etc.).

1.3 RESEARCH OBJECTIVES AND OUTLINE

The objectives of this study include:

- a) Estimation of user costs incurred by pavement roughness;
- b) Estimation of environmental costs for additional maintenance activities to maintain pavement in a smooth condition;
- c) Development of a smartphone application, Roughness Capture, to collect vehicle vertical acceleration data using smartphone accelerometer capabilities;
- d) Analysis of acceleration data to obtain pavement [perceived] profile;
- e) Calculating pavement roughness from the pavement profile using the MATLAB quarter car simulation;

- f) Validation of the Roughness Capture smartphone application generated results by comparing to those obtained by an industry standard inertial profiler on pavement sections in Illinois;
- g) Locating potholes and bumps, and generating a map representing pavement roughness values or quality of pavement in terms of smoothness;

The outline can be summarized as shown in Figure 1.1.

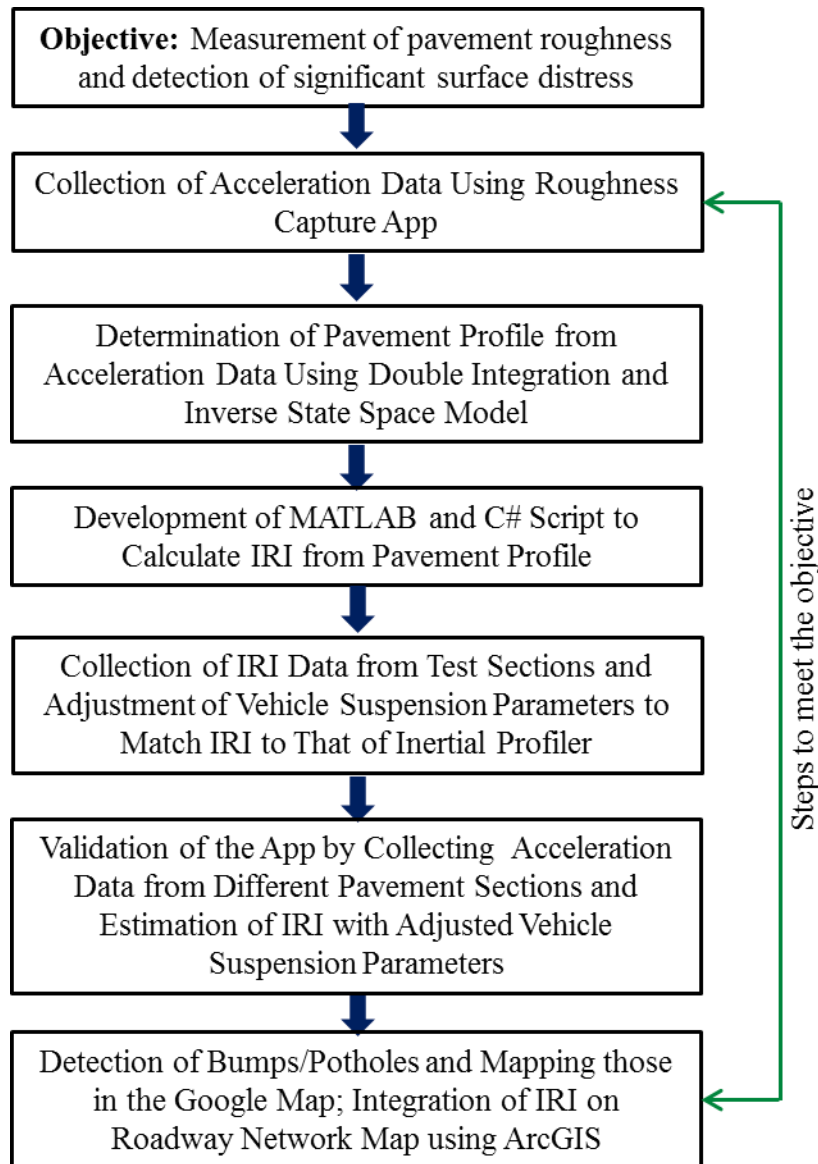


Figure 1.1: Outline of This Dissertation

1.4 ORGANIZATION OF THIS DISSERTATION

This dissertation is organized into 7 chapters. Chapter two through seven are organized as follows:

- CHAPTER 2 – Effect of Pavement Roughness on User Costs

This chapter quantifies user costs incurred by pavement roughness, including fuel consumption, tire, repair and maintenance, and depreciation costs. Agency investments required to keep pavements in a smooth state have been compared with user cost savings resulting from smooth roads.

- CHAPTER 3 - Environmental Assessment of Construction Activities to Reduce Roughness

This chapter provides a life cycle assessment of pavement construction, maintenance and rehabilitation (CMR) activities, linked to the analysis presented in Chapter 2. Environmental costs of CMR activities have been performed to compare with savings in user costs associated with smoother roads.

- CHAPTER 4 – Pavement Roughness

This chapter describes currently available methods and techniques for pavement roughness measurement. It also introduces features of the android-based smartphone phone application developed in this study.

- CHAPTER 5 – Analysis of Acceleration Data

This chapter provides detailed descriptions of the double integration and state space modeling schemes used for acceleration data analysis to determine pavement profile. MATLAB and C# scripts have been developed to eliminate the need to use ProVAL to determine pavement roughness from pavement profile. Pavement roughness data were collected using different vehicles and smartphones, and vehicle suspension parameters were calibrated in the model to match IRI values to those of the inertial profiler. Model validation was performed on 14 additional pavement sections.

- CHAPTER 6 – Detection of Localized Distress and Visualize IRI on ArcGIS Map

This chapter describes detection of localized pavement distresses such as bumps and potholes by filtering the vehicle vertical acceleration data. Integration of IRI data onto a roadway network map is also presented.

- CHAPTER 7 - Summary, Conclusions and Future Extensions

- REFERENCES

- APPENDIX

CHAPTER 2

EFFECT OF PAVEMENT ROUGHNESS ON USER COSTS

2.1 BACKGROUND

Not long after the construction of a pavement or a new pavement surface, various forms of deterioration begin to accumulate due to the harsh effects of traffic loading combined with weathering action. This deteriorated pavement condition, which is the sum effect of a number of distinct deterioration modes or ‘distresses,’ increases not only agency costs but also user costs. There are many indices that represent pavement condition. International Roughness Index (IRI) is widely used to quantify pavement smoothness. From the driving comfort viewpoint, smoothness is considered as the most important aspect of pavement condition, and it is especially important for pavements with elevated speed limits. Highway agencies generally have their own specifications of IRI level for different classes of roadways for new pavements and also in their service life. Roughness increases user costs including fuel, repair and maintenance, depreciation, and tire costs. User costs across a vehicle fleet resulting from increased roughness is undoubtedly significant, but has not been well quantified in light of newly available prediction tools.

In this study, pavement roughness is used to estimate user costs associated with overall pavement surface condition [5, 6]. According to ASTM E867-06, pavement roughness is defined as "The deviation of a surface from a true planar surface with characteristic dimensions that affect vehicle dynamics and ride quality" [7]. After a detailed investigation, the International Roughness Index (IRI) was chosen as the standard reference roughness index. IRI is used to quantify pavement roughness, with units of inch/mile or m/km. IRI depends on different pavement factors including age, environment, traffic loading, pavement structure and drainage, pavement layer strength, stiffness, and the amount and severity of cracking, potholes, raveling, rutting, etc. Roughness (IRI) is determined from a mathematical model, which simulates the vehicle’s suspension response to roughness at a speed of 50 mph. The model is referred to as a “quarter car simulation,” as a quarter-car model (one wheel of a passenger vehicle) with two degrees of freedom on a rough pavement is used to estimate IRI.

Pavement roughness significantly affects user costs, as it has an effect on fuel consumption, repair and maintenance costs, vehicle depreciation, tire costs, etc. While Zaniewski et al. (1982) reports (from a study based on survey of truck fleet owners) that the effect of roughness on fuel consumption is not statistically significant at a 95% confidence level, more recent studies performed by the World Bank using the HDM-4 model (vehicle operating cost model) indicates that pavement roughness does indeed increase fuel consumption [8]. Zaabar and Chatti (2010) have calibrated the HDM-4 model for US conditions [9]. Jackson (2004) reported, based on study of five pavement sections in Florida, that a 10% reduction in roughness would raise fuel economy by about 1.3% [10]. The NCHRP 1-33 study concluded that a 1 inch/mile increase in IRI would result in a \$280 (in 1999 dollars) increase in repair and maintenance costs for a passenger car operated on primary road [5], which would amount to approximately \$375 in 2011. Drivers prefer to drive on smoother pavements even though it might require taking a longer route, thereby increasing fuel costs.

The objectives of this chapter are to: (a) estimate different types of user costs incurred by pavement roughness, and; (b) compare agency investments for different maintenance and rehabilitation strategies and associated roughness-related user costs. A comparison of previous studies with the current study is summarized in Table 2.1.

Table 2.1: Factors Considered in Previous Studies versus Current Study

Category	Previous Studies	Current Study
User costs	<ul style="list-style-type: none"> ○ Included only a subset of total user cost, i.e., repair and maintenance or depreciation ○ Fuel consumption not considered ○ Total user costs for a single vehicle or the fleet considered for different acceptable and unacceptable IRI levels for different classes of highways ○ Incomplete link between user costs and IRI 	<ul style="list-style-type: none"> ○ Includes a comprehensive array of user costs related to roughness ○ Fuel consumption considered using calibrated HDM-4 model ○ Total user cost for a single vehicle and 10,000 AADT was considered for Interstate, primary, and secondary roads ○ Functional relationship between IRI level and user costs
Agency Costs	<ul style="list-style-type: none"> ○ Agency costs not considered along with user cost 	<ul style="list-style-type: none"> ○ Agency costs considered and compared with user costs related to roughness
Miscellaneous	<ul style="list-style-type: none"> ○ Historical or IRI data from transportation agency were used 	<ul style="list-style-type: none"> ○ MEPDG program was used to predict IRI at different traffic and weather condition with different initial IRI level

The following sections provide background on the various user costs needed to conduct a life cycle cost analysis (LCCA) considering user costs and their relation to pavement roughness. FHWA (1998) defines LCCA as “. . . a process for evaluating the total economic worth of a usable project segment by analyzing initial costs and discounted future cost, such as maintenance, user, reconstruction, rehabilitation, restoring, and resurfacing costs, over the life of the project segment” [11].

2.2 PAVEMENT COSTS

Although agency costs for a given pavement facility are very significant at the time of initial construction and when major rehabilitation activities performed, pavement user costs may also be significant when the total fleet using those facilities is considered. Pavement agency costs include initial construction, maintenance, rehabilitation, and engineering administration. Pavement user costs include fuel, oil, tire repair and replacement, vehicle maintenance and repair, depreciation, travel time delay, and driver discomfort/injury.

2.3 AGENCY COSTS

Various DOT's have their own unique pavement rehabilitation and maintenance (R&M) strategies. In this paper, four alternative strategies have been considered. Cost information for different rehabilitation and maintenance techniques was collected from DOT's as retrieved from the literature. As these data were collected from different sources, data was inflated using the relevant Consumer Price Index (CPI) and expressed in 2011 dollars. According to FHWA (2011), "the Consumer Price Index (CPI) measures the changes in the cost of purchasing products and services" [12]. FHWA also maintains a similar cost index for highway construction activities. According to FHWA (2011), the Federal-aid highway Construction Index (CI) is computed based on the unit costs of excavation, resurfacing, and construction, and reflects cost changes for materials such as reinforcing steel, bituminous concrete, Portland cement and other ingredients for highway projects across the country. As CI is not available for most recent years, CPI was used in this paper.

2.4 PAVEMENT USER COSTS

2.4.1 Fuel Cost

Fuel is an important component of pavement user costs, and has been reported to account for as much as 50-75% of total pavement user costs [13]. Fuel consumption depends on vehicle class, and factors that affect fuel consumption include vehicle type, class, age, vehicle technology, pavement surface type, pavement condition, speed, roadway geometry, environment, etc. According to the American Automobile Association (2011), the composite national average driving cost per-mile for 2010 was 58.5 cents, based on \$2.88 per gallon fuel cost [14]. Fuel consumption is directly related to forces acting on the vehicle, including aerodynamic, rolling resistance, gradient, curvature, and inertial forces. Zaniewski (1989) reported that fuel consumption of automobiles is not dependent on pavement surface type [15]. Lu (1985) reported that pavement rolling resistance depends on pavement roughness, and that an IRI reduction of 129 inch/mile will result in a 10% drop in rolling resistance [16]. A decrease in rolling resistance by 10% increases fuel economy by 1% to 2%, according to TRB Special Report 286 [17]. This increase in fuel economy would save about 1.75 to 3.5 billion gallons of fuel per year of the 175.2 billion gallon consumed by the total highway fleet in the year 2008 [18], if this

improvement in rolling resistance could be attained. Thus, maintaining pavement surface smoothness could potentially save billions of dollars annually in the US.

There are many models available to estimate vehicular fuel consumption, which are often termed as vehicle operating cost (VOC) models. The models include: (a) Texas Research and Development Foundation (TRDF) model; (b) World Bank's HDM-4 model; (c) Saskatchewan models; (d) ARFCOM: Australian Road Fuel Consumption model; (e) New Zealand VOC model; (f) South African VOC models, and; (g) Swedish mechanistic model for simulations on road traffic (VETO). HDM-4, the most recent VOC model, clearly shows that pavement roughness affects fuel consumption. As the HDM-4 model was developed based upon data from developing countries, Zaabar and Chatti (2010) calibrated the model to consider US conditions [9]. In fuel consumption model, vehicle speed was assumed to be at least 45 mph. They estimated the increase in fuel consumption based on pavement roughness for different types of vehicles, which was converted into equation (2.1) form for the purposes of this study:

$$\% \text{ Increase in fuel consumption for IRI increases} = 0.01573 \times \text{IRI} - 0.996 \quad (2.1)$$

Here, IRI is pavement roughness expressed in units of inches/mile. This above equation was used to estimate increase in pavement user costs, as described later in this chapter.

The Environmental Protection Agency (EPA) estimates annual fuel costs for different types of vehicle. For this study, arbitrarily, a mid-sized Honda Accord M-6 car was selected. According to EPA (2010), fuel cost for this car is 15.12 cents/mile considering 15000 miles driven per year (55% city, 45% highway) and a fuel price of \$3.78/gal [19].

2.4.2 Repair and Maintenance Costs

Repair and maintenance includes user costs (parts and labor) required because of vehicular wear and tear. Zaniewski et al. (1982) developed the only model found in the literature based on US conditions. The World Bank's recent HDM-4 model is based on data from developing countries [20]; however, Zaabar and Chatti (2010) reported repair and maintenance cost predictions by the HDM-4 model is reasonable for US conditions [9]. According to HDM-4, the effect of pavement roughness on repair and maintenance cost is negligible at low (193 inch/mile) IRI. However, Zaniewski et al. (1982) modified a World Bank study which was based on data from Brazil to

investigate the effect of roughness on repair and maintenance costs and proposed adjustment factors based on the present serviceability index (PSI) parameter, which provides a numeric rating of current pavement condition. According to the authors, the multiplying factor for repair and maintenance cost would be 1.00 at a PSI value of 3.5. Later PSI values were converted to IRI (Table 2.2) using a transfer equation generated by Hall and Correa in 1999 [21].

Table 2.2: Multiplying Factors (MF) for Repair and Maintenance Costs Generated from Zaniewski et al. (1982)

PSI	(IRI), inch/mile	MF for Passenger Car and Pickup Trucks	Vehicle Class	Average Cost, \$/1000-mile		
				Zaniewski et al. (1982)	2007 Value, Zaabar and Chatti (2010)	2011 Cost
4.5	40	0.83	Small Car	34.50		
4.0	63	0.90	Medium Car	41.84	64.73	69.77
3.5	84	1.00	Large Car	48.33		
3.0	123	1.15	Pick Up	53.12	83.31	89.81
2.5	180	1.37	Light Truck	99.59	148.24	159.80
2.0	320	1.71	Medium Truck	140.82	190.83	205.71
1.5	610	1.98	Heavy Truck	140.82	191.95	206.92

The equation (2.2) was fitted to find a relationship between IRI and repair and maintenance (R&M) cost.

$$\text{Multiplying Factor (MF) for R\&M} = -5 \times 10^{-6} \times \text{IRI}^2 + 0.0049 \times \text{IRI} + 0.6239 \quad (2.2)$$

$$R^2 = 0.9986$$

Where, IRI is in inch/mile

Zaniewski et al. (1982) proposed repair and maintenance costs for different types of vehicles and Zaabar and Chatti (2010) updated this cost to 2007 dollar value. In this study, cost information was updated to 2011 dollar value to estimate additional user costs incurred as a result of pavement roughness.

2.4.3 Depreciation Cost

Chesher et al. (1981) reported, from a study performed based on developing countries data, that vehicular depreciation rate is dependent on pavement roughness [22]. Studies performed in developed countries have also shown that roughness affects depreciation costs. Vehicle depreciation cost depends on mileage driven and age of vehicle. According to Haugodegard et al. (1994), a major portion (70%) of depreciation cost depends on vehicle age and a minor part (30%) on mileage. They also observed that mileage-related depreciation depends on pavement roughness. Zaniewski et al. (1982) studied depreciation cost based on a survey and vehicle registration data. They proposed adjustment factors based on a PSI of 3.5. Table 2.3 represents multiplying factor for depreciation cost.

Table 2.3: Multiplying Factor for Depreciation Cost based IRI and Zaniewski et al. (1982)

Present Serviceability Index (PSI)	International Roughness Index (IRI), inch/mile	MF for Passenger Car and Pickup Trucks
4.5	40	0.98
4.0	63	0.99
3.5	84	1.00
3.0	123	1.02
2.5	180	1.04
2.0	320	1.06
1.5	610	1.09

The equation (2.3) was developed using data reported in Table 2.3 to establish a formulaic relationship between IRI and depreciation cost.

$$\text{Multiplying Factor (MF) for Depreciation} = -1 \times 10^{-6} \times \text{IRI}^2 + 0.0007 \times \text{IRI} + 0.9535 \quad (2.3)$$

$$R^2 = 0.9983$$

where, IRI is in units of inches/mile. This equation was used in this study to estimate depreciation cost at different levels of IRI.

FHWA (2002) reported average vehicle depreciation cost of different types vehicles [23]. This study found that mileage related depreciation costs for a medium or large sized auto is 9.8 cents/mile in 1995 dollars. According to Barnes and Langworthy (2004), a baseline depreciation cost of an automobile in highway and smooth pavement condition is 6.2 cents/mile in 2003 dollars [24]. Applying the CPI, this depreciation cost would be 7.53 cents/mile in 2011 dollars, which has been subsequently used in this paper to estimate additional cost incurred by pavement roughness.

2.4.4 Tire Costs

Zaniewski et al. (1982) developed an adjustment factor to estimate tire cost as a function of pavement condition, using a PSI of 3.5 as reference, where tire cost increases with pavement roughness [5]. The effect of distance traveled and tire load are greater than that of pavement roughness on tire wear [5]. Tire wear depends on roughness, and highly abrasive aggregate has an effect on tire wear [5]. Haugodegard et al (1994) showed, based on a Norwegian study, a definite increasing trend of tire wear with pavement roughness [2]. Table 2.4 presents multiplying factors for tire cost.

Table 2.4: Multiplying Factor for Tire Cost based IRI and Zaniewski et al. (1982)

Present Serviceability Index (PSI)	International Roughness Index (IRI), inch/mile	MF for Passenger Car and Pickup Trucks
4.5	40	0.76
4.0	63	0.86
3.5	84	1.00
3.0	123	1.16
2.5	180	1.37
2.0	320	1.64
1.5	610	1.97

The equation (2.4) was fitted from Table 2.4 to find a relationship between IRI and tire cost.

$$\text{Multiplying Factor (MF) for Tire Cost} = -9 \times 10^{-6} \times \text{IRI}^2 + 0.0064 \times \text{IRI} + 0.5133 \quad (2.4)$$

$$R^2 = 0.9989$$

Where, IRI is in inch/mile. This equation was used in this study to estimate tire cost at different levels of IRI.

According to Barnes and Langworthy (2003), baseline tire cost for an automobile operated on a highway with a smooth pavement condition is 0.9 cents/mile in 2003 dollars [24]. By using CPI, this tire cost is 1.1 cents/mile in 2011 dollar which has been later used to estimate additional cost incurred due to pavement roughness.

2.5 ROUGHNESS PREDICTION

Pavements begin deteriorating after construction due to traffic loads and environmental factors. Pavement surface roughness increases with the extent and severity of various distresses, which affect ride quality, safety, travel speed, and vehicle operating costs. There are many pavement roughness models which were developed using different distresses for new and overlaid pavements [25]. In this study, the IRI model that appears on the MEPDG was used to predict pavement roughness [26]:

$$IRI = IRI_0 + 0.0150*SF + 0.400*FC_{Total} + 0.0080*TC + 40*RD \quad (2.5)$$

Where, IRI_0 = Initial IRI, inch/mile

SF = Site Factor

FC_{Total} = Area of fatigue cracking (combined alligator, longitudinal, and reflection cracking under the wheel path), in percentage of total lane area

TC = Length of transverse cracking in feet per mile

RD = Average rut depth measured in inches

The following inputs were used for MEPDG analysis of 12-inch full depth asphalt pavement, along with program default values:

AADT = 10000

Asphalt Binder = PG 64-22

Asphalt creep and strength data: University of Illinois, Buttlar group database

Initial IRI = 63 inch/mile and 70 inch/mile

Climate: Champaign, IL

Design life: 20 years

Table 2.5 shows the predicted IRI of a 12-inch, full-depth asphalt pavement.

Table 2.5: Prediction of IRI Using MEPDG Software Program

Year	IRI (When Initial IRI = 63 inch/mile)	IRI (When Initial IRI = 70 inch/mile)
1	76.3	83.3
2	80.1	87.1
3	83	90
4	86.6	93.6
5	89.6	96.6
6	93.5	100.5
7	98.5	105.5
8	101.4	108.4
9	104.3	111.3
10	108.3	115.3
11	111.2	118.2
12	114.6	121.6
13	117.8	124.8
14	121.2	128.2
15	124.9	131.9
16	128.3	135.3
17	131.6	138.6
18	135.4	142.4
19	138.8	145.8
20	142.5	149.5

Perera and Kohn (2006) reported that, for pavement sections with IRI greater than 97 inch/mile before applying an overlay, the IRI after placing the overlay was reduced to between 52 to 76 inch/mile [27]. They also reported that IRI values would be less than 64 inch/mile after the application of an overlay when pre-overlay IRI values of less than 97 inch/mile were present. Thus, for roughness prediction of pavement following rehabilitation, an IRI level of (63 inch/mile) was assumed in this study. Maintenance represents pavement improvement activities

which are performed when pavement is in a structurally sound, good condition. Al-Mansour et al. (1994) studied the effect of crack sealing, chip seal, and sand seal on roughness in flexible pavements used on interstate and state highways [28]. They reported low benefits in roughness reduction due to maintenance activities in the case of new pavements and increased benefit in roughness reduction for maintenance applied to aged pavements. Hall et al. (2002) studied the effect of various maintenance activities, including slurry seal, chip seal, crack seal, and thin overlays on pavement roughness [29]. Based upon a statistical analysis, they reported that the effect of chip seals, crack seals, and slurry seals were not significant compared to a control section which did not receive a maintenance treatment. However, thin overlays were found to reduce pavement roughness significantly. In this study, no improvement in IRI was considered for pavements undergoing chip seals, slurry seals, and crack seals, while a roughness reduction resulting in a restored IRI level of 63 inch/mile was assumed following the application of an overlay. Although rate of change of IRI for overlays is higher than new pavement IRI deterioration, the same rate was considered for simplicity of calculation in this study.

2.6 ESTIMATION OF COST DUE TO PAVEMENT ROUGHNESS

Different types of pavement user costs were estimated by using the equations and user cost data provided in the above sections. Table 2.6 shows increases in user costs i.e. fuel consumption, repair and maintenance, depreciation, and tire cost, at different levels of IRI as predicted by the AASHTO Mechanistic Empirical Pavement Design Guide (MEPDG) software program when IRI is greater than 63.3 inch/mile. Total roughness-related user costs are also shown in Table 2.6 for a fleet of 10,000 vehicles, assumed to travel an average of 12,000 miles per year. From Table 2.6, it can be seen that a vehicle owner will incur an additional \$129/year for a vehicle driven on road with an IRI of 110 inch/mile, which is considered to be an adequate smoothness level for a primary road. This additional user cost would be higher (\$478/year) if the same vehicle were driven on road with an IRI of 200 inch/mile, which is the highest acceptable IRI level for a primary road.

Table 2.6: Total User Cost Increased due to Pavement Roughness

IRI, inch/mile	Increase in Fuel Cost, \$/mile from Eq. (1)	Increase in R&M Cost by Eq. (2), \$/mile	Increase in Depreciation Cost by Eq.(3), \$/mile	Increase in Tire Cost by Eq. (4), \$/mile	Total Increase in User Cost, \$/mile	Total Cost per Year for 10,000 vehicle, \$	Total Cost per Year per vehicle, \$
63.00	0.00000	0	0	0	0.00000	-	-
76.3	0.00031	0	0.00008	0	0.00039	\$46,428	\$5
80.1	0.00040	0	0.00024	0	0.00063	\$75,841	\$8
83	0.00046	0	0.00035	0	0.00082	\$98,113	\$10
86.6	0.00055	0.000742	0.00050	0	0.00179	\$214,581	\$21
89.6	0.00062	0.001575	0.00061	0.00016	0.00297	\$356,126	\$36
93.5	0.00071	0.002648	0.00077	0.00036	0.00449	\$538,386	\$54
98.5	0.00083	0.004009	0.00096	0.00061	0.00641	\$769,284	\$77
101.4	0.00090	0.00479	0.00106	0.00076	0.00751	\$901,780	\$ 90
104.3	0.00097	0.005565	0.00117	0.00090	0.00861	\$1,033,230	\$103
108.3	0.00106	0.006625	0.00132	0.00110	0.01011	\$1,212,824	\$121
100 ¹	0.00087	0.004413	0.00101	0.00069	0.00698	\$837,947	\$84
110 ²	0.00111	0.007072	0.00138	0.00118	0.01074	\$1,288,548	\$129
125 ³	0.00146	0.010931	0.00190	0.00188	0.01618	\$1,941,125	\$194
175 ⁴	0.00265	0.022673	0.00340	0.00390	0.03262	\$3,914,234	\$391
200 ⁵	0.00324	0.027896	0.00401	0.00472	0.03987	\$4,784,164	\$478
250 ⁶	0.00443	0.037047	0.00495	0.00600	0.05242	\$6,290,776	\$629

Agency costs for four different maintenance and rehabilitation (M&R) strategies were estimated. The effects of M&R activities on pavement roughness were estimated from data found through literature review [29]. Table 2.7 shows agency costs for four alternative M&R strategies. To calculate life-cycle cost of pavement, a 35 year analysis period and a 3% discount rate was considered. A comparison was then made between agency costs and costs related to pavement roughness, as shown in Table 2.1.

¹ IRI level for adequate smooth pavement of Interstate highway

² IRI level for adequate smooth pavement of Primary roads

³ IRI level for adequate smooth pavement of Secondary roads

⁴ IRI level for inadequate smooth pavement of Interstate highways

⁵ IRI level for inadequate smooth pavement of Primary roads

⁶ IRI level for inadequate smooth pavement of Secondary roads

Table 2.7: Pavement Maintenance and Rehabilitation (M&R) Strategies (1-mile)

Alternative 1			Alternative 2		
Year	Action	Cost	Year	Action	Cost
0	New Pavement	\$206712	0	New Pavement	\$206712
3	Crack Seal (4 yrs)	\$1500	3	Crack Seal (4 yrs)	\$1500
7	Crack Seal (4 yrs)	\$1500	7	Mill & Patch 20% Spot Repair	\$18050
10	2" Overlay (10 yrs)	\$92810	15	2" Mill & 2" Overlay	\$94090
13	Crack Seal (4 yrs)	\$1500	18	Crack Seal (4 yrs)	\$1500
16	Slurry Seal (4 yrs)	\$11265	20	Mill & Patch 20% Spot Repair	\$18050
20	2" Mill & 2" Overlay	\$94090	27	1.5" Mill & 3" Overlay	\$110860
23	Crack Seal (4 yrs)	\$1500	30	Crack Seal (4 yrs)	\$1500
26	Chip Seal (5 yrs)	\$12530	35	Salvage Value	-\$33258
30	2" Mill & 2" Overlay	\$94090			
35	Salvage Value	-\$47045			
	Present Worth =	\$367,115		Present Worth =	\$332,735
	EUAC =	\$ 17,085		EUAC =	\$ 15,485
Alternative 3			Alternative 4		
Year	Action	Cost	Year	Action	Cost
0	New Pavement	\$206,712	0	New Pavement	\$206,712
3	Crack Seal (4 yrs)	\$1,500	3	Crack Seal (4 yrs)	\$1,500
5	Chip Seal (5 yrs)	\$12,530	5	Crack Seal (4 yrs)	\$1,500
10	1.5" Overlay (10 yrs)	\$77,585	9	Mill & Patch 20% Spot Repair	\$18,050
14	Crack Seal (4 yrs)	\$1,500	12	Chip Seal (5 yrs)	\$12,530
17	Slurry Seal (4 yrs)	\$11,265	17	2" Mill & 2" Overlay	\$94,090
20	2" Mill & 2" Overlay	\$94,090	20	Crack Seal (4 yrs)	\$1,500
23	Crack Seal (4 yrs)	\$1,500	23	Slurry Seal (4 yrs)	\$11,265
26	Fog Seal (2 yrs)	\$9,700	27	1.5" Overlay (10 yrs)	\$77,585
30	1.5" Overlay (10 yrs)	\$77,585	30	Crack Seal (4 yrs)	\$1,500
35	Salvage Value	-\$38,792	35	Salvage Value	-\$15,517
	Present Worth =	\$359,962		Present Worth =	\$325,497
	EUAC =	\$ 16,752		EUAC =	\$ 15,148

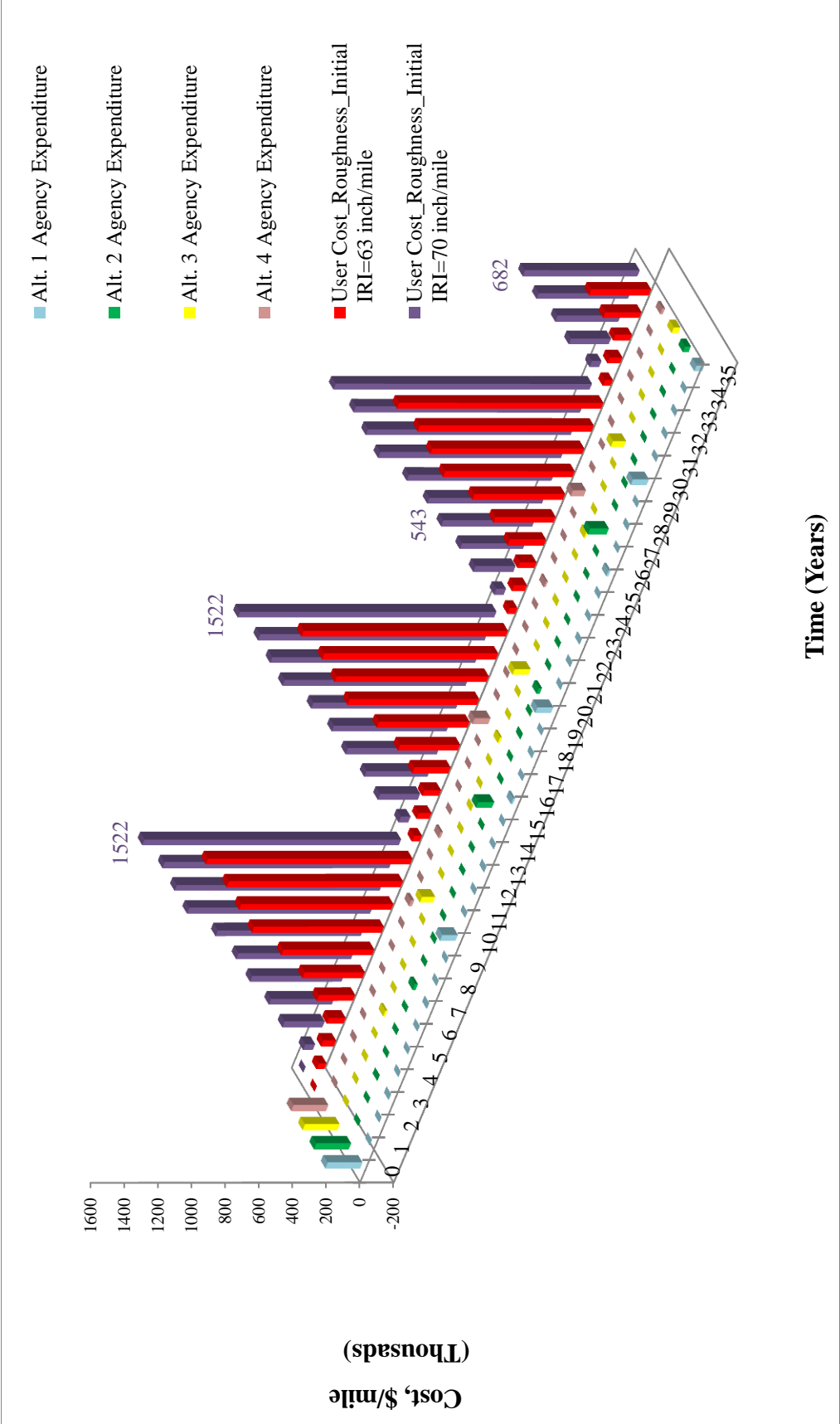


Figure 2.1: Comparison between Agency Costs and User Costs Related to Pavement Roughness

In Figure 2.1, roughness cost was calculated assuming 12,000 mile/year and a 10,000 annual average daily traffic (AADT) level. It can be seen that the present worth (PW) of the pavement from the LCCA was found to be about \$350,000, whereas cost related to roughness was about \$9,910,000 to \$15,460,000 depending on the initial roughness of the pavement. This finding suggests that highway agencies only expend about 2.3% to 3.6% of the amount that is spent by users as a result of pavement roughness over the period of the LCC.

In this paper, agency costs and costs incurred because of pavement roughness were considered, not total vehicle operating cost. Figures 2.2 and 2.3 show that vehicle maintenance and repair costs increase significantly with IRI, amounting to about 56% to 60% of the total costs considered, depending upon initial IRI.

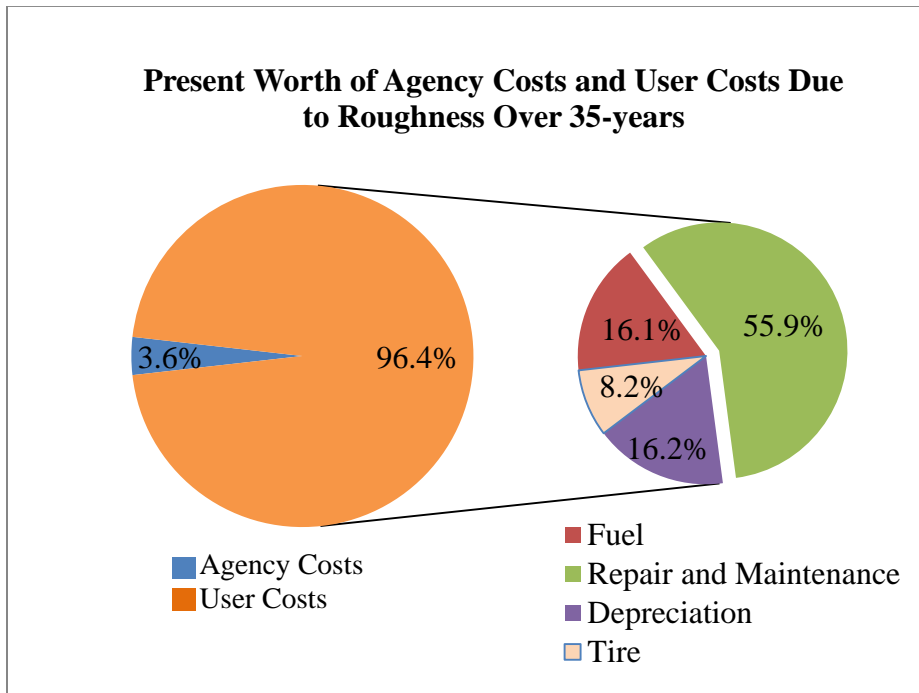


Figure 2.2: Present Worth of Agency Costs and User Costs Related to Roughness Over 35-Year Analysis Period of Pavement (Initial IRI = 63 inch/mile)

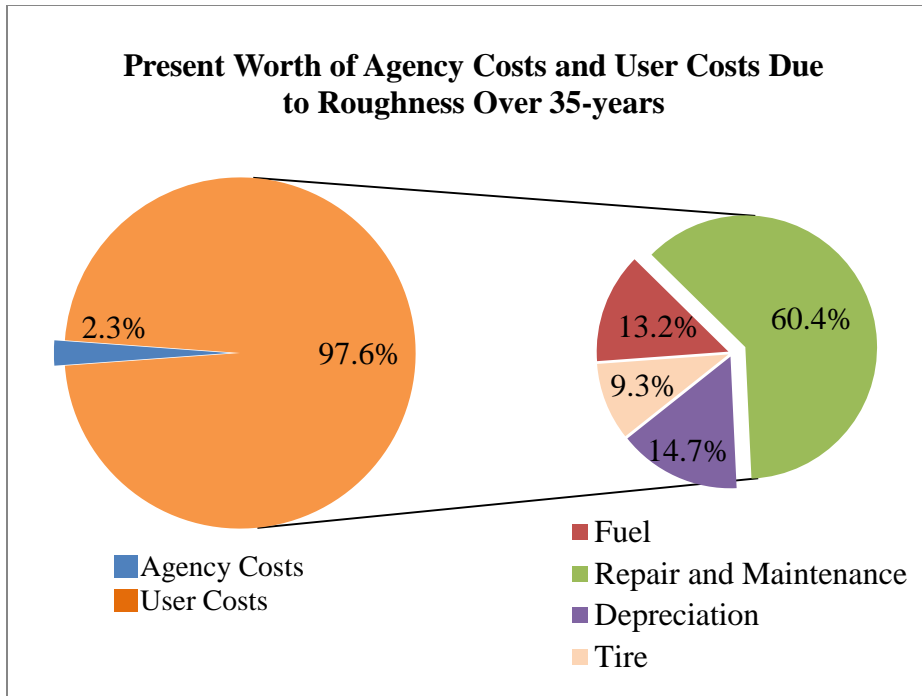


Figure 2.3: Present Worth of Agency Costs and User Costs Related to Roughness Over 35-Year Analysis Period of Pavement (Initial IRI = 70 inch/mile)

The present analysis strongly suggests that increased investment in pavement maintenance and rehabilitation activities aimed at reducing pavement roughness could result in a many-fold savings in user costs. It is acknowledged that the typical values, models and other assumptions used in this study will vary from region to region, and will change with time (e.g., with changes in fuel, material, and vehicle maintenance costs, changes in transportation policies, etc.). A spreadsheet-based program is currently being developed to facilitate the LCCA analysis performed herein, which will allow this model to be readily applied in various regions across the US and abroad. Table 2.8 provides a sensitivity analysis comparing agency vs. user costs for differing average daily traffic (ADT) levels and analysis periods. It was assumed that agency cost would be 10% less and 10% more for 8,000 ADT and 12,000 ADT, respectively compared to 10,000 ADT, to account for full-depth asphalt design pavement thickness variation as a function of design traffic. Although these two variables clearly affect agency and user costs, the overall conclusion of the study (users bear the bulk of the financial burden when pavements become rough) is unchanged.

Table 2.8: Sensitivity Analysis for Traffic Level and Analysis Period

Average Daily Traffic Level and Yearly User Cost			
Traffic Level (ADT)	Agency Cost	User Cost	
		Initial IRI = 63 inch/mile	Initial IRI = 70 inch/mile
8,000	\$330,400	\$7,928,341	\$12,368,748
10,000	\$367,115	\$9,910,426	\$15,460,936
12,000	\$403,825	\$11,892,512	\$18,553,123
Analysis Period and Yearly User Cost			
Analysis Period (years)	Agency Cost	User Cost	
		Initial IRI = 63 inch/mile	Initial IRI = 70 inch/mile
35	\$367,115	\$9,910,426	\$15,460,936
40	\$388,723	\$11,345,212	\$17,409,807
45	\$405,547	\$11,561,089	\$17,929,249

A final analysis is now presented to further demonstrate that increased pavement maintenance activities will be paid off many times over in reduced user costs. Table 2.9 shows the maintenance and rehabilitation strategy used to conduct this analysis. Table 2.10 shows increases in user costs.

Table 2.9: An Example of an Enhanced Maintenance and Rehabilitation Strategy for a 1-Mile Section of Roadway

Year	Action	Cost			
0	New Pavement	\$206,712		Present of Worth of Alternative 1	\$367,115
3	Crack Seal (4 yrs)	\$1,500		Present Worth of this M&R	\$475,325
7	2" Mill & 2" Overlay	\$94,090		Additional Investment	\$108,209
10	Crack Seal (4 yrs)	\$1,500		Roughness related user costs for Alternative 1 with initial IRI 63 in/mile	\$9,910,426
13	2" Mill & 2" Overlay	\$94,090		Roughness related user costs for this M&R with initial IRI 63 in/mile	\$4,740,484
16	Slurry Seal (4 yrs)	\$11,265		Reduction of user costs	\$5,169,943
20	2" Mill & 2" Overlay	\$94,090		Roughness related user costs for Alternative 1 with initial IRI 70 in/mile	\$15,460,936
23	Crack Seal (4 yrs)	\$1,500		Roughness related user costs for this M&R with initial IRI 70 in/mile	\$9,725,724
26	2" Mill & 2" Overlay	\$94,090		Reduction of user costs	\$5,735,212
30	2" Mill & 2" Overlay	\$94,090			
35	Salvage Value	-\$47,045			
	Present Worth (PW) =	\$475,325			
	EUAC =	\$22,121			

Table 2.10: User Costs for the Enhanced M&R Strategy

Year	Initial IRI of Pavement = 63 inch/mile				Initial IRI of Pavement = 70 inch/mile		
	IRI, Inch/mile	Total Increase in User Cost, \$/mile	Total Cost per year for 10,000 vehicle, \$	Total Cost per Year per vehicle, \$	IRI, Inch/mile	Total Increase in User Cost, \$/mile	Total Cost per year for 10,000 vehicle, \$
0	63	0	\$ -	\$ -	70	0	\$ -
1	76.3	0.000386899	\$ 46,428	\$ 5	83.3	0.000481	\$ 57,709
2	80.1	0.000632008	\$ 75,841	\$ 8	87.1	0.001986	\$ 238,297
3	83	0.000817608	\$ 98,113	\$ 10	90	0.003124	\$ 374,906
4	86.6	0.001788174	\$ 214,581	\$ 21	93.6	0.004525	\$ 543,034
5	89.6	0.002967715	\$ 356,126	\$ 36	96.6	0.005683	\$ 681,909
6	93.5	0.004486547	\$ 538,386	\$ 54	100.5	0.007173	\$ 860,773
7	76.3	0.000386899	\$ 46,428	\$ 5	83.3	0.000481	\$ 57,709
8	80.1	0.000632008	\$ 75,841	\$ 8	87.1	0.001986	\$ 238,297
9	83	0.000817608	\$ 98,113	\$ 10	90	0.003124	\$ 374,906
10	86.6	0.001788174	\$ 214,581	\$ 21	93.6	0.004525	\$ 543,034
11	89.6	0.002967715	\$ 356,126	\$ 36	96.6	0.005683	\$ 681,909
12	93.5	0.004486547	\$ 538,386	\$ 54	100.5	0.007173	\$ 860,773
..
34	86.6	0.001788174	\$ 214,581	\$ 10	90	0.003124	\$ 374,906
35	89.6	0.002967715	\$ 356,126	\$ 21	93.6	0.004525	\$ 543,034
Present Worth (PW) =			\$4,740,484	Present Worth (PW) =			\$9,725,724

If the enhanced M&R strategy shown in Table 2.9 is used, it would require an additional transportation agency expenditure in terms of present worth of \$108,209 more over the 35-year analysis period. According to Table 2.9, this would save a whopping \$5,169,943 to \$5,735,212 (52% to 37%) of user costs over the 35-year life cycle depending on the initial roughness of the pavement. Stated otherwise, increased maintenance activities resulting in smoother pavement condition over the life of the pavement will have about a 50-fold return on investment in terms of reduced user costs. Additional justification for the increased maintenance expenditures can be argued from a sustainability standpoint; increased pavement maintenance activities will significantly reduce fuel consumption and tire wear over the life of the pavement, and will extend the overall life of pavement system (the enhanced M&R strategy results in a higher salvage value and therefore a higher remaining life in the pavement section at the end of the 35-year analysis period, thereby delaying reconstruction). It is hoped that the present analysis will provide compelling information that can be used by transportation policy makers to make a

strong case for increased maintenance and rehabilitation activities to help reduce the financial burden carried by users resulting from rough pavement.

2.7 CONCLUSIONS

Roughness is an important aspect of pavement condition which significantly effects driver comfort, and moreover, user costs. A comprehensive investigation was conducted to study the effect of pavement roughness on agency and user costs. Some unique features of the research conducted include: (a) A comprehensive array of user costs related to roughness were considered; (b) fuel consumption was computed using a calibrated HDM-4 model; (c) total user costs for a single vehicle and 10,000 AADT was considered for Interstate, primary, and secondary roads; (d) a functional relationship between IRI level and user costs was developed; (e) agency costs were simultaneously considered and compared with user costs in the context of pavement roughness, and; (f) the newly released MEPDG program was used to predict IRI at different traffic levels and weather condition and with different initial IRI level. The analysis conducted demonstrated that user costs including fuel consumption, repair and maintenance, depreciation, and tire costs dramatically increase with increased pavement roughness, which far outweigh agency costs associated with the construction and maintenance of the facility itself. For the two main examples presented, agency costs based upon typical maintenance practices by state DOTs were in the range of 2.3 to 3.6% of the combined costs (agency plus user) associated with a unit section of roadway.

By investing in additional maintenance (resurfacing every 7 years instead of every 10 years, on average) would save a whopping \$5.1 M to \$5.7 M (52% to 37%) of user costs over the 35-year life cycle depending on the initial roughness of the pavement, as compared to the additional \$108,000.00 agency investment required for this additional rehabilitation step. This equates to a 50-fold return on investment in terms of reduced user costs. Additional justification for the increased maintenance expenditures can be argued from a sustainability standpoint; increased pavement maintenance activities will significantly reduce fuel consumption and tire wear over the life of the pavement, and will extend the overall life of pavement system. Additional analyses are recommended to verify the results obtained herein and to expand the findings to include more pavement types, rehabilitation strategies, etc. Furthermore, it is recommended that

the analysis conducted herein be incorporated into more holistic life cycle analysis, so that the hypothesized benefits resulting from enhanced maintenance and rehabilitation activities can be quantified in conjunction with pavement system sustainability. It is surmised that by adding sustainability concepts into the equation, the case for investing in practices that promote smoother pavements will be further justified.

CHAPTER 3

ENVIRONMENTAL ASSESSMENT OF CONSTRUCTION ACTIVITIES TO REDUCE ROUGHNESS

3.1 INTRODUCTION

According to the 2009 Report Card for America's Infrastructure, poorly maintained roadways cause user delay costs amounting to \$78.2 billion per year, while repairs and vehicle operating expenses cost vehicle owners an additional \$67 billion a year [30]. About 72.4% of urban roads are in minimum satisfactory ride quality condition. Furthermore, the budget allocated for the improvement of highways is only \$70.3 billion per year, which is about 38% of the estimated cost to sustain highway infrastructure condition to an acceptable level over the long run.

According to the National Asphalt Pavement Association (NAPA), annual hot-mix asphalt production in the US is about 500 million tons. About 90% roads and highways are surfaced with asphalt concrete [31]. According to the Federal Highway Administration (FHWA), annual production of aggregate is about 2 billion tons, but the demand will increase to 2.5 billion tons by 2020 [32]. The amount of resources and investment needed to keep the transportation network in good condition, and methods to go about this in a sustainable manner, need to be thoroughly analyzed. Life cycle cost analysis (LCCA) and life cycle assessment (LCA) are powerful tools that can be used to assess economic and environmental impacts associated with resource usage and infrastructure investments.

LCA quantifies environmental impacts associated with products and services (e.g., pavements in this study), and considers inputs and outputs of a product or system [33]. There are many reasons to conduct LCA to evaluate various pavement construction and maintenance alternatives, including: (a) identification of opportunities to improve the environmental performance of maintenance and rehabilitation activities over the facilities life cycle; (b) informing decision-makers in industry, government or non-government organizations; (c) selection of relevant indicators of environmental performance including measurement techniques, and; (d) implementing eco-friendly activities such as the increased use of reclaimed asphalt pavement materials [34]. For instance, in an effort to minimizing emission generated due to construction

and maintenance activities, about 60 million tons of reclaimed material are reintroduced into pavement systems annually in the US [31]. LCA consists of four phases: goal and scope definition; inventory analysis; impact assessment, and; interpretation. A functional unit is defined in an LCA; for example, a 1-mile, 1-lane roadway section is typically considered as a functional unit. Establishing a functional unit is extremely important because it relates inputs and outputs of the LCA analysis and enables a fair comparison of different rehabilitation and maintenance activities when all phases of an LCA are considered. An ideal LCA considers five phases of pavement life, including: materials; construction; use; maintenance and rehabilitation (M&R), and; end-of-life.

Matthews et al. (2001) studied the external costs of air emissions from the transportation sector which are not directly paid by users, such as environmental costs resulting from the production of materials, equipment, services, etc. It was reported that emission costs can be 1%-45% of total cost for transportation services. They also stated that emission costs for transportation equipment manufacturing, construction and operation materials such as crude petroleum and natural gas can be 0.3-11% and 1-100% of total cost, respectively [34]. Lee et al. (2010) studied the environmental benefits of using recycled materials using LCA and reported that application of recycled materials in base and subbase layers of pavement can reduce carbon dioxide emissions by 20%, energy consumption by 16%, and hazardous waste generation by 6% [35]. Brillet et al. (2006) reported that construction and maintenance of roadways and vehicle operation are not independent [36]. This is because while pavement M&R activities improve the smoothness of roads and, therefore; consumption related to use is decreased, the additional M&R activities required to improve smoothness result in extra consumption and emission. Kuchkvar and Tatari (2012) studied ecologically-based LCA of continuously reinforced concrete and hot-mix asphalt pavement and reported that materials extraction and production related emission are less than that of transportation and manufacturing for facilities involving long hauling distances [37]. Cass and Mukherjee (2011) investigated greenhouse gas emissions for highway construction operations and reported that more than 90% carbon dioxide (CO₂) emissions were generated due to material production, equipment used, and fuel used during construction [38]. It is evident from a review of the literature that long term assessment of pavement using LCCA-LCA and including agency costs, user costs, and environmental costs is necessary to obtain a holistic evaluation of rehabilitation strategies and sustainable construction approaches.

In Chapter 2, it has been demonstrated that a 50-to-1 return on investment ROI could be realized by maintaining smooth pavement condition throughout the life of a pavement. However, the cost associated with the environmental impact of construction, maintenance, and rehabilitation (CMR) activities was not considered. The objectives of this study are to: (a) analyze environmental impacts of CMR activities used in pavement engineering; (b) estimate and compare agency costs, user costs due to roughness [extracted from a previous study presented by the authors], and emission costs due to CMR activities, and; (c) estimate emission costs associated with pavement roughness. By considering the cost associated with the environmental impact of CMR activities, a more realistic estimate of the ROI associated with maintaining relatively smooth pavement throughout its service life was assessed.

3.2 MODELING APPROACH

Two LCA programs were used in this study: PaLATE and MOVES. PaLATE is a life cycle assessment tool developed by Horvath (2004) which estimates environmental impact of pavement materials used in the construction and maintenance of pavements [39]. This excel based program allows the user to input the materials and equipment used throughout the service life of the pavement and evaluates the associated environmental impacts. Energy requirements and emitted air pollution depend on fuel efficiency, productivity, and engine size used in every phase of pavement construction and maintenance. PaLATE uses an economic input-output life cycle assessment (EIO-LCA) method [40], which is a model that assumes that emission are linearly related to materials and resources utilized. PaLATE estimates environmental emissions such as carbon dioxide (CO₂), nitrogen oxide (NO_x), pollutant matters (PM₁₀), sulfur dioxide (SO₂), carbon monoxide (CO), lead (Pb), mercury (Hg), potential leachates, hazardous waste generated, human toxicity potential (cancer and non-cancer), and energy consumption. It should be noted that PaLATE evaluates environmental impacts during construction and maintenance phases only; therefore, another program is required to estimate emissions during use/operation phase of the life cycle of the pavement.

To analyze environmental impacts of vehicle use/operation, the Motor Vehicle Emission Simulator (MOVES) program was used. MOVES was developed by Environmental Protection Agency (EPA) in 2010 to estimate road emissions of vehicles, and the latest version of the

MOVES program was released in 2012 [41]. Estimation of emissions using this program is more accurate than that of previous models such as MOBILE 6.2. MOVES was developed based on emission test results and a thorough understanding of vehicle emissions. MOVES can be used to estimate emissions of air pollutants and greenhouse gases (GHG) such as carbon dioxide (CO₂), nitrous oxide (N₂O), and methane (CH₄) at a chosen time frame and for different geographic criteria, including: nation, county, and project. Project-specific data is required, including meteorological data, road type distribution, vehicle type-vehicle miles traveled, vehicle age distribution, average speed distribution, fuel type, etc.

3.3 SYSTEM DEFINITION

In this study, life cycle cost analysis and life cycle assessment (LCCA-LCA) were applied to a 1-mile, 1-lane asphalt pavement section, following the approach taken in our previous study (20). First, a pavement was designed using the AASHTO M-E PDG program with a 35 year analysis period [42]. The analysis period was selected to be sufficiently long to illustrate the difference among various alternative strategies. The following describes the inputs of the M-E PDG analysis conducted, where a 12-inch thick full-depth asphalt pavement was designed. Figure 3.1 presents a flow diagram describing how LCCA-LCA was incorporated in this study.

<u>Parameters/Criteria:</u>	<u>Type/Amount</u>
AADT:	10,000
Asphalt Binder:	PG 64-22
Initial IRI:	63 inch/mile
Design life:	20 years
Climate:	Champaign, IL
Asphalt creep and strength data:	University of Illinois, Buttlar group database

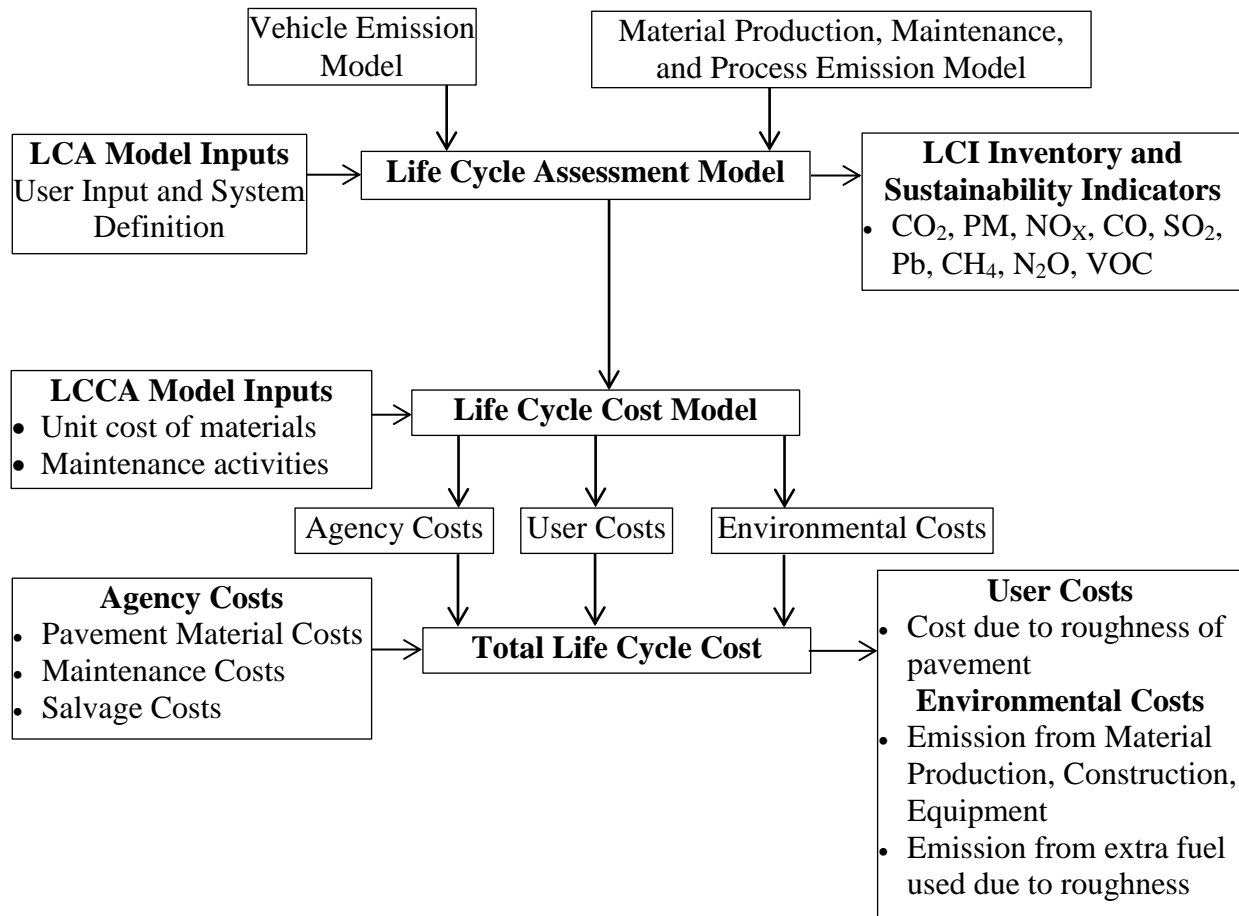


Figure 3.1: Combined Life-Cycle Cost and Life-Cycle Assessment Flow Diagram

It was assumed that the pavement was constructed over a 6-inch crushed stone base. Two different maintenance and rehabilitation strategies were considered over the 35 year analysis period. In the so called basic approach, activities such as crack sealing, chip sealing, slurry sealing, placement of a 2-inch overlay, and placement of a 2-inch milling operations were considered. More roughness was allowed to occur in the basic approach, as only minor rehabilitation was considered throughout the analysis period. Hall et al. (2002) investigated the contribution of several maintenance activities on the reduction of roughness for a given pavement. Their study showed that activities such as crack sealing, chip seals, and slurry seals do not reduce roughness, whereas overlays reduce roughness significantly [29]. In the so-called alternative approach considered herein, more comprehensive rehabilitation strategies were considered, which result in a smoother pavement throughout its life as compared to the basic approach.

Note that estimated environmental emissions and associated impacts and costs related to construction, maintenance, and rehabilitation (CMR) activities will strongly depend on the inputs selected and models used. In this study, emissions of CMR activities were estimated using the PaLATE program described earlier. Material hauling distances was assumed as having a maximum of 30 miles in this study. Obviously, environmental emissions increase with material hauling distance and will be different for different construction situations. Environmental emissions related to vehicle use/operation were estimated using the MOVES program which was developed by the Environmental Protection Agency (EPA) and has been widely employed by the researcher community. While it can be argued that usage of different assumptions, models, etc., could change the estimated emissions and associated environmental costs, the results strongly suggest that these variations would not alter the overall findings of this study with respect to the ROI associated with maintaining smooth pavement throughout its service life.

3.4 ROUGHNESS RELATED USER COSTS

User costs related to pavement roughness has been calculated in Chapter 2, and summary of the finding has been shown in Table 3.1.

Table 3.1: User Costs due to Pavement Roughness

Agency Costs	Present of Worth of Alternative Approach	\$653,701
	Present Worth of Basic Approach	\$545,491
	Additional Investment Require	\$108,210
User costs	Roughness related user costs for Basic Approach	\$9,910,426
	Roughness related user costs for Alternative Approach	\$4,740,484
	Reduction of user costs	\$5,169,943
Emission Costs	Emission Cost for Alternative Approach	\$87,686

3.5 POLLUTION DAMAGE COST RATES

Although no standard monetary value has been assigned to various pollutants, many existing studies considered different values for each pollutant. Unit costs of pollutants are estimated based on their impacts on health. Unit cost of pollutants and greenhouse gases depends on

population density and land cover of the construction site [43]. It is assumed that the emission of these pollutants and greenhouse gases have a substantial adverse effect on health in metropolitan areas with higher population densities. Thus, unit costs associated with emissions is higher in urban areas than rural areas. Tol (2005) reported that damage cost of carbon dioxide (CO₂) varies in the range of \$5-125 per ton, and reported that most estimates are in the lower range [44]. Tol et al. (2001) stated that “estimates [of carbon dioxide emission cost] in excess of \$50/ton requires relatively unlikely scenario of climate change, impact sensitivity, and economic values” [45]. Emission damage costs were collected from Kendall et al. (2008) and adjusted to 2011 dollar using consumer price index (CPI). Damage cost was reported by Tol (2003) based on cost effectiveness and cost benefit of various emission and climatic scenarios [46]. In this study, emission damage costs of pollutants and greenhouse gases were obtained from a recent (2011) FHWA report [43] and Kendall et al. (2005) [47] report as presented in Table 3.2.

Table 3.2: Emission Cost Rates Kendall et al. [47]

	CO ₂ , tons	NO _x , tons	PM ₁₀ , tons	SO ₂ , tons	CO, tons	Pb, tons
Rural Cost Rate, \$/ton	26	8,712	980	26	0	588
Urban Cost Rate, \$/ton	26	8,712	7,526	208	2	4,845

3.6 ENVIRONMENTAL COSTS

Environmental Costs were estimated from emissions generated by various activities related to pavement such as pavement materials production, transportation, and equipment used during construction. Pavement Life-cycle Assessment Tool for Environmental and Economic Effects (PaLATE) provides emissions of five criteria-pollutants defined by Environmental Protection Agency (EPA) and major greenhouse (CO₂) gas. The criteria-pollutants include carbon monoxide (CO), nitrogen oxides (NO_x), sulfur dioxide (SO₂), lead (Pb), and particulate matter (PM₁₀). This program estimates emissions resulting from the production of pavement materials, transportation of those materials to the site, and construction processes.

3.6.1 Emission Calculation

In this study, emissions due to material production, transportation to the construction site, and construction process was obtained by PaLATE. Table 3.3 describes materials, processes, and equipment considered in this study for the CMR activities in the two different approaches investigated.

Table 3.3: Details of Material Quantities, Process, and Equipment Used for CMR

Stage	Item	Quantity, yd ³		Material Source to Site Distance, mile	Transportation Mode
		Basic Approach	Alternative Approach		
Initial Construction	Virgin Aggregate	2206	2206	20	Dump Truck
	Bitumen	141	141	30	Tanker Truck
	Gravel (Base)	98	98	20	Dump Truck
Maintenance and Rehabilitation	Virgin Aggregate	1256	1917	20	Dump Truck
	Bitumen	70.4	117	30	Tanker Truck
	Asphalt Emulsion	35	17.4	30	Tanker Truck
	RAP Material	782	1955	-	
	Hot-in-Place Recycling (HIPR)	782	1955	-	
	Crack Sealing	0.26	0.19	30	Tanker Truck
Process		Equipment Used			
HMA Production		Asphalt Mixing in Batch Plant			
Asphalt Paving		Paver, Pneumatic Roller, Tandem Roller			
Milling		Milling Machine			
Crushing Plant		Excavator, Wheel Load, Dozer, Generator			
HIPR		Heating Machine, Asphalt Mixer, Pneumatic Roller, Tandem Roller			

The PaLATE program accounts for emissions due to all phases of material production. For asphalt production, this includes extraction, transportation/storage, heating, distillation, cooling, and final processing. According to Unruh (2002), a major part of the energy required to produce and construct asphalt pavement is incurred in the distillation process for heating and for steam generation [48]. Stipple (2001) reported that 40% of energy consumed by bitumen during the refining process, and rest of the energy used by the lighter products [49]. But Zapata and Gambatese (2005) reported that mixing and drying of aggregates are major steps which consumed a major portion of the energy during construction of asphalt pavements [50]. They suggested that significant amounts of energy can be conserved by changing the storage and drying processes of aggregates.

Emission due to the traffic use phase was estimated by MOVES, which was developed by EPA. Two different traffic levels (10,000 and 15,000 AADT) were considered in both basic and alternative approaches. Figure 3.2 shows emissions generated by 15,000 passenger cars over 35 years in an urban area along with pavement construction emissions. As initial construction is identical in both basic and alternative approaches, emission is also same. In maintenance phase, CO₂ emission is about 115 tons/mile and 191 tons/mile in basic and alternative approach, respectively. Because of more frequent heavy rehabilitation in alternative approach, emission is higher than that of basic approach. But CO₂ emission related to pavement roughness is less in alternative approach (240 tons/mile) than basic approach (325 tons/mile) because of the smoother pavement.

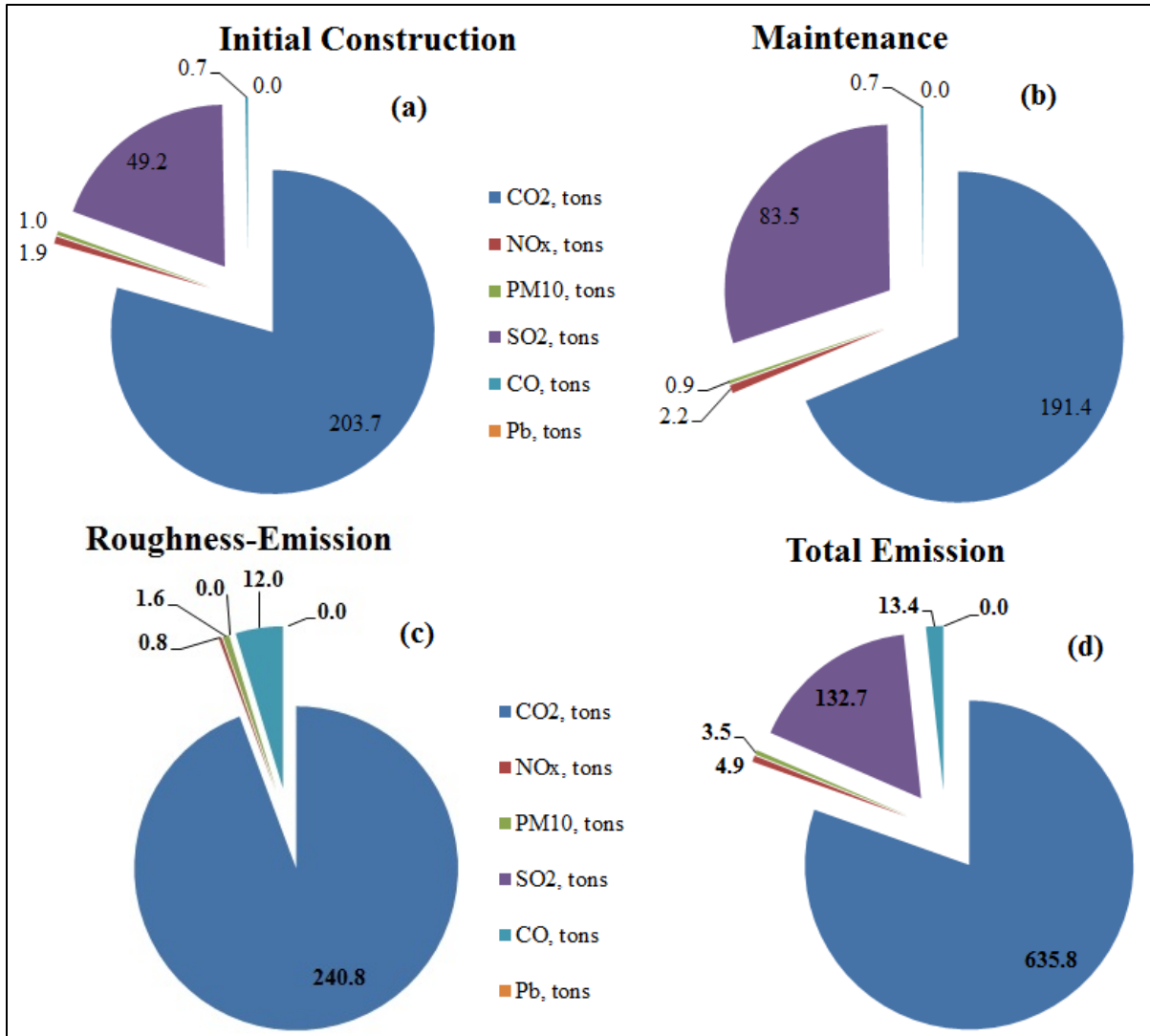


Figure 3.2: Emission of Alternative Approach for Urban Area Over 35-Year Pavement Service Life: (a) Initial Construction, (b) Maintenance, (c) Emission Due to Pavement Roughness, and (d) Total Emission

Zaabar and Chatti (2010) studied the effect of roughness on fuel consumption of vehicles, and reported that fuel consumption increases with pavement roughness and can increase as high as 4 percent depending on IRI level [51]. In the current study, their model was used to estimate additional fuel resulting from pavement roughness. The MOVES program was used to calculate rate of emission of air pollutants and greenhouse gases. This rate was used to estimate emission due to fuel utilized by vehicles due to roughness and is reported in this paper as roughness-related emissions. Pollution damage costs were estimated using rates reported by Kendall et al. (2005).

Tables 3.4 and 3.5 show emissions and cost data for urban area for basic and alternative approaches using 15,000 AADT.

Table 3.4: Emissions by Category and Associated Environmental Cost: Basic Approach - Urban Area

Emissions Category	CO2, tons	NOx, tons	PM10, tons	SO2, tons	CO, tons	Pb, tons
Initial Construction	204	2	1	49	1	0.0002
Maintenance	115	1	1	45	0	0.0002
Vehicles - 35years	87764	292	588	3	4391	11
Roughness Related	325	1	2	0	16	0.04
Total Emissions	88408	296	592	97	4409	11
Est. Envir. Cost, \$/ton	26	8712	7526	208	2	4845
Total Environmental Cost, \$	\$2,274,301	\$2,581,150	\$4,453,547	\$20,261	\$10,802	\$51,089
Total = \$9,391,150						
Portion of Emissions due to Init. Constr. and Maint.	319	3	2	94	1	0.0004
Est. Envir. Cost, \$/ton	26	8712	7526	208	2	4845
Cost, \$	\$8,206	\$27,243	\$12,095	\$19,602	\$3	\$2
Total = \$67,151						
Portion of Emissions due to Roughness	325	1	2	0	16	0.04
Est. Envir. Cost, \$/ton	26	8712	7526	208	2	4845
Cost, \$	\$8,360	\$9,421	\$13,503	\$2	\$40	\$188
Total = \$31,514						

Table 3.5: Emissions by Category and Associated Environmental Cost: Alternative Approach - Urban Area

Emissions Category	CO2, tons	NOx, tons	PM10, tons	SO2, tons	CO, tons	Pb, tons
Initial Construction	204	2	1	49	1	0.0002
Maintenance	191	2	1	83	1	0.0002
Vehicles - 35years	87764	292	588	3	4391	10.5058
Roughness Related	241	1	2	0	12	0.0288
Total Emissions	88400	297	592	136	4405	10.5350
Est. Envir. Cost, \$/ton	26	8712	7526	208	2	4845
Total Environmental Cost, \$	\$2,274,092	\$2,587,036	\$4,454,407	\$28,301	\$10,792	\$51,041
Total = \$9,405,669						
Portion of Emissions due to Init. Constr. and Maint.	395	4	2	133	1	0.0004
Est. Envir. Cost, \$/ton	26	8712	7526	208	2	4845
Cost, \$	\$10,162	\$35,569	\$14,307	\$27,643	\$3	\$2
Total = \$87,686						
Portion of Emissions due to Roughness	240.82	0.80	1.61	0.01	12.05	0.03
Est. Envir. Cost, \$/ton	26	8712	7526	208	2	4845
Cost, \$	\$6,195	\$6,982	\$12,150	\$2	\$30	\$140
Total = \$25,498						

From Table 3.4 and Table 3.5, it can be noticed that emission of air-pollutants and greenhouse gases in urban area are higher in alternative approach than that of basic approach. Carbon dioxide (CO₂) emission is same for the initial construction phase but higher for alternative approach in maintenance phases and roughness related emission. As more major rehabilitation and maintenance activities were applied in alternative approach, shown in Table 2.9, emission is higher in this case. Increases in carbon dioxide and sulfur dioxide emissions in maintenance activities are significant, about 66% and 84%, respectively. But roughness-emission was reduced in the alternative approach as pavement was kept smoother using more rehabilitation. From Table 3.4 and 3.5, it can be seen that both carbon dioxide and carbon monoxide emissions related to pavement roughness were reduced by 25% in the alternative approach. Vehicle emissions for

15,000 AADT was also estimated over the 35-year analysis period and reported in Tables 3.4 and 3.5. Emissions due to construction and maintenance of pavement are very low compared to vehicle emission. Costs of emissions were also reported in Table 3.4 and 3.5. Emission costs in the alternative approach due to maintenance and rehabilitation is 30% higher than that of the basic approach over the 35 year service life of the pavement, but roughness-emission cost is about 20% less than that of basic approach. As a result, it can be seen that pavement smoothness compensates for emissions that are generated as a result of the additional rehabilitation required to maintain the higher level of smoothness.

Tables 3.6 and 3.7 show emission and cost information of a 1-mile rural roadway section, where analysis was performed using 10,000 AADT over a 35 year period.

Table 3.6: Emissions by Category and Associated Environmental Cost: Rural Area

	CO ₂ , tons	NO _x , tons	PM ₁₀ , tons	SO ₂ , tons	CO, tons	Pb, tons
Initial Construction	204	2	1	49	1	0.0002
Maintenance	115	1	1	45	0	0.0002
Vehicles - 35years	58510	196	394	2	2941	7.03
Roughness Related	217	1	1	0	11	0.03
Total Emissions	59045	199	397	96	2953	7.06
Est. Envir. Cost, \$/ton	26	8712	980	26	0	588
Total Environmental Cost, \$	\$1,518,936	\$1,737,320	\$388,811	\$2,476	0	\$4,152
Total = \$3,651,695						
Portion of Emissions due to Init. Constr. and Maint.	319	3.127	1.607	94.126	1.161	0.0004
Est. Envir. Cost, \$/ton	26	8712	980	26	0	588
Cost, \$	\$8,206	\$27,243	\$1,575	\$2,421	0	0
Total = \$39,446						
Portion of Emissions due to Roughness	217	1	1	0	11	0.03
Est. Envir. Cost, \$/ton	26	8712	980	26	0	588
Cost, \$	\$5,573	\$6,281	\$1,172	\$0	0	\$15
Total = \$13,042						

Identical maintenance and rehabilitation activities were applied to urban and rural roads. Therefore, emissions due to initial construction and maintenance are the same in both rural and urban roads for the same type of approach (basic or alternative). However, monetary values of rural and urban emissions are different as shown in Table 3.2. Using this rural emission cost rate, the cost of emissions in both the basic and alternative approaches were estimated as shown in Tables 3.6 and 3.7. It can be seen that emission cost due to construction and maintenance activities over the 35 year service life the of pavement is 29% higher in the alternative approach as compared to that of the basic approach. The reason behind this result is the application of more major rehabilitation in the alternative approach. At the same time, roughness-emission was reduced by 24% in the alternative approach because of smooth pavement, which nearly compensated for the environmental impact of the additional rehabilitation activity required to produce smoother pavement throughout the 35 year analysis period.

Table 3.7: Emissions by Category and Associated Environmental Cost: Alternative Approach - Rural Area

	CO2, tons	NOx, tons	PM10, tons	SO2, tons	CO, tons	Pb, tons
Initial Construction	204	2	1	49	1	0.00
Maintenance	191	2	1	83	1	0.00
Vehicles - 35years	58510	195	392	2	2928	7.00
Roughness Related	160.5	0.5	1.1	0.0	8.0	0.02
Total Emissions	59065	199	395	135	2937	7.0
Est. Envir. Cost, \$/ton	26	8712	980	26	0	588
Total Environmental Cost, \$	\$1,519,449	\$1,736,547	\$387,288	\$3,469	0	\$4,130
Total = \$						\$3,650,883
Portion of Emissions due to Init. Constr. and Maint.	395	4	2	133	1	0.0004
Est. Envir. Cost, \$/ton	26	8712	980	26	0	588
Cost, \$	\$10,162	\$35,569	\$1,863	\$3,415	0	\$ 0
Total = \$						\$51,008
Portion of Emissions due to Roughness	160.549	0.534	1.076	0.006	8.033	0.019
Est. Envir. Cost, \$/ton	26	8712	980	26	0	588
Cost, \$	\$4,130	\$4,655	\$1,055	0	0	\$11
Total = \$						\$9,851

3.7 SENSITIVITY OF EMISSION COST TO ROUGHNESS AND TRAFFIC VOLUME

The effects of roughness and traffic volume on emission cost were also performed using the urban emission cost rate as shown in Figure 3.3. From Figure 3.3, it can be seen that emission costs increase with roughness and traffic volume. Roughness-emission costs for a 1-mile section of with a maximum allowable IRI level (110 inch/mile) of primary road is about \$40,000 for 15,000 AADT over the 35-year service life. But roughness-emission costs can increase to as high as \$105,000 for inadequately smooth 1-mile pavement section of a secondary road with 10,000 AADT over a 35-year service life. Pavement with International Roughness Index (IRI) level 100, 110, and 125 inches/mile are considered as adequate smoothness level for Interstate, primary,

and secondary road pavements. When pavement IRI level is higher than adequate smoothness level, it is considered as rough pavement.

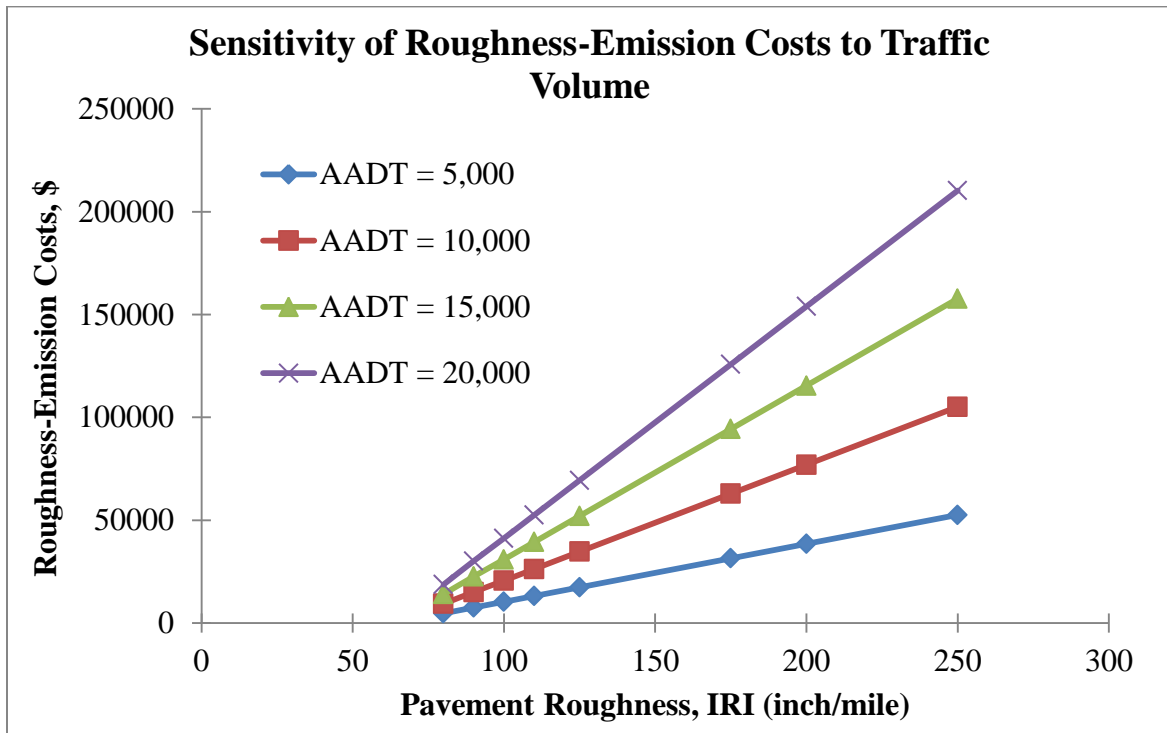


Figure 3.3: Sensitivity of Roughness-Emission Cost to Pavement Roughness and Traffic Volume

3.8 AGENCY INVESTMENT, USERS, AND EMISSIONS COSTS

Agency costs, user costs due to pavement roughness, and emission costs due CRM and roughness have are shown in Figure 3.4. From Figure 3.4, it can be seen that emissions cost due to CRM and roughness is only about 1% and 0.3%, respectively, whereas agency cost and user costs are about 5% and 94%. After splitting the user costs, it can be seen that about 54% of these costs are related to vehicle repair and maintenance. As mentioned earlier, an additional agency investment of \$108,209 over 35 years can reduce user costs from \$9.9 million to \$4.7 million with a benefit/cost ratio of 48. As a result of these additional agency M&R activities, extra emissions with a cost of about \$20,535 are generated, however; the achieved smoothness reduces the roughness emission cost by an amount of \$6,016. Clearly, from a user cost standpoint, it is good policy to maintain roads at a high level of smoothness, as millions of dollars are saved for users over the 35 year analysis period, as compared to the very modest additional environmental

cost required to maintain the pavement in a smooth condition (difference between \$20,535 and \$6,016, or about \$14,500). Although the environmental costs associated with the two M & R strategies considered were relatively small as compared to user costs, it was nevertheless important to conduct a thorough LCA to demonstrate that the results presented in Chapter 2 were still applicable when environmental effects were considered. Whereas it was reported, in Chapter 2, a potential 50-to-1 return on investment as a result of maintaining pavement in a smooth condition, this Chapter, which includes LCA along with LCCA, indicates that a 48-to-1 return on investment can be realized by maintaining smooth pavement.

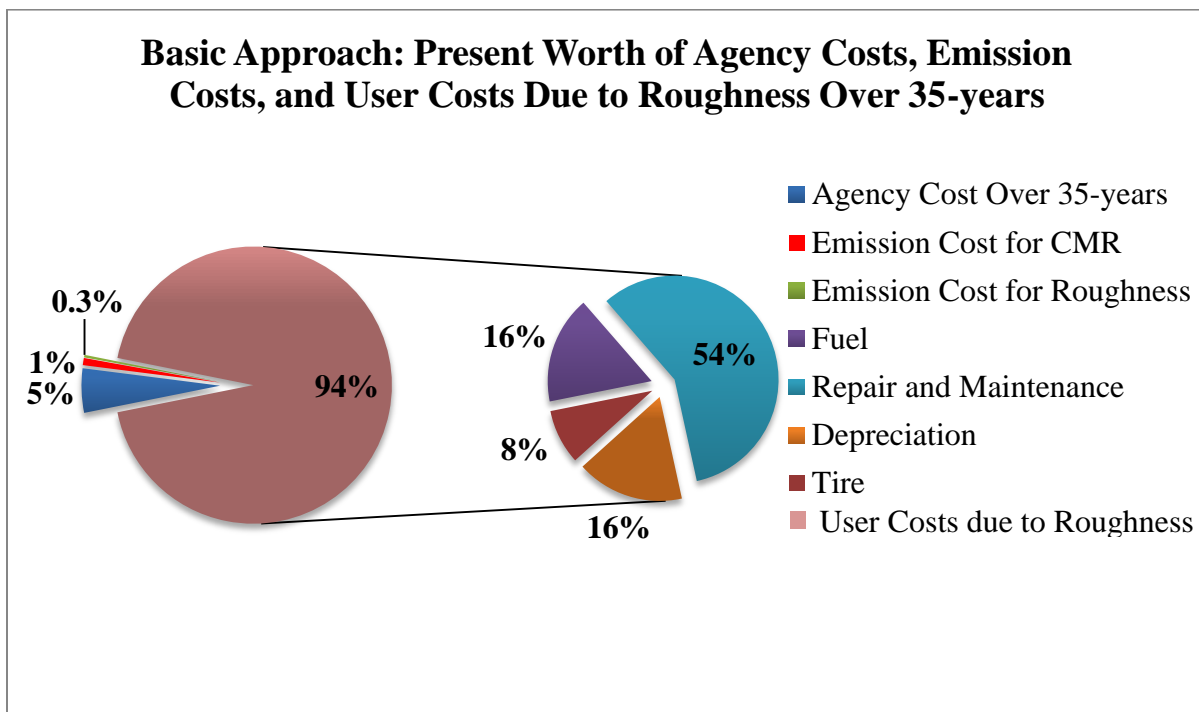


Figure 3.4: Agency Costs, Emission Costs, and User Costs Due to Roughness

3.9 CONCLUSION

It is important to maintain pavement in good condition, otherwise, significant amount of user related costs can be incurred, along with other costs such as emission costs. From this study, the following conclusions can be drawn:

(a) Emissions related to initial construction were same for both basic and alternative approach because of the identical design, construction materials, and process. More frequent major

rehabilitation were adopted in alternative approach which increased emissions amount in maintenance phase but reduced roughness related emission by keeping in smoother state.

(b) Emission costs associated with additional rehabilitation (maintaining a smooth pavement throughout service life) in the alternative approach were very low compared to savings in user costs that are realized as a result of maintaining the pavement in a smooth condition.

(c) In the basic approach (pavement allowed to become rough during service life), user costs due to roughness is about \$9.9 million (94%) whereas costs to the agency, emission costs due to CMR, and emission costs due to roughness were about \$545,491 (5%), \$67,151 (1%), and \$31,514 (0.3%), respectively over the 35 year analysis period.

(d) In the alternative approach, which requires an additional \$108,210 investment in M & R over the 35 year analysis period, user costs associated with roughness is about \$4.7 million (about 52% less than that associated with the basic approach), whereas agency costs, emissions costs due to CMR, and emissions costs due to roughness were calculated as \$653,701, \$87,686, and \$25,498, respectively.

(e) An additional agency investment of \$108,209 over a 35-year design period for one mile/one lane of roadway can provide a 48-to-1 return on investment in terms of reduced user costs, even when environmental costs are considered. In a previous study, a 50-to-1 return on investment was estimated; however, environmental costs associated with additional M & R activities were ignored.

CHAPTER 4

PAVEMENT ROUGHNESS

4.1 PAVEMENT ROUGHNESS

Pavement roughness is a measure of surface irregularities that adversely affect pavement ride quality. Driver satisfaction depends primarily on the ride quality of a pavement. Therefore, to increase driver satisfaction, transportation agencies often provide a monetary incentive to the contractor to exceed the requirements of smoothness specification [52]. According to NCHRP Web Document 42, initially smooth pavements remain smooth over time and provide longer service life [53]. According to Perera et al. (2005), three vehicle responses relate to pavement roughness (IRI), including road meter response, vehicle vertical acceleration, and tire load [54]. The American Association of State Highway Officials (AASHO) study revealed that the serviceability of a pavement from the driver's perspective mainly depends on surface roughness [55].

Basing the definition of pavement roughness as distortions in the pavement surface, it follows that road roughness evaluation requires measurement of the longitudinal profile of the pavement in the vehicle wheel path. For engineering interpretation, the measurements are usually handled with a mathematical model that generates summary statistics for the length of pavement being evaluated. Pavement roughness is expressed by different indices including the International Roughness Index (IRI), Ride Number (RN) and Profile Index (PI).

For newly constructed pavements, most of the States use roughness related specification to provide incentives or disincentives, and the profilograph is used to measure pavement profile. The California profilograph is mainly used to measure profile index (PI) [56]. Profile index is estimated by computing the number of scallops in the profile trace that are not in a blanking band. The widely used blanking band used in the United States is 0-0.2 inch. The Ride Number is a subjective rating based index and closely related to pavement surface ratings from a panel of human subjects. It was developed in the NCHRP project 1-23 conducted by Janoff et al. in the 1980s and published as NCHRP Report 275 [57, 58]. It represents rideability of pavements on a scale 0 to 5.0 where 0 represents an unrideable road and 5.0 characterizes a perfectly rideable

surface. In the United States, the most widely used index is the IRI which was developed in the 1980s in a study supported by the World Bank. Most transportation agencies now collect IRI data for their roadway networks. The Moving Ahead for Progress in the 21st Century (MAP-21) legislation requires transportation agencies report IRI data every year [59]. IRI is computed using a quarter-car simulation to translate pavement profile to a roughness index, as developed by Sayers et al. [60].

4.2 QUARTER-CAR MODEL TO IRI CALCULATION

Figure 4.1 shows the quarter car model, which has five components including the body mass supported by a single tire, the axle mass, a vertical spring representing a tire, a suspension spring and a damper [61].

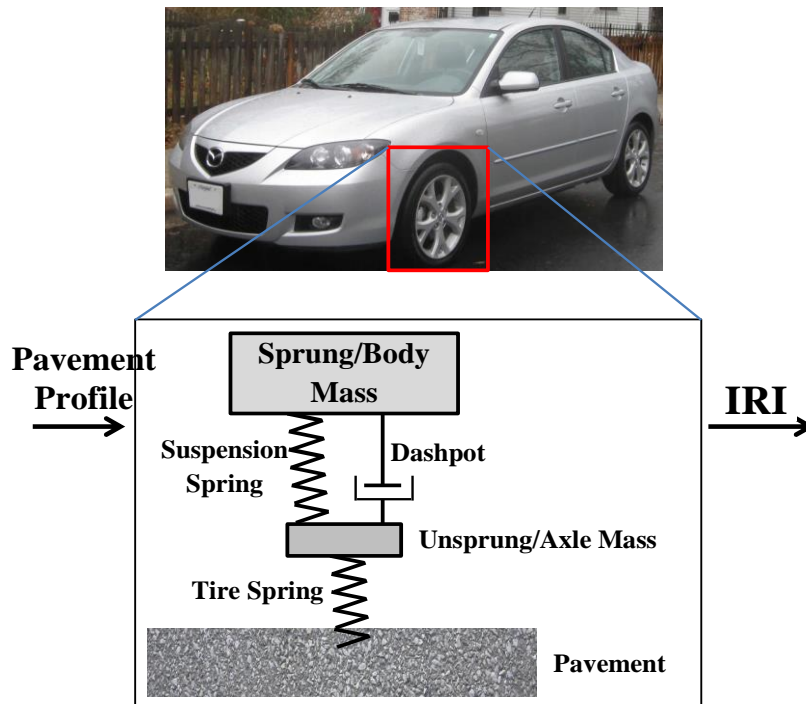


Figure 4.1: Schematic Illustrating International Roughness Index Calculation (After [54])

The suspension deflection is determined by the simulation and normalized by the distance traveled by the vehicle in the simulation to obtain the average suspension motion over the simulated distance.

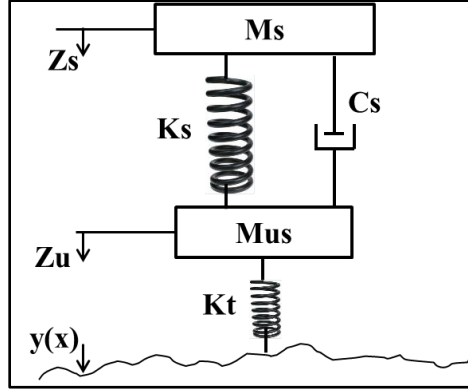


Figure 4.2: Parameters in Quarter-Car Model

By normalizing these equations by sprung mass, M_s :

$$Z_s'' + C(Z_s' - Z_u') + K_2(Z_s - Z_u) = 0$$

$$uZ_u'' + C(Z_u' - Z_s') + K_2(Z_u - Z_s) + K_1(Z_u - y) = 0$$

Where $\frac{C_s}{M_s} = C$, $\frac{K_s}{M_s} = K_2$, $\frac{K_t}{M_s} = K_1$, and $\frac{M_{us}}{M_s} = u$

The IRI is estimated as a sum of accumulation of the quarter-car simulated motion between the sprung and unsprung masses in the model which is averaged over the length L of the pavement profile:

$$IRI = \frac{1}{L} \int_0^{L/V} (Z_s' - Z_u') dt$$

The obtained value is expressed as IRI with a unit of inch/mile or m/km. Generally, a software program is used to determine the IRI from measured pavement profile. A profile obtained from each wheel path is used to determine IRI, and the average value is then reported.

4.3 HALF-CAR MODEL

Unlike quarter-car model, the whole rear axle is considered in half-car model (Figure 4.3). If the spring and damper coefficients and tires stiffness are the same on both sides of the rear axle, there will not be any cross coupling motion. Therefore, when tires stiffness are the same when collecting pavement profile data, there will be either linear or rotational motion.

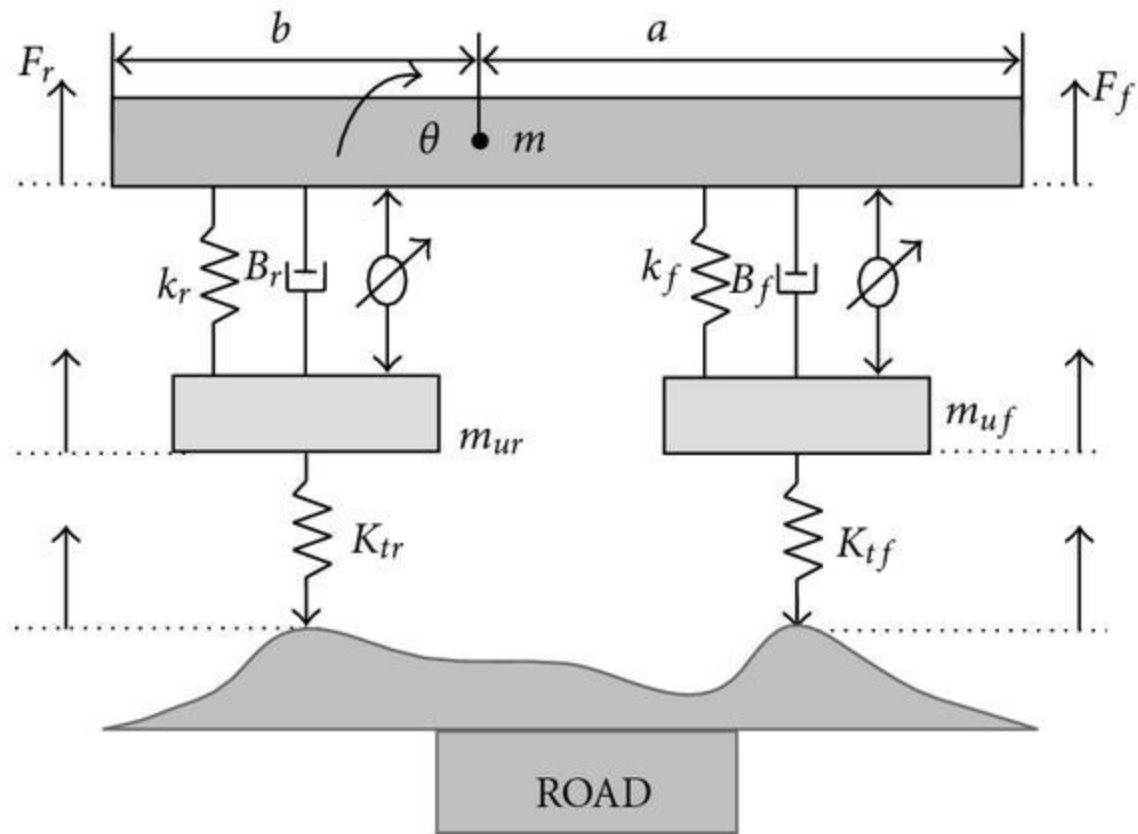


Figure 4.3: Half-Car Model [62]

As a result, the average of left and right wheel profile collected with a quarter-car model tends to negate the need for the more complex half-car model. The half-car model will assess equal or lower roughness index as compared to the quarter-car model, rendering the simpler quarter car analysis as conservative.

4.4 LIMITATIONS OF IRI

As quarter-car model can be used with wide range of equipment, it is beneficial to use quarter-car model instead of half-car model. However, there are limitations of quarter-car model which have been listed below [61]:

- IRI does not provide any idea of the type of pavement distresses that creating pavement roughness

- Multiple pavement sections can have same IRI value although pavement distresses are not the same
- Data collected at low speed can generate false peaks in the computed inertial profile; therefore, they lead to false spikes in the IRI parameter
- Accelerometer sensitivity affects pavement roughness
- Due to the nature of Butterworth and moving average filters and their implementation on equipment, the resulting IRI numbers are generally comparable; however, the resulting profiles produced are not quite as comparable even if the same filter and parameters are applied

Pavement ride quality can be classified based on IRI. According to the U.S. Department of Transportation (1999), pavement ride can be categorized into five groups [63], as shown in Table 4.1.

Table 4.1: Pavement Ride Quality Based on Roughness [63]

Category	IRI Rating (inch/mile)		Interstate and NHS Ride Quality
	Interstate	Non-Interstate	
Very Good	< 60	< 60	Acceptable 0 - 170
Good	60 - 94	90 - 94	
Fair	95 - 119	95 - 170	
Poor	120 - 170	171 - 220	Less than acceptable > 170
Very Poor	> 170	> 220	

4.5 EXISTING ROUGHNESS MEASUREMENT SYSTEMS

Although pavement profile measurements were of major interest to researchers decades ago, most agencies now conduct pavement roughness measurement on a routine basis [64]. While many devices and methods are available to evaluate pavement ride quality, most are not currently utilized because of low accuracy and/or measurement inefficiencies. A historical review of pavement roughness measurement technology and devices are summarized below.

- Pavement profile measuring technology started with rod and level surveys and straightedge measurements in the early 1900s [65]

- A response-type road roughness measurement system (RTRRMSI) such as the BPR Roughometer, was developed in the 1940s. This device involved a single-axle trailer with a single tire towed by a vehicle [66].
- Profilograph technology such as California profilograph and Rainhart profilograph emerged in 1960s, and has been available for many years and exists in a variety of different forms, configurations, and brands [66].
- Road meters, such as the Mays Ride Meter, are also RTRRMS systems that were developed in 1960s [65].
- The first high-speed inertial profiler was developed by Elson Spangler and William Kelley at the General Motors Research Corporation [67]. The Automatic Road Analyzer (ARAN), Dynatest, SSI, Ames Engineering, and International Cybernetics Corporation (ICC) inertial profilers are now widely used.

The devices that are typically used in the US can be divided into four categories:

- Calibration and construction control systems
- Response-type systems
- Manual devices
- Non-contact profile measurement systems

4.5.1 Manual Devices

There are several manual devices available to measure pavement roughness including the rolling straightedge, rod and level, face dipstick, and ARRAB walking profilometer. These devices, such as the rod and level, dipstick, and walking profilometer are generally used to measure the accuracy of an inertial profiler. Basically, pavement profile data is collected from test sections having a range of pavement distresses, and results are compared with the inertial profiler to check whether the inertial profiler is measuring the correct roughness.

The Rolling Straightedge was one of first methods developed to measure pavement smoothness. A rolling straightedge consists of a rigid beam having a fixed wheel on each end and a third wheel capable of vertical movement located at the middle of the straightedge. An indicator is attached to the middle wheel which records the deviation of the pavement at the center wheel relative to the plane of the rolling straightedge. However, it has been found that rolling straightedge is not able to capture and reflect longer features that can attribute significant roughness. Moreover, its slow operating speed and manual operation make it incompatible for testing under traffic and safety issues are also concerned. With these operating problems, straightedges are quickly becoming out-of-dated and impractical for general use due to inefficiency and inaccuracy [67].



Figure 4.4: A Rolling Straightedge [66]

Most accurate pavement profile can be measured by the rod and level as described in ASTM E 1364 [68]. While collecting data using rod and level, it is very important to meet the level resolution specified by the ASTM standard [53].

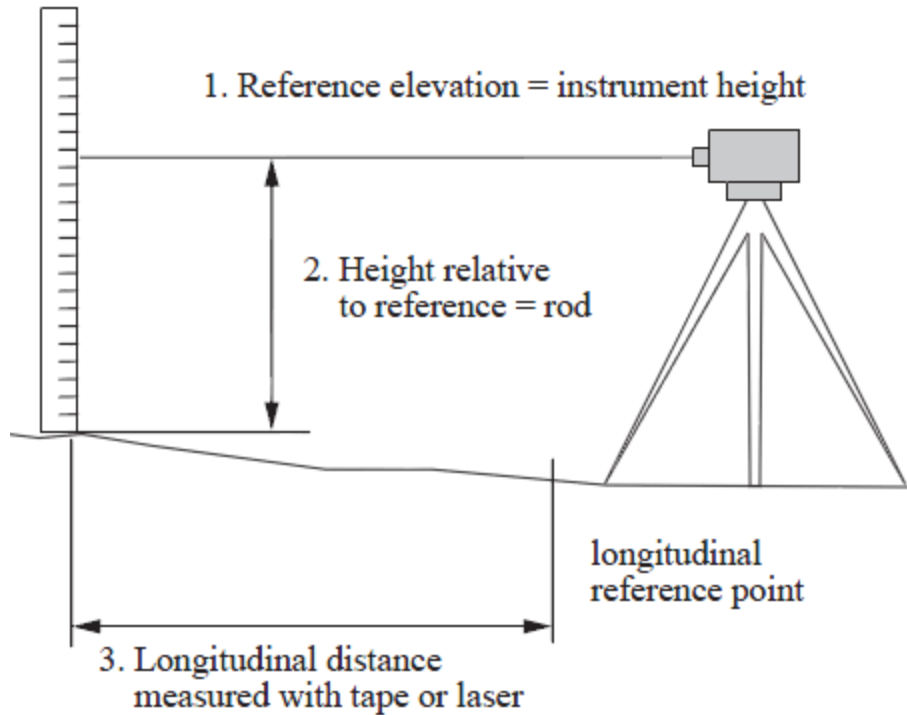


Figure 4.5: Rod and Level to Measure Pavement Profile [69]

Although the Dipstick originally was developed for evaluating the evenness of building slabs, it has emerged as one of the simplest device to measure pavement profile and can collect data at higher rates than rod and level [70]. With the dipstick, a sensor is mounted to make its axis and line passing through footpad contact points to be in the same plane, and an accelerometer measures the slope of the frame. Knowing the frame and distance between the feet allows determination of the change in elevation between the feet.

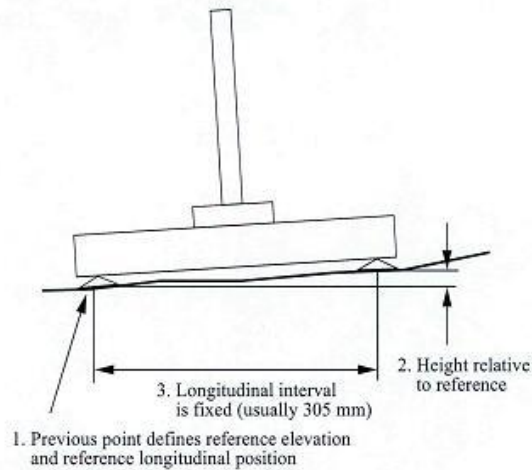


Figure 4.6: A Schematic Illustration of Dipstick [71]

4.5.2 Calibration and Construction Control Devices

Calibration and construction control devices are generally used to check the profile of the new constructed layer which includes California profilographs, dipsticks, Ames profilographs, and Rainhart profilograph. Profilographs are generally used for construction inspection, quality control, and acceptance of smoothness of concrete pavement. The California profilograph was widely used for over fifty years. There is a rigid beam or frame in profilographs which is supported by wheels at both ends and center. The midpoint wheel moves vertically and a strip chart recorder for capturing the movement of recording wheel. Pavement roughness measured by the profilographs is expressed as Profile Index (PI) in inch/mile. However, the California profilograph can only evaluate 1.9 to 3.1 miles of pavement per hour. It has been reported that profilographs tend to amplify or attenuate true pavement profile [54].

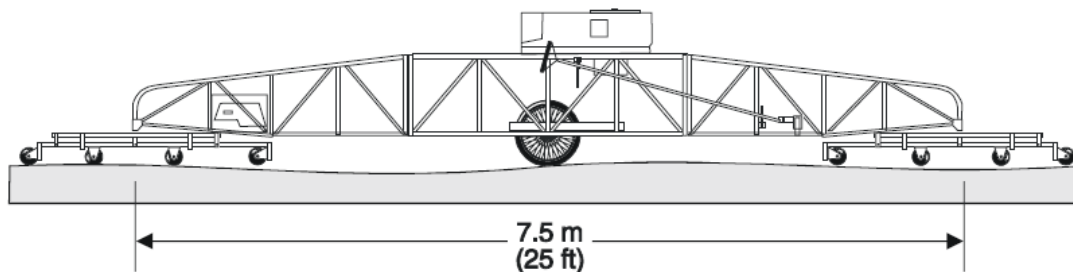


Figure 4.7: California Profilograph [65]

4.5.3 Response-Type Roughness Measurement Systems

The devices measure the response of the vehicle to the roughness of the pavement. Response-type systems include Bureau of Public Roads (BPR) roughometer and Maysmeter. The Bureau of Public Roads (BPR) roughometer was the first high-speed system to measure pavement roughness [53]. Figure 7 shows a sketch of the BPR Roughometer. The main component of the BPR roughometer is a wheel which simulates quarter of a vehicle. The wheel moves vertically with respect trailer frame which is accumulated. In BPR roughometer, pavement roughness is expressed as inch/mile, and data can be collected at a speed of 20 mph.

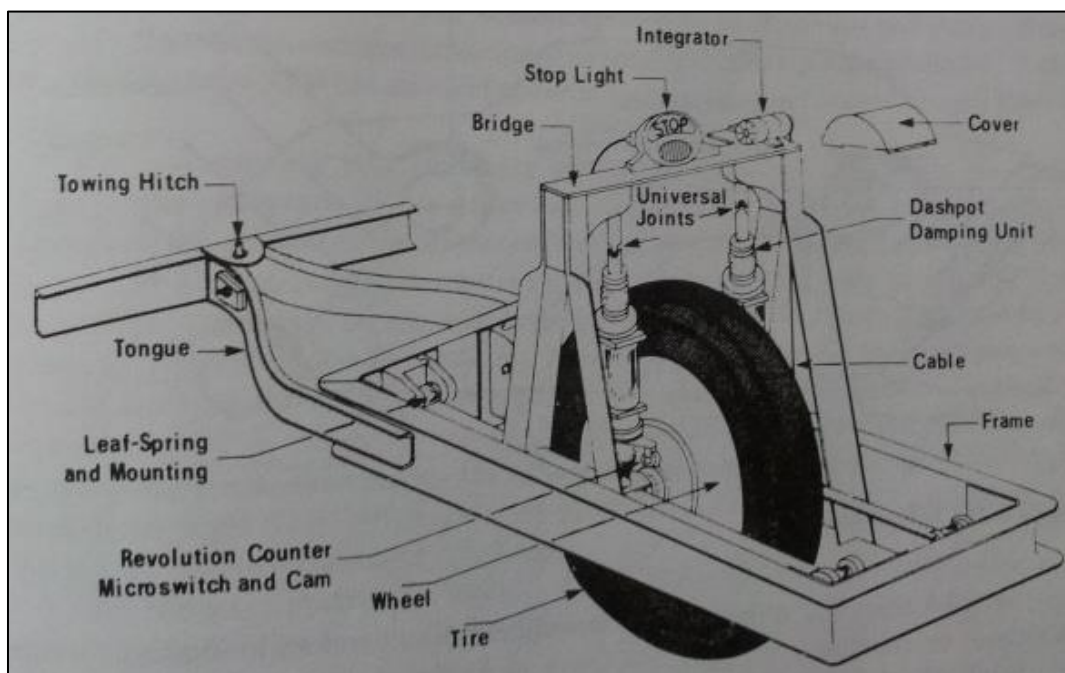


Figure 4.8: Bureau of Public Roads (BPR) Roughometer [72]

4.5.4 Non-Contact Profile Measuring Devices

Noncontact profile-measuring systems include K.J. Law Roughness Surveyors, Laser Road Surface Testers, South Dakota Profilometers, Automatic Road Analyzers (ARAN), and Surface Dynamic Profilometers. ARRAB (Australian Road Research Board), ICC SurPRO (International Cybernetics Corporation), and SSI (Surface Systems and Instruments) are the most widely used reference profilers. With these shortcomings, efficient, automated, and highly repeatable inertial

profilometers were developed. According to Woodstrom [64], modern inertial profilometers require four basic sub-systems:

- Accelerometers to determine the height of the vehicle relative to an inertial frame of reference
- Height sensors to measure the instantaneous riding height of the vehicle relative to a location on the road below the sensor
- Distance or a speed sensor to determine of the position of the vehicle along the length of the road (nowadays combined with GPS)
- Computer hardware and software for computation of the road profile



Figure 4.9: Automated Pavement Profiler and Equipment on a Typical Data Collection Van

Pavement roughness measured by inertial profilers is expressed by IRI. IRI is used to measure roughness in 47 states within the US; however, at least 10 different approaches have been used to collect IRI [65]. Not only do variations exist among the tools used to collect pavement profile, but different analysis methods are also used (choice of wheel path data, averaging techniques).

Besides shortcomings and expenses associated with current pavement roughness measurement systems, this study was also motivated by other potential benefits of having a smart-phone based roughness measurement system, such as crowd sourcing for real-time pavement condition

assessment (pothole or other pavement defect detection) and the ability to inform users about route choice in terms of user costs and sustainability (fuel use/emissions/carbon footprint).

4.6 APPLICATION OF SMARTPHONE TO MEASURE PAVEMENT ROUGHNESS

With the advancement of cellphone technology, now smartphones are not only used for making calls or sending emails but also utilized device such as navigation, emergency response, etc. It has been realized that accelerometer sensor of smartphones can be utilized to measure pavement roughness.

4.6.1 Development of Roughness Capture Application

Pavement surface irregularities lead (non-planar road profile) leads to vertical accelerations in moving vehicles. The magnitude of vertical acceleration depends on the severity and frequency of pavement distresses and other surface irregularities, vehicle suspension characteristics, and vehicle speed. A 3-axis accelerometer enabled cellphone can be used to collect vehicle vertical acceleration data, as demonstrated in previous studies, such as those conducted at the Massachusetts Institute of Technology [73] to identify localized pavement defects. An android-based cellphone application has been developed in the present study that can capture acceleration for the purpose of characterizing pavement roughness and individual pavement distresses. Figure 4.9 shows vehicle vertical acceleration data collected using Roughness Capture, an android-based smartphone application developed by Applied Research Associates in Champaign, Illinois and validated by researchers at the University of Illinois under a project sponsored by the NexTrans University Transportation Center.



Figure 4.10: Illustration of Smartphone Based Roughness Capture System

Modern smartphones are equipped with a number of sensors including multi-axis accelerometers, temperature probes, gyroscopes, light intensity sensors, magnetic field sensors, etc. [74]. The Roughness Capture application collects acceleration in three orthogonal directions, a timestamp, and GPS coordinates and stores them in an ASCII text file. Data collection rate is specified by the user, generally in the range of 10 – 140 samples per second, but higher sampling rates are possible depending upon smartphone hardware. In general, the higher the data collection rate, the better the accuracy of the estimated pavement profile (with diminishing returns at very high sampling rates).

CHAPTER 5

ACCELERATION DATA ANALYSIS METHOD

5.1 INTRODUCTION

In this chapter, a vehicle dynamic model, an analysis of vehicle vertical acceleration to obtain pavement profile, and a numerical method to determine pavement roughness from conventional (inertial profiler) and smartphone-based data collection approaches are presented. The effects of smartphone type and vehicle type on pavement roughness measurement are also presented.

5.2 VEHICLE DYNAMIC MODEL

Profile-based pavement roughness measurement systems rely on an idealized mechanical simulation of a standard vehicle (or a portion thereof). Mathematical models describing vehicle response have been used since the 1940s [60]. The most popular indices derived from these mechanical simulations come from quarter-car and half-car models [60]. These models provide a quantitative measure of how pavement roughness affects the vehicle movement and IRI, which can in turn be used to produce measures and classifications of road condition, estimated rider comfort and to assess road safety.

5.2.1 Quarter-Car Model

A schematic of a quarter-car model is shown in Figure 5.1, where M_s represents one-fourth of the sprung vehicle mass (mass carried by the suspension, or ‘above’ axles) and Z_s is its displacement; K_s and C_s are the suspension spring and damper coefficients, respectively; M_{us} is the unsprung mass, which includes the mass of the wheels, brakes, axles, and so forth; and Z_t is its displacement. Finally, K_t represents the stiffness of the tire as represented by a spring element.

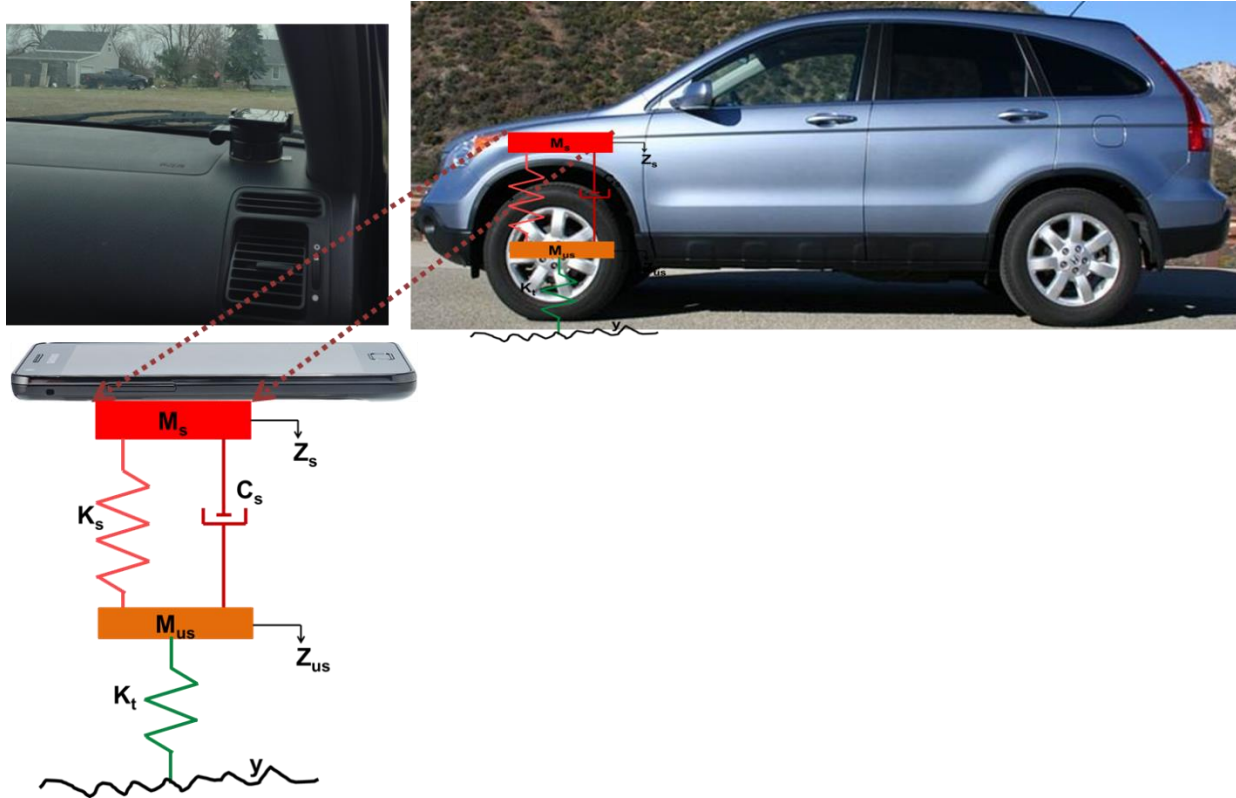


Figure 5.1: Schematic of Quarter-Car Model [after 60]

The differential equations of quarter-car model are given below [60]:

$$M_s Z_s'' + C_s(Z_s' - Z_{us}') + K_s(Z_s - Z_{us}) = 0 \quad (5.1)$$

$$M_{us} Z_{us}'' + C_s(Z_{us}' - Z_s') + K_s(Z_{us} - Z_s) + K_t(Z_{us} - y) = 0 \quad (5.2)$$

5.2.2 Model State-Space Representation

To estimate pavement roughness using the quarter-car model, pavement profile (y) is required. From a smartphone application, it is possible to collect vehicle vertical acceleration data based on the vehicle response to pavement. Moreover, acceleration data is collected by fixing the smartphone on the dashboard of the vehicle using a consumer-grade cell phone dashboard mount (Figure 5.1). A quarter-car model can be represented and solved by the state-space model. Equations 5.1 and 5.2 have been used to develop this system where no input (y) is available [75]. Therefore, we seek to estimate pavement profile using the state-space model. The state-space

model of a continuous-time system can be expressed by a system of n linear differential equations. These equations can be expressed in matrix form by the following equations.

$$\frac{d}{dt}x(t) = \dot{x}(t) = Ax(t) + Bw(t) \quad (5.3)$$

$$y(t) = Cx(t) + Dw(t) \quad (5.4)$$

Where;

x = state vector

A = state matrix

B = input matrix

C = output matrix

D = direct transition matrix

w = input

y = output

Here, y is considered as output and w is considered as input. An n^{th} -order dynamic system can be represented by n^{th} -order differential equation in a state-space representation (Eqn. 5.5) [75].

$$\frac{d^n y}{dt^n} + a_1 \frac{d^{n-1} y}{dt^{n-1}} + \dots + a_{n-1} \frac{dy}{dt} + a_n y = w \quad (5.5)$$

Differential Equation 5.5 can be reduced to a system of first order differential equation by considering,

$$x_1 = y$$

$$x_2 = \frac{dy}{dt}$$

$$x_3 = \frac{d^2 y}{dt^2}$$

$$x_n = \frac{d^{n-1} y}{dt^{n-1}}$$

which, after taking derivatives leads to

$$\frac{d}{dt}(x_1) = \dot{x}_1 = \frac{dy}{dt} = x_2$$

$$\frac{d}{dt}(x_2) = \dot{x}_2 = \frac{d^2 y}{dt^2} = x_3$$

$$\frac{d}{dt}(x_n) = \dot{x}_n = \frac{d^n y}{dt^n}$$

Now, substituting these in Equation 5.5, we get,

$$\dot{x}_n + a_1 x_n + \dots + a_{n-1} x_2 + a_n x_1 = w$$

$$\dot{x}_n = -a_1 x_n - \dots - a_{n-1} x_2 - a_n x_1 + w$$

The state-space form is given by:

$$\begin{bmatrix} \dot{x}_1 \\ \dot{x}_2 \\ \vdots \\ \dot{x}_{n-1} \\ \dot{x}_n \end{bmatrix} = \begin{bmatrix} 0 & 1 & 0 & \dots & 0 \\ 0 & 0 & 1 & \dots & 0 \\ \vdots & \vdots & \vdots & \ddots & \vdots \\ 0 & 0 & \vdots & \vdots & 0 \\ -a_n & -a_{n-1} & -a_{n-2} & \dots & -a_1 \end{bmatrix} \begin{bmatrix} x_1 \\ x_2 \\ \vdots \\ x_{n-1} \\ x_n \end{bmatrix} + \begin{bmatrix} 0 \\ 0 \\ \vdots \\ 0 \\ 1 \end{bmatrix} w \quad (5.6)$$

Equation 5.6 can be written as,

$$\dot{x} = Ax + Bw \quad (5.7)$$

$$\text{Where } A = \begin{bmatrix} 0 & 1 & 0 & 0 & 0 \\ 0 & 0 & 1 & 0 & 0 \\ & & & & 0 \\ 0 & 0 & & 0 & 1 \\ -a_n & -a_{n-1} & -a_{n-2} & & -a_1 \end{bmatrix} \text{ and } B = \begin{bmatrix} 0 \\ 0 \\ 0 \\ 0 \\ 1 \end{bmatrix}$$

The output equation can be written as:

$$y = [1 \quad 0 \quad 0] \begin{bmatrix} x_1 \\ x_2 \\ \\ x_{n-1} \\ x_n \end{bmatrix} \quad (5.8)$$

Where $C = [1 \quad 0 \quad 0]$ and $D = 0$.

5.2.2.1 State Space Model Utilization in Road Profile Estimation

The state-space model can be used to estimate pavement profile from collected acceleration data.

The differential equations from the quarter-car model can be re-written as:

$$M_s Z_s'' + C_s(Z_s' - Z_u') + K_s(Z_s - Z_u) = 0$$

After rearranging this equation for Z_s'' , it can be written as,

$$Z_s'' = -\frac{K_s}{M_s} Z_s - \frac{C_s}{M_s} Z_s' + \frac{K_s}{M_s} Z_u + \frac{C_s}{M_s} Z_u' \quad (5.9)$$

$$M_{us} Z_u'' + C_s(Z_u' - Z_s') + K_s(Z_u - Z_s) + K_t(Z_u - y) = 0$$

After rearranging this equation for Z_u'' , it can be written as,

$$Z_u'' = \frac{K_s}{M_{us}} Z_s + \frac{C_s}{M_{us}} Z_s' - \frac{K_s + K_t}{M_{us}} Z_u - \frac{C_s}{M_{us}} Z_u' + \frac{K_t}{M_{us}} y \quad (5.10)$$

Considering,

$$X_1 = Z_s; \quad X_1' = Z_s' = X_2; \quad Z_s'' = X_2'$$

$$X_3 = Z_u; \quad X_3' = Z_u' = X_4; \quad Z_u'' = X_4'$$

Equations 5.9 and 5.10 can be rewritten by the following equation in state space matrix form:

$$\begin{bmatrix} X_1' \\ X_2' \\ X_3' \\ X_4' \end{bmatrix} = \begin{bmatrix} 0 & 1 & 0 & 0 \\ -\frac{K_s}{M_s} & -\frac{C_s}{M_s} & \frac{K_s}{C_s} & \frac{C_s}{M_s} \\ 0 & 0 & 0 & 1 \\ \frac{K_s}{M_{us}} & \frac{C_s}{M_{us}} & -\frac{(K_s + K_t)}{M_{us}} & -\frac{C_s}{M_{us}} \end{bmatrix} \begin{bmatrix} X_1 \\ X_2 \\ X_3 \\ X_4 \end{bmatrix} + \begin{bmatrix} 0 \\ 0 \\ 0 \\ \frac{K_t}{M_{us}} \end{bmatrix} y$$

This equation can be written in form of general state-space model,

$$X' = AX + By \quad (5.11)$$

From Eqn. 5.11, matrices A and B can be written as

$$A = \begin{bmatrix} 0 & 1 & 0 & 0 \\ -\frac{K_s}{M_s} & -\frac{C_s}{M_s} & \frac{K_s}{C_s} & \frac{C_s}{M_s} \\ 0 & 0 & 0 & 1 \\ \frac{K_s}{M_{us}} & \frac{C_s}{M_{us}} & -\frac{(K_s + K_t)}{M_{us}} & -\frac{C_s}{M_{us}} \end{bmatrix} \quad B = \begin{bmatrix} 0 \\ 0 \\ 0 \\ \frac{K_t}{M_{us}} \end{bmatrix}$$

Acceleration at sprung mass level (Z_s'') can be obtained as:

$$Z_s'' = CX + Dy \quad (5.12)$$

where $C = \begin{bmatrix} -\frac{K_s}{M_s} & -\frac{C_s}{M_s} & \frac{K_s}{M_s} & \frac{C_s}{M_s} \end{bmatrix}$ and $D = \begin{bmatrix} \frac{K_t}{M_{us}} \end{bmatrix}$

In Eqn. 5.13, output (Z_s'') is a known quantity, e.g., the smartphone app collects it, while road profile (y) is unknown. Therefore, an inverse solution scheme is needed. According to Fairman (1998), Eqn. 5.13 can be rearranged as [76]:

$$y = \frac{Z_s''}{D} - \frac{CX}{D} \quad (5.13)$$

substituting y in Equation 5.12 gives,

$$X' = \left(A - \frac{BC}{D} \right) X + \frac{B}{D} y \quad (5.14)$$

As a result, new state matrices in the state space system can be written as:

$$A_1 = A - \frac{BC}{D}$$

$$B_1 = \frac{B}{D}$$

$$C_1 = \frac{1}{D}$$

$$D_1 = \frac{C}{D}$$

This model has been developed in MATLAB. Vehicle mass and suspension parameters are collected from vehicle specifications and other published articles [77, 78, 79, 80]. Table 5.1 shows vehicle suspension parameters of four different cars.

Table 5.1: Vehicle Mass and Suspension Parameters

Properties	Ford Fiesta [77]	1997 Honda Accord [78]	Gillespie (1992) [79]	Golden Car [80]
Sprung Mass (M_s), kg	216.75	414	240	250
Unsprung Mass (M_{us}), kg	28.85	40	36	37.5
Suspension Spring Constant (K_s), N/m	21,700	90,000	980	15,825
Suspension Dashpot Coefficient (C_s), N.s/m	1,200	9,000	16,000	1,500
Tire Stiffness (K_t), N/m	184,000	400,000	160,000	163,250

5.3 ESTIMATION OF PAVEMENT PROFILE

Two approaches have been explored in this study to estimate pavement profile from acceleration data. These approaches involve integration of acceleration data and inverse state space model application, as explained in the following sections.

5.3.1 Acceleration Data Filtering

Smartphones have accelerometers made of very small piezoelectric sensors, which can measure acceleration along x, y, and z axes. The LIS311DLH accelerometer chip is currently the most commonly used in smartphones [81]. Accelerometers embedded into smartphones are very small with a typical size of around 0.12x0.12x0.04 inch (3x3x1 mm) [81], and require very little power. Despite their small size, low cost, and low power consumption, they are able to measure acceleration data to up to six decimal points, generally in unit of m/sec^2 [81], and can collect hundreds of data points per second.



Figure 5.2: A Typical Accelerometer Used in Smartphone [82]

Once data is captured, there are two reasons to filter acceleration data: (a) to remove noise existing in the data, and (b) to meet roughness estimation requirement as roughness is sensitive by the wavelength of pavement surface disturbance ranging from 4 to 100 feet (1.23 to 30.48 m).

Acceleration data collected with the smartphone application contains noise. This noise can be produced due to the electronic circuit which converts motion into voltage signal. Mechanical noise can be introduced from the accelerometer sensor itself [83]. Therefore, it is necessary to remove noise from acceleration data before further analysis.

The gain of the IRI transfer function for the profile is shown in Figure 5.3 [84]. The gain is a dimensionless quantity that represents the weighting applied by the IRI to the pavement profile. It can be noticed that IRI is not equally responsive to the all wavelengths of pavement profile. It can be seen that roughness is mostly influenced by the wavelength ranging from 4 to 100 feet (1.23 to 30.48 m), whereas maximum sensitivity resides in the range of 8 to 51 feet (2.46 to 15.54 m) because of the high gain for profile slope (Figure 5.3).

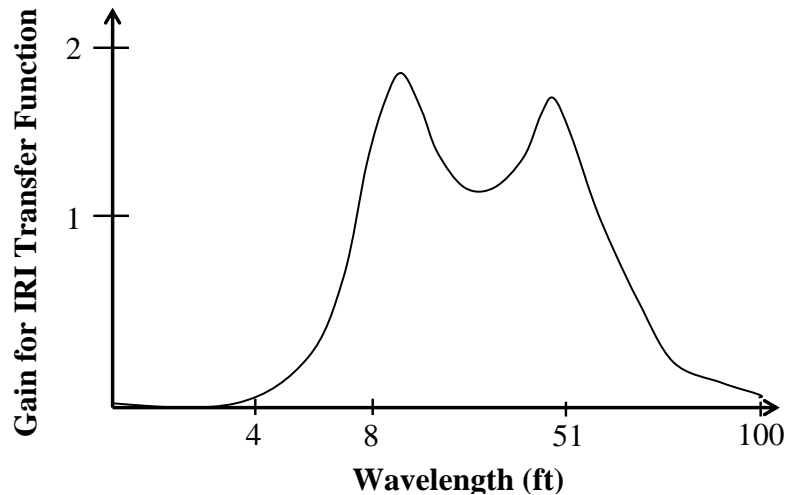


Figure 5.3: Wavelength for Pavement Roughness Sensitivity [after 84]

Both low-pass and high-pass filters have been utilized to remove wavelengths greater than 100 feet (30.48 m) and less than 4 feet (1.22 m), respectively from the acceleration data. A low-pass filter retains the portion of the spectrum of the signal having wavelengths lower than the cutoff wavelength, while attenuating the portion of the spectrum with wavelengths lower than the cutoff value. Figure 5.4 shows an ideal low-pass filter in terms of filtered magnitude response.

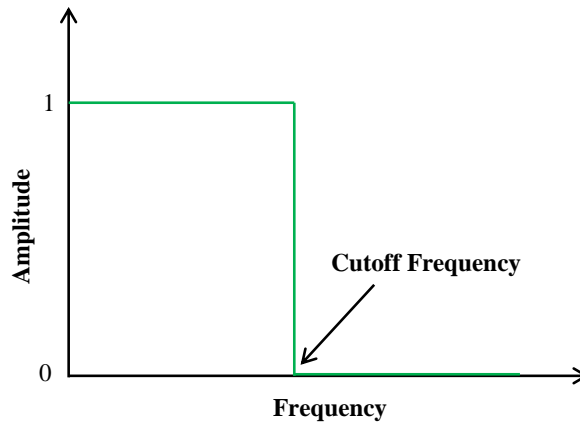


Figure 5.4: An Ideal Low-Pass Filter with Cutoff Frequency

A high-pass filter retains the portion of the spectrum of the signal above the cutoff frequency and attenuates the portion having frequencies lower than the cutoff frequency. Figure 5.5 shows an ideal high-pass filter in terms of magnitude response.

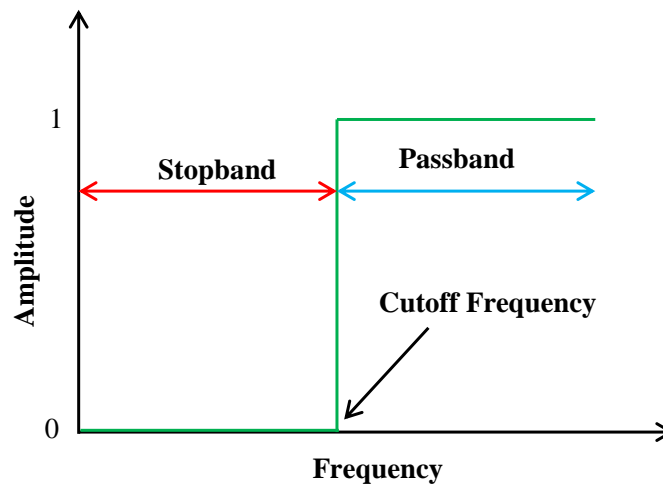


Figure 5.5: Magnitude Response of an Ideal High-Pass Filter

5.3.2 Integration of Acceleration Data

Acceleration data was processed by an in-house MATLAB code to obtain pavement profile data (double integration of acceleration data), and then the estimated pavement profile was analyzed using in-house developed MATLAB script (Section 5.4.1) to estimate roughness in terms of IRI. This process of data analysis is shown in Figure 5.6.

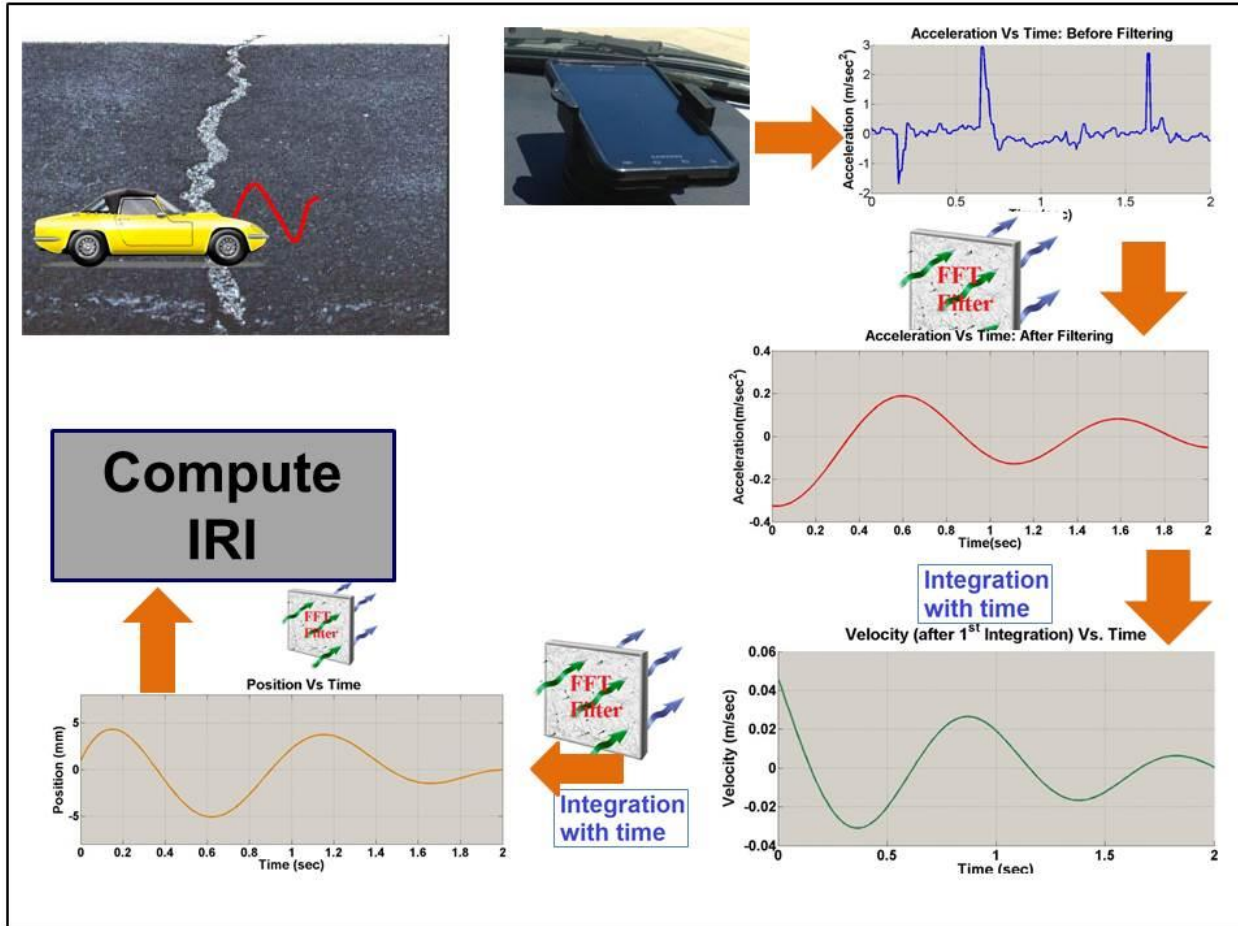


Figure 5.6: Acceleration Data Analysis by Integration and Roughness Estimation

The following steps are completed during the double integration procedure:

- (a) Filter acceleration data using a high-pass filter to remove acceleration drift
- (b) Integrate acceleration data to obtain velocity
- (c) Apply high-pass filter to velocity to eliminate the necessity for an initial condition (initial velocity)
- (d) Perform integration on filtered velocity to obtain displacement
- (e) Apply high-pass filter to displacement to eliminate the necessity for an initial condition (initial displacement)

An illustrative example is now provided. Consider a wave as expressed by Eqn. 5.16. If a small acceleration drift (0.008 ft/sec^2 or 0.0024 m/sec^2) is added to the Eqn. 5.16; Eqn. 5.17 can be obtained as:

$$A = 0.1 \sin(2\pi \times 0.5t) + 0.1 \sin(2\pi \times 10t) \quad (5.15)$$

$$A = 0.1 \sin(2\pi \times 0.5t) + 0.1 \sin(2\pi \times 10t) + 0.008 \quad (5.16)$$

There are quite a few methods to integrate acceleration data, including the rectangular method, the trapezoidal rule, and Simpson's rule. In this study, the trapezoidal rule has been used to integrate acceleration data to obtain velocity and displacement. The integration process using the trapezoidal rule is shown in Figure 5.7.

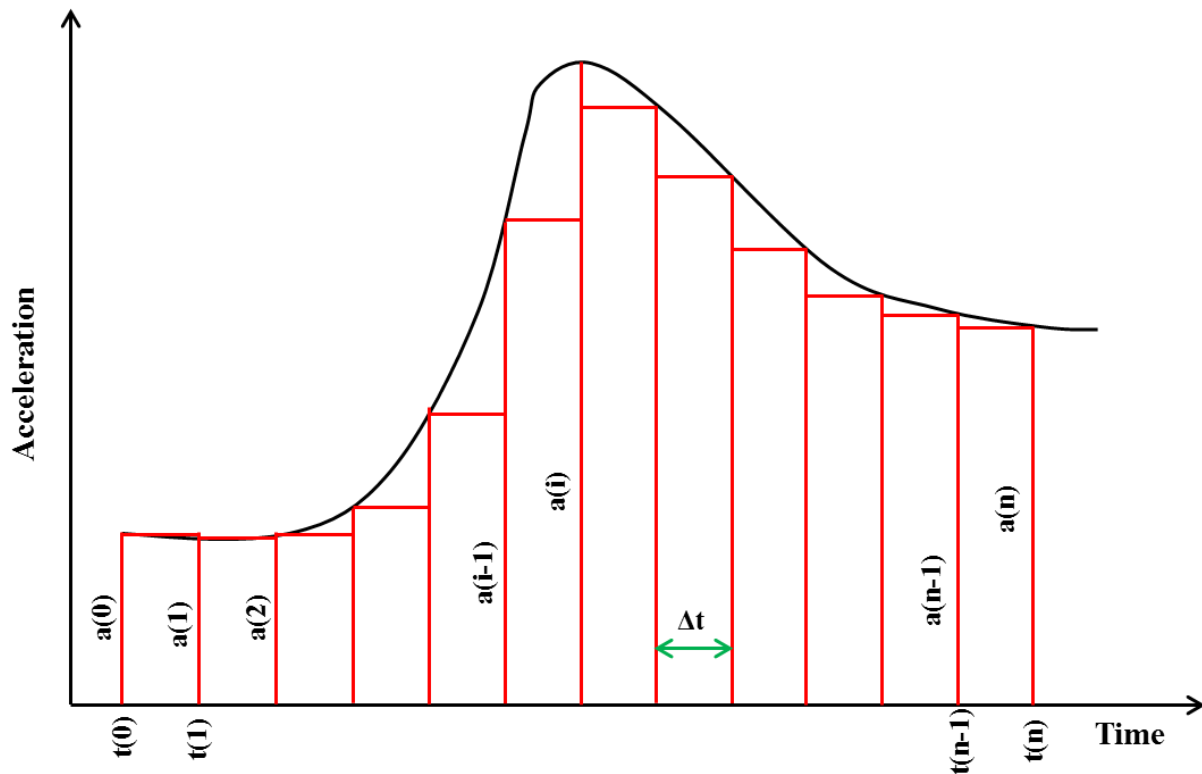


Figure 5.7: Integration by Trapezoidal Rule

The integration is performed using the trapezoidal rule, i.e., equation (5.18).

$$\int_{t(0)}^{t(n)} a(t) dt = \sum_{i=1}^n \left(\frac{a(i-1) + a(i)}{2} \right) \Delta t \quad (5.17)$$

After double integrating Eqn. 5.16 and Eqn. 5.17 with and without filtering, Figures 5.8, 5.9, 5.10 are obtained.

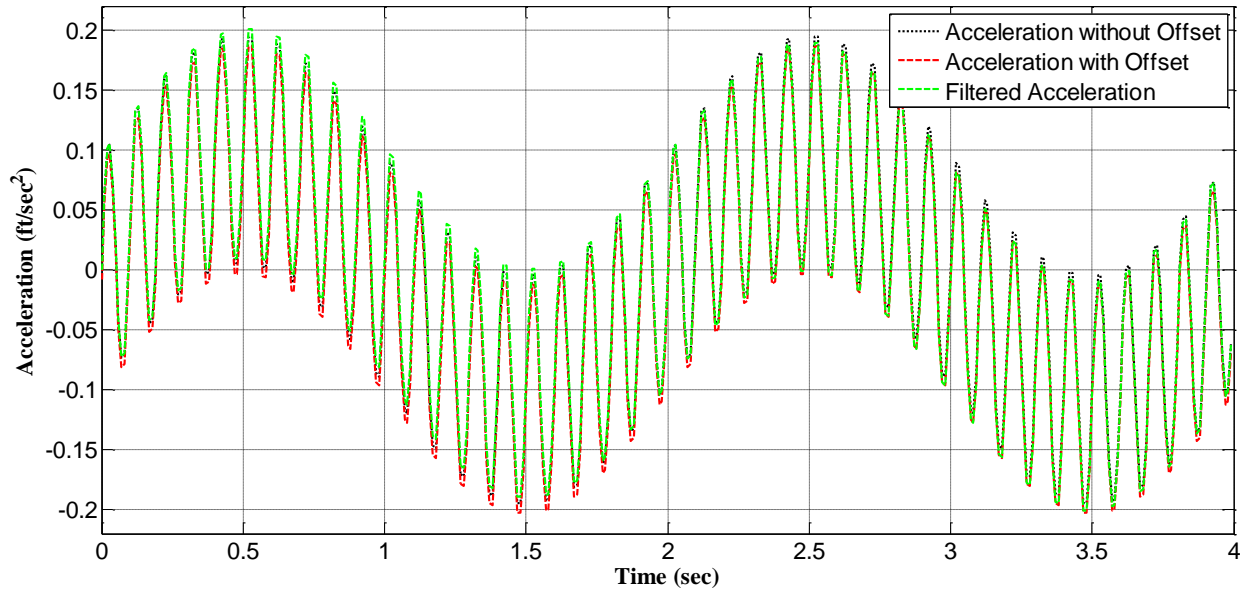


Figure 5.8: Acceleration Data, Acceleration Data with Offset, and Filtered Acceleration Data

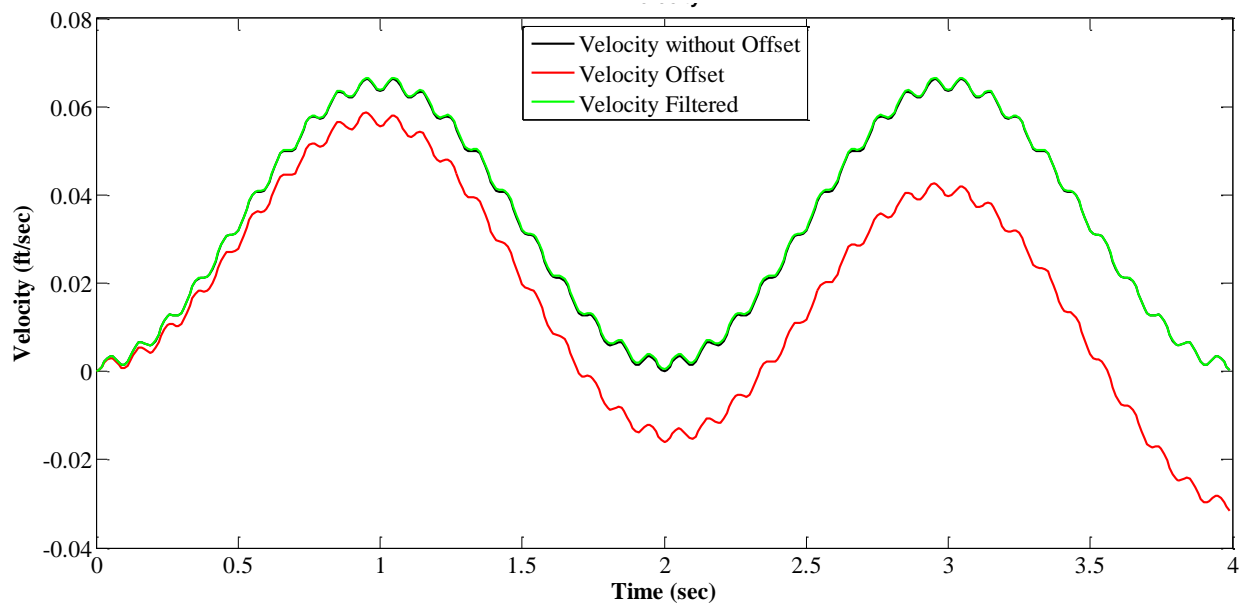


Figure 5.9: Estimated Velocity, Velocity with Offset, and Filtered Velocity Data

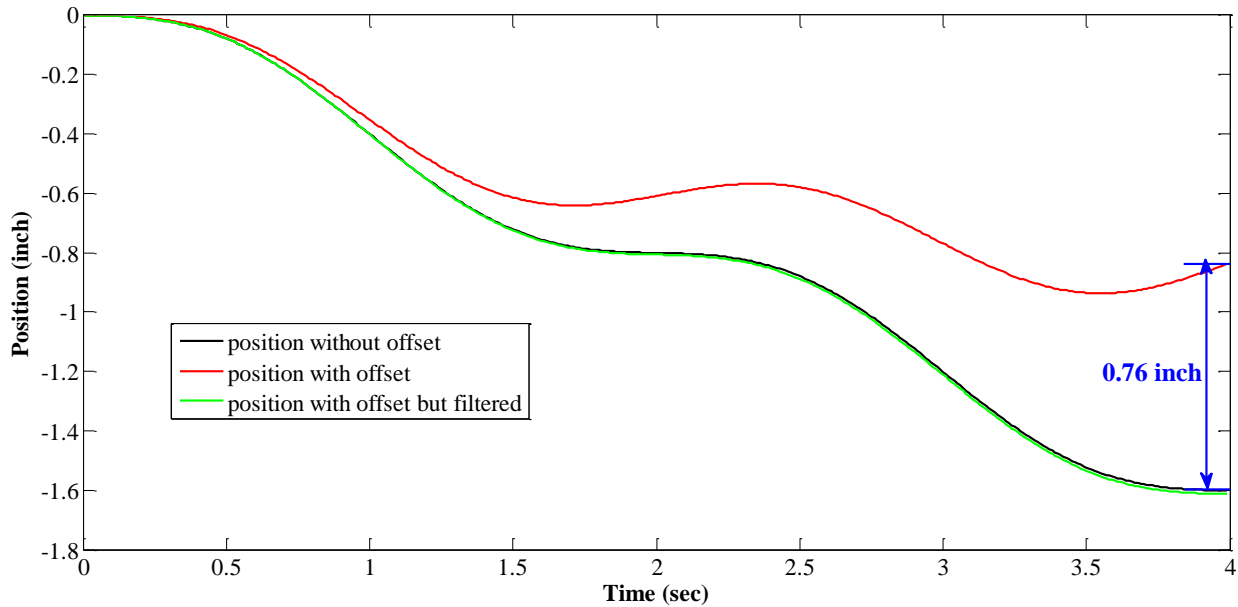


Figure 5.10: Estimated Displacement, Displacement with Offset, and Filtered Displacement Data

From Figure 5.10, it can be seen that there is significant error in the position that is obtained without filtering the acceleration data. Although the added acceleration offset is very small (0.008 ft/sec^2 or 0.0024 m/sec^2), a position offset of 0.76 inch (19.3 mm) accumulates after just after 4 seconds as compared to that obtained using the proposed data filtering scheme.

5.3.3 Inverse State-Space Model

The inverse state-space model has been implemented using MATLAB as described in Section 5.2.1.1 to estimate pavement profile from vehicle vertical acceleration data. First, acceleration data was filtered to remove wavelengths that are less than 4 feet (1.23 m) and greater than 100 feet (30.48 m). Then, vertical acceleration data was used as an input to obtain road profile.

5.4 DETERMINATION OF PAVEMENT ROUGHNESS

To determine pavement roughness using standard techniques, pavement profile is required. Inertial profilers are commonly used to collect road profile data, and often the software program *Profile Viewer and Analysis*, or ProVAL, is used to determine IRI. The ProVAL software was developed by the Transtec Group and sponsored by Federal Highway Administration (FHWA) and the Long Term Pavement Performance Program (LTPP) [85]. In the current study, a

MATLAB script was developed, following the requirements of ASTM E 1926-08 to estimate pavement roughness from the profile determined from vehicle vertical acceleration data [86].

5.4.1 Development of a MATLAB Script to Calculate IRI

Currently, obtained vehicle vertical acceleration data are used to calculate position data which is considered here as perceived pavement profile. This profile data is then typically analyzed with the ProVAL software program to calculate IRI. However, to calculate IRI directly from a smartphone, a MATLAB script has been developed following ASTM E1926 – 08. The output of this script is similar to those of the ProVAL program, as indicated by the close proximity to the unity line when plotted as in Figure 5.11.

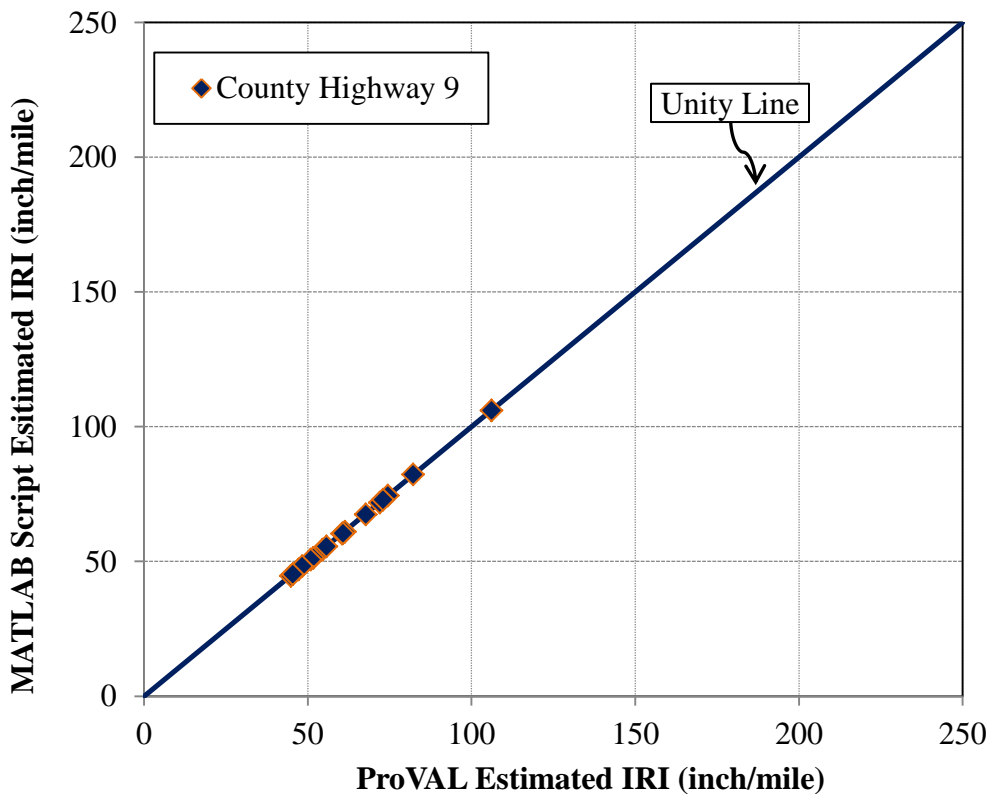


Figure 5.11: Comparison of MATLAB and ProVAL Generated IRI for County Highway 9

5.5 PROJECT APPROACH

After the development of methods to determine pavement roughness from the vehicle vertical acceleration data, acceleration data has been collected from three different test sections. The

steps involved in this project have been shown in Figure 5.12. Vehicle vertical acceleration data was collected using different smartphones and vehicles; acceleration data was analyzed by double integration and the inverse state-space model to obtain road profile, a MATLAB script was used to determine IRI, and IRI values were then integrated with ArcGIS Map to provide a spatial presentation of data, which may be useful for pavement management purposes.

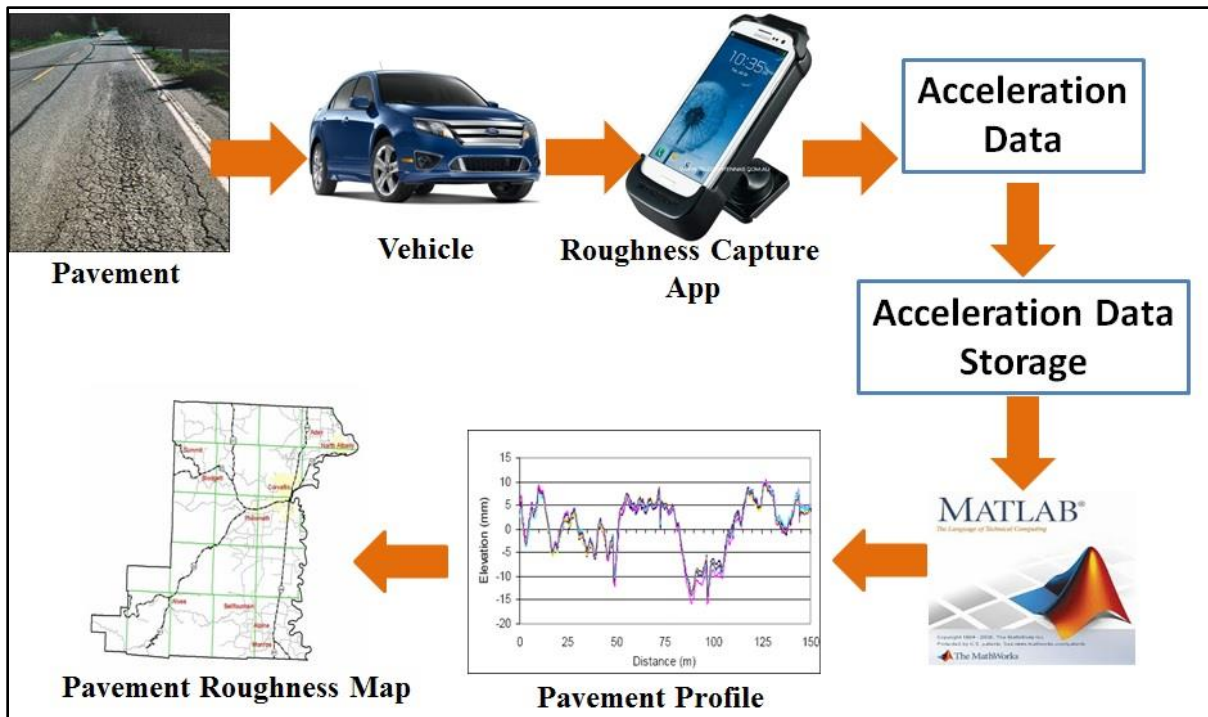


Figure 5.12: Project Approach

5.5.1 Data Collection

Data collection included collection of vehicle vertical acceleration data, storage and retrieval of data from smartphones, and collection of pavement profile data from an inertial profiler. Data collection was generally performed at a driving speed of 50 ± 2 mph. Android-based smartphones manufactured by different vendors were utilized in conjunction with the Roughness Capture application. For validation of the new Roughness Capture app, a Honda CRV equipped with an inertial profiler was used to collect reference pavement profile data. Pavement profile data along with vehicle driving speed and traveled distance were collected. While collecting profile data using the inertial profiler, smartphones were mounted on the dashboard using a standard car mount (Figure 5.13), and the Roughness Capture application was used to collect acceleration

data, GPS location, and a timestamp. Table 5.2 shows test sections and the list of smartphones and vehicles used for data collection from the test sections.



Figure 5.13: Acceleration Data Collection Using Smartphone Application

Table 5.2: Test Section, Vehicle, and Smartphone Models for Acceleration Data Collection

Vehicle	Pavement Section	Smartphone
Mazda3	County Highway 32, 9, 23	Samsung SII, Nexus 4, Motorola Droid, Samsung S4
Honda CRV	County Highway 32, 9, 23	Samsung SII, Nexus 4, Motorola Droid, Samsung S4
Dodge Avenger	County Highway 32, 9, 23	Samsung SII, Nexus 4, Motorola Droid, Samsung S4
Chevrolet Impala	County Highway 32, 9, 23	Samsung SII, Nexus 4, Motorola Droid, Samsung S4, Samsung SM 900GV

Three test sites were selected from three different county highways within a 10 mile radius of Rantoul, IL, and having a wide range of pavement roughness. Figure 5.14 shows the location of test sections. Test sites were 2-miles long, and the test vehicle was driven at target speed of 50

mph in the rightmost driving lane. Site 1 was the northbound lane of County Highway 32 east of Rantoul, IL. Site 2 was the westbound lane of County Highway 9, and Site 3 was on the southbound lane of County Highway 23. A minimum of two data collection runs were conducted at each site, with five replications used in selected instances to assess Roughness Capture repeatability.



Figure 5.14: Location of Test Sections

During this study, a data collection rate of 140 points/second was used. Preliminary trials showed that a maximum of about 140 points/second can be reliably obtained from the range cellphones used in this study. For the standard speed of 50 mph, the vehicle travels 880 inches/second. Thus, the spacing of acceleration data points was 6.29 inches.

5.5.2 Data Analysis

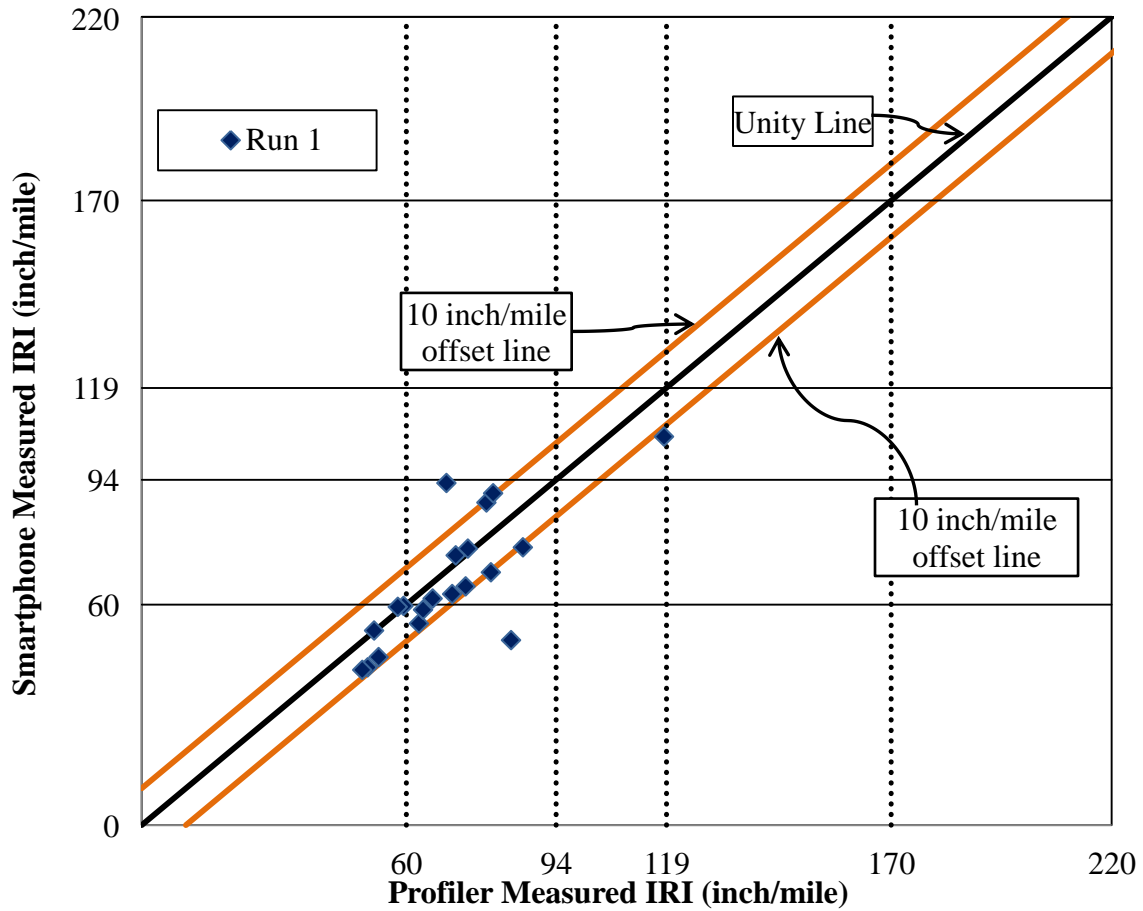
Vehicle acceleration data collected by roughness capture was analyzed to estimate pavement roughness. First, acceleration data was processed by an in-house MATLAB code to obtain pavement profile data (double integration of acceleration data and inverse state-space), and then the estimated pavement profile was analyzed using another MATLAB script to estimate roughness in terms of IRI of each 0.1-mile section across the 2-mile long test sections. The

detailed mathematical procedure used was presented in Section 5.2.1.1. It is acknowledged that the current smartphone-based approach does not produce a true profile of pavement surface, but rather a ‘perceived profile.’ This is due the effects of dampening provided by the vehicle suspension system. Simultaneously, an inertial profiler was used to estimate pavement profile, and the ProVAL software [85] was then used to calculate average IRI for 0.1-mile sections across the 2 mile test sites.

5.6 COMPARISON OF IRI ESTIMATED BY APP AND DATA COLLECTION VEHICLE

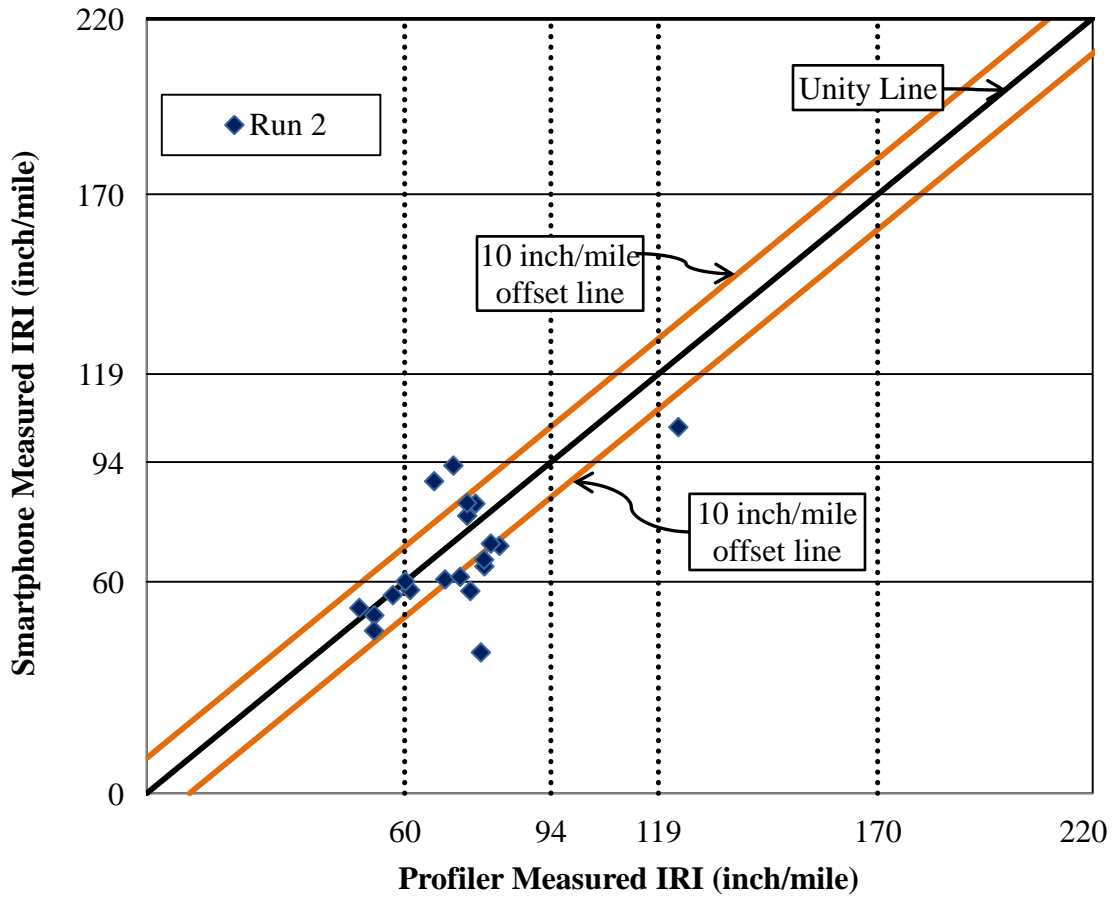
5.6.1 IRI Measured from Acceleration Integration Process

To collect data with Roughness Capture application, a Honda CRV car (inertial profiler car) and a Samsung Galaxy SII phone were used. Figure 5.15 shows pavement roughness values estimated by the Roughness Capture application and an industry standard inertial profiler for two different runs at County Highway 32. IRI values of every 0.1-mile section of the 2-mile section were plotted (20 points). A good correlation between the two methods was observed without the need for system calibration. It has been assumed that acceptable results would be obtained if the Roughness Capture application was able to calculate IRI within ± 10 inch/mile of that measured by inertial profiler over the vast majority of 0.1 mile sections investigated. For reference, two horizontal lines were drawn at 10 inch/mile offsets from the unity line to help visualize the magnitude of deviation of the smartphone measured IRI values from those of inertial profiler. It can be seen that most of the values (seventeen sections out of twenty) were in the 10 inch/mile offset band, indicating a very good correspondence between the two methods. In Figure 5.15(a), only one 0.1-mile section showed distinctly different IRI values, indicating that the pavement ride category assessment for that particular section might differ from the reference by one category. In Figure 5.15(b), only three 0.1-mile sections were outside of the 10 inch/mile offset lines. Although some differences exist, it appears that the same overall pavement management decision would be reached for the 2-mile section using the IRI values determined using either approach.



(a)

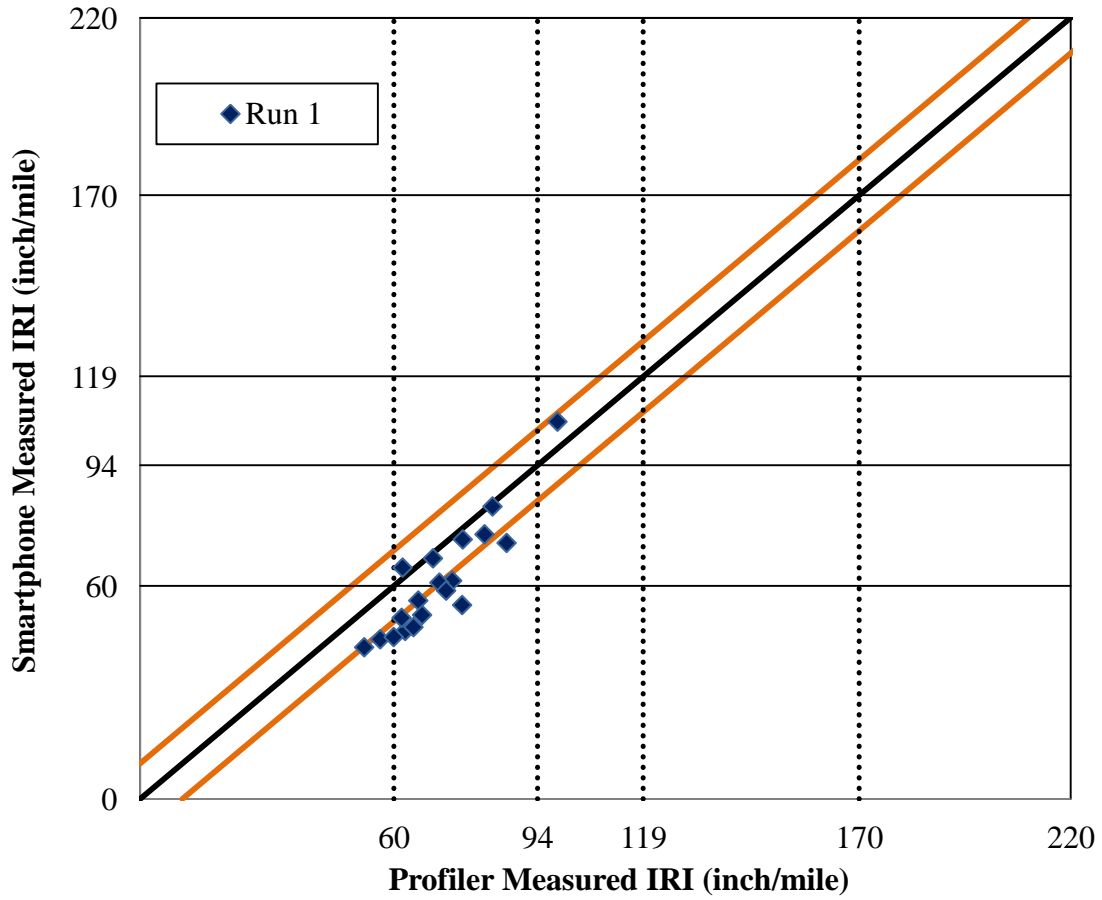
Figure 5.15: Comparison of Pavement Roughness Data Measured by Cellphone Application and Inertial Profiler for County Highway 32: (a) Run 1 and (b) Run 2



(b)

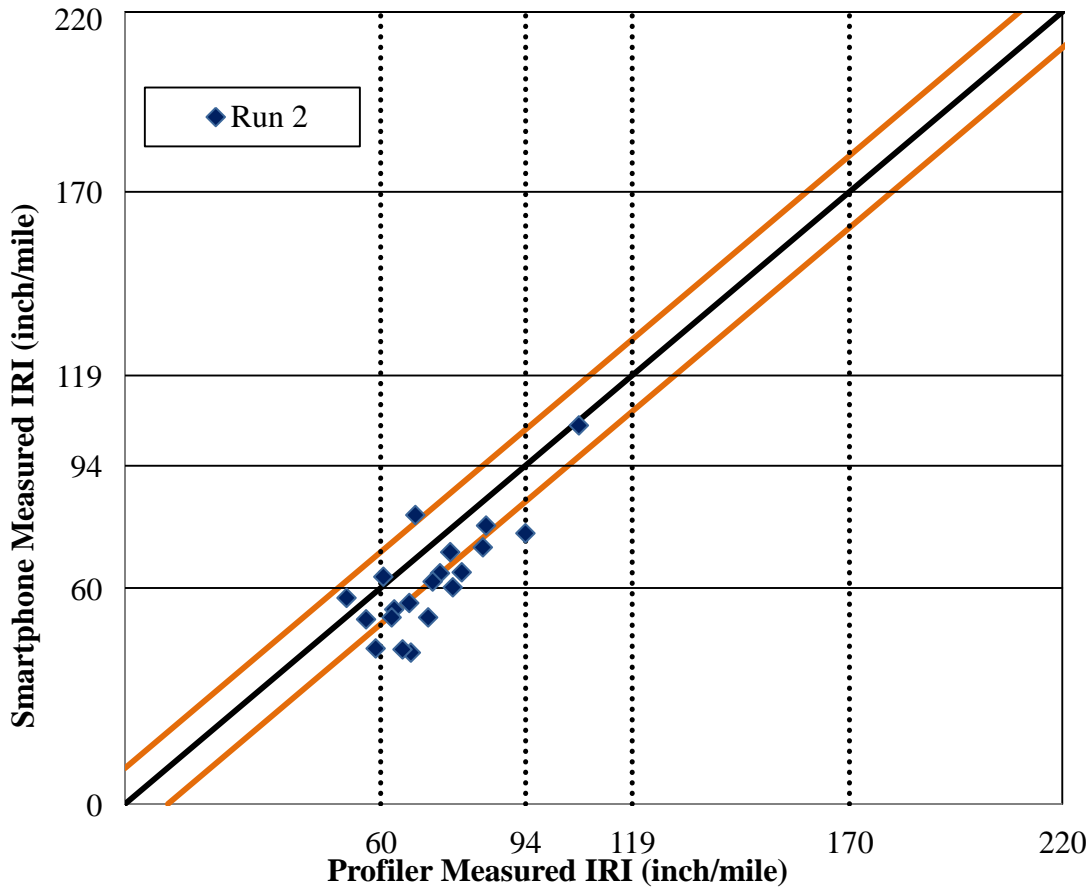
Figure 5.15 (cont.)

Figure 5.16 shows the pavement roughness measured by the Roughness Capture application and inertial profiler for two different runs conducted at county highway 9. Again, IRI values estimated by the Roughness Capture smartphone application corresponded closely to those measured by the inertial profiler system without the need for system calibration.



(a)

Figure 5.16: Comparison of Pavement Roughness Data Measured by Cellphone Application and Inertial Profiler for County Highway 9: (a) Run 1, and (b) Run 2



(b)

Figure 5.16 (cont.)

Figure 5.17 shows the pavement roughness values measured for County Highway 23, which had relatively higher pavement roughness. In this section, it was observed that the uncalibrated smartphone measured IRI values were below the unity line (IRI was underpredicted). As stated earlier, acceleration data was sampled at a longitudinal distance of 6.29 inches in the smartphone based system using a 140 sample/section data collection rate. In contrast, the more sophisticated inertial profiler system collects data at intervals of less than 1 inch. Due to the high pavement roughness and high number of significant vehicle acceleration events, it is speculated that the 140 samples/second data collection rate used might have contributed to the underprediction of pavement roughness in this section. Another explanation is the heightened effect of damping resulting from the vehicle suspension system, which is not currently accounted for in the double

integration analysis scheme. However, vehicle suspension system has been considered using the state space model, which is presented later in section 5.6.2.

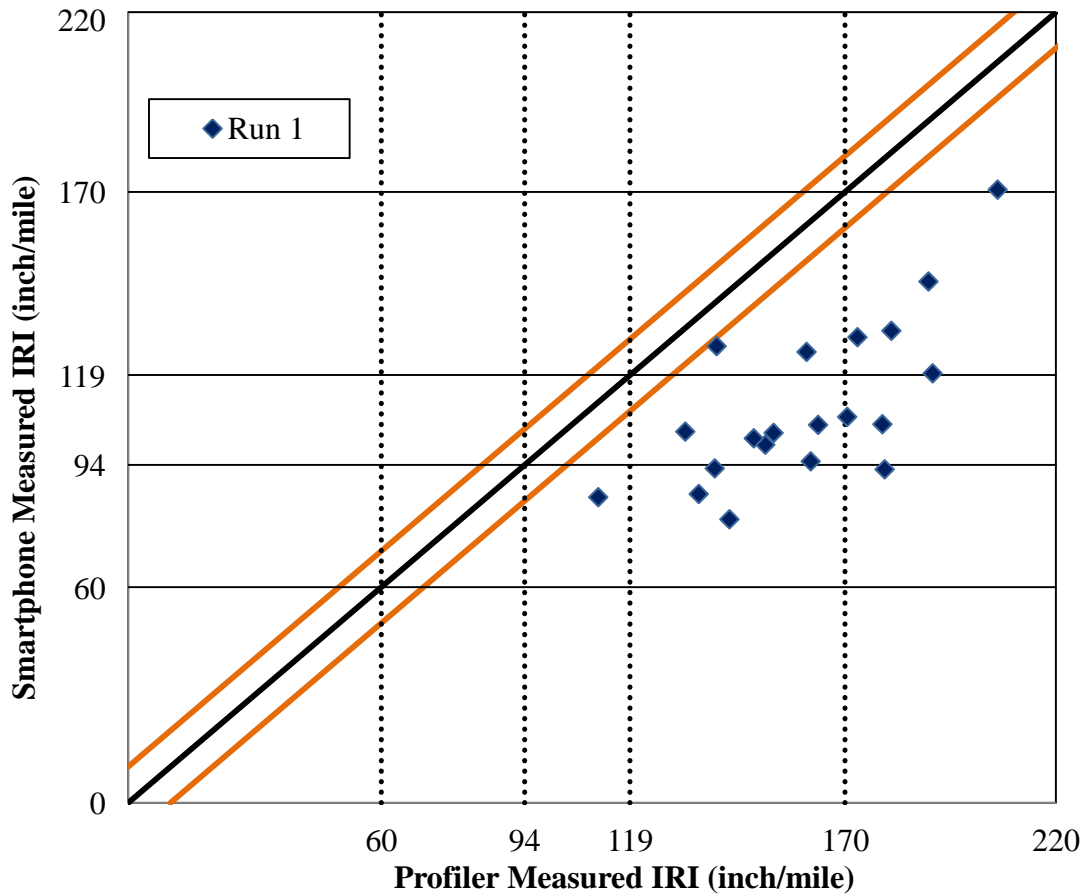


Figure 5.17: Comparison of Pavement Roughness Data Measured By Cellphone Application and Inertial Profiler at County Highway 23

5.6.1.1 Repeatability of Smart Phone based IRI Estimated by Double Integration Scheme

Figures 5.18 through 5.20 show IRI data for every 0.1-mile section of CH32, CH9, and CH23, respectively. IRI data was collected five times to assess the repeatability of the Roughness Capture android-based smartphone application. The x-axis values represent the distance along the driving lane whereas y-axis values chart the IRI measured by the roughness capture app. Pavement ride categories as presented earlier in Table 4.1 were used to form the y-axis scale. It appears that the effects of vehicle suspension on the damping of the vertical acceleration of the ‘sprung mass’ portion of the vehicle (where the cell phone is mounted) is higher on rougher roads, as measured IRI values at CH 23 are lower than reference values of IRI. Here, the average

COV's are 11, 9, and 9 percent at CH 32, CH 9, and CH 23, respectively. In comparison, the COV of measuring IRI with an inertial profiler may be less than 5 percent, but considering the cost of measuring IRI via an inertial profiler [3], a COV of 10 percent for the smartphone-based Roughness Capture application appears to be quite reasonable. The importance of precisely matching the location of pavement segments when comparing smartphone based roughness to the reference data from a data collection van was very apparent when analyzing the data from this section. With extra effort to improve location matching, COV was found to decrease.

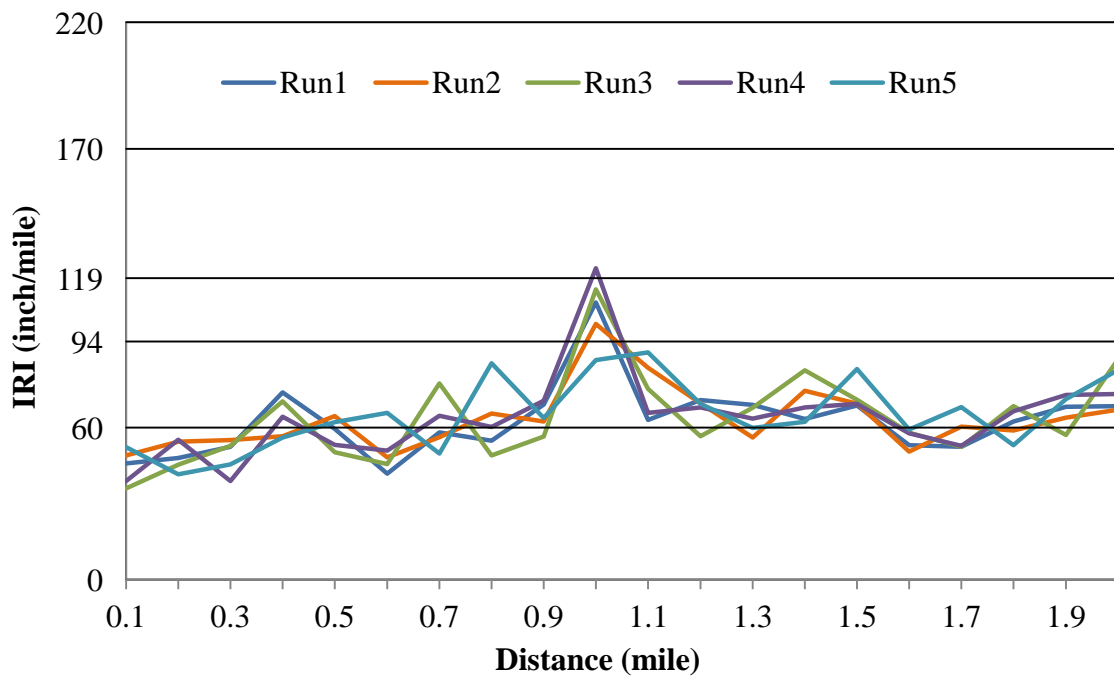


Figure 5.18: Estimation of IRI at County Highway 32 over Five Different Runs

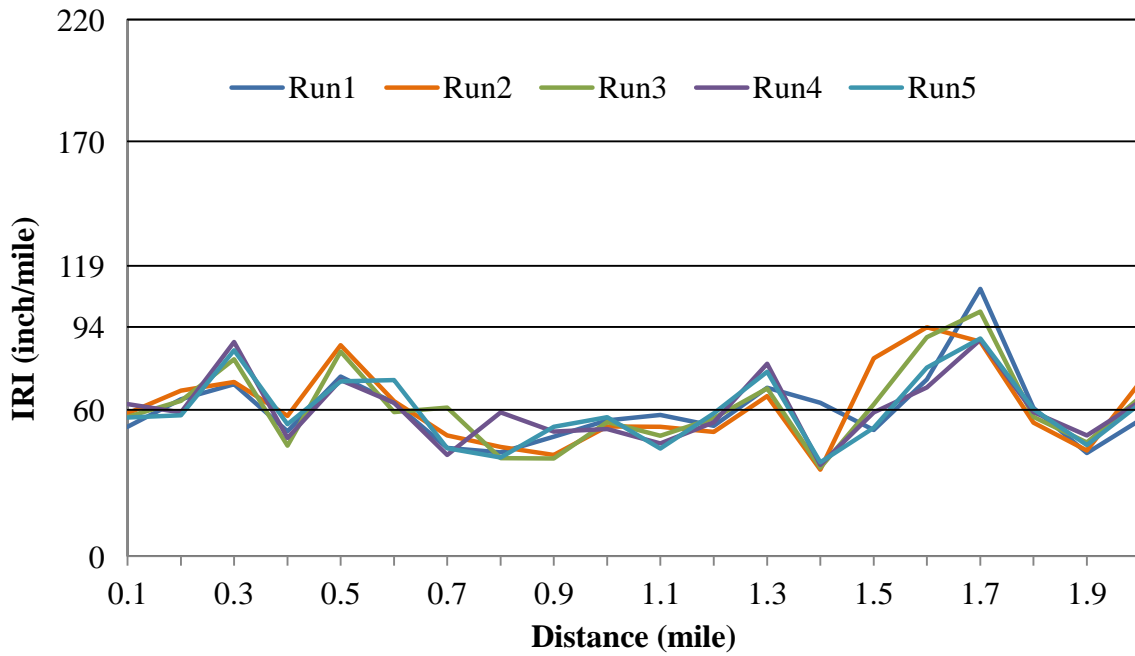


Figure 5.19: Estimation of IRI at County Highway 9 over Five Different Runs



Figure 5.20: Estimation of IRI at County Highway 23 over Five Different Runs

Table 5.3 shows average IRI measured by the Roughness Capture App, standard deviation, and coefficient of variance (COV) of every 0.1-mile section of each testing site. From the left portion of the table, it can be seen that most of the COV's are less than 15 percent except for a few sections. For one pavement section, the COV was estimated as 22 percent. The highest COV measured was 28 percent, within section 2. Given the fact that it was impossible to drive the test vehicle along the exact same path in terms of vehicle wander; the repeatability of IRI measurements with the roughness capture app appears to be acceptable for the purpose of collecting useful pavement condition data in a rapid, inexpensive manner. This conclusion is further justified considering the possibility of using crowd sourcing to obtain a large number of measurement replications, which can then be used to arrive at a more accurate and possibly real-time pavement condition assessment.

Table 5.3: Repeatability of Roughness Capture Application to Measure IRI

County Highway 32			County Highway 9			County Highway 23		
Average IRI, inch/mile	St. Dev.	COV	Average IRI, inch/mile	St. Dev.	COV	Average IRI, inch/mile	St. Dev.	COV
44.4	6.8	15	57.5	3.4	6	89.5	9.2	10
48.9	5.9	12	62.5	4.1	7	109.0	5.5	5
48.9	6.7	14	79.0	7.7	10	90.0	4.6	5
64.2	8.0	12	51.3	4.8	9	103.9	15.2	15
57.9	6.0	10	77.5	7.1	9	93.5	10.0	11
50.5	9.2	18	64.1	4.9	8	140.9	8.0	6
61.2	10.5	17	48.1	7.7	16	150.1	11.8	8
63.0	14.0	22	45.3	7.8	17	120.4	15.9	13
64.4	5.6	9	46.9	5.8	12	123.2	5.7	5
106.9	13.8	13	54.5	1.9	4	95.6	6.3	7
75.5	11.4	15	50.1	5.5	11	85.8	12.3	14
66.9	5.8	9	54.8	2.9	5	110.2	11.5	10
63.3	5.4	9	71.5	5.5	8	114.0	24.8	22
70.2	8.5	12	42.0	11.7	28	141.5	9.4	7
72.3	6.1	8	61.3	11.9	19	100.0	8.6	9
55.7	3.7	7	80.5	10.8	13	99.5	5.7	6
57.2	6.9	12	95.1	9.5	10	125.2	7.3	6
61.8	6.2	10	58.4	2.5	4	96.1	7.3	8
66.7	6.4	10	45.4	2.8	6	82.9	15.8	19
75.7	8.8	12	63.6	5.6	9	96.9	4.2	4

5.6.1.2 Summary of Roughness Measurement by Double Integrating Scheme

So far, the results presented were for the measurement and analysis approach whereby roughness is estimated through double integration and filtering of acceleration data collected with smart phones. Before presenting an improved analysis method to consider vehicle suspension effects, the results the aforementioned approach are first summarized, as follows:

- IRI values measured with the smartphone application Roughness Capture were similar to those collected with the inertial profiler for the two test sites having low to medium roughness, with very few outliers observed. Even the outliers were in the same ride category or within one ride category of the reference measurement. These results were obtained without the need for system calibration or the use of a more sophisticated analysis system to consider vehicle suspension damping effects.
- At test site 3, which had relatively high roughness, the smartphone based system produced measured IRI values which were substantially lower than those collected with the inertial profiler. It is speculated that a higher sampling rate and/or the inclusion of a vehicle suspension model may be needed to bring the values into closer correlation, which is the subject of Section 5.6.2.
- The repeatability of the roughness capture application was found to be acceptable for the intended application. For test site 1, the coefficient of variance (COV) was in the range of 7-22, where only one value exceeded 20 percent, and most values were less than 15 percent. At site 2 and site 3, COV's were as low as 4 percent. COVs were higher than 20 percent for only 3 of the 40 test sections.
- As vehicles suspension systems vary widely, vertical acceleration data collected by smartphones mounted in different vehicles will be dampened to differing degrees. To address this phenomenon, additional modeling to estimate the effects of motion dampening of the sprung mass due to the vehicle suspension is needed. The model must consider effects of vehicle mass and suspension system characteristics of the actual survey vehicle being used for data collection, and through modeling, develop an improved estimate of actual pavement profile by numerically removing dampening effects. By feeding in the improved, rougher estimate of pavement profile into the quarter car model (instead of using the vertical trajectory of the cab of the vehicle, whose

trajectory is dampened by the vehicle suspension system), an IRI value closer to that obtained with the industry standard inertial profile should be obtained.

In the following section, a state space model is introduced into the analysis scheme in order to estimate an improved estimate of pavement profile and therefore an improved IRI estimate.

5.6.2 Roughness Measurement considering State Space Model

By ignoring vehicle mass and suspension system effects and using the vertical trajectory of the vehicle cab (sprung mass) as an estimate of pavement profile, the double integration scheme used alone was found to underpredict pavement IRI, especially for very rough pavements. Thus, an improved modeling scheme which adds a state space model to numerically remove suspension system dampening effects was developed. The state space model can be used to model vehicle mass and suspension system effects, where acceleration data collected from smartphones mounted on the vehicle dashboard and collected using Roughness Capture can be used as an input to determine pavement profile. In the development of this new model, the Roughness Capture application was used to collect vehicle vertical acceleration data from the same test sites (county highway 32, county highway 9, and county highway 23). Acceleration data was again filtered to remove acceleration values with wave lengths less than 4 feet and greater than 100 feet to meet the requirements of ASTM E 1926-08. The inverse state-space system has been implemented using a MATLAB script to determine an improved estimate of pavement profile from the vehicle sprung mass vertical acceleration data. Then, the quarter-car model MATLAB script was applied to calculate pavement roughness (IRI) from the improved pavement profile estimate. Pavement roughness estimation using the inverse state-space model approach is summarized in Figure 5.21.

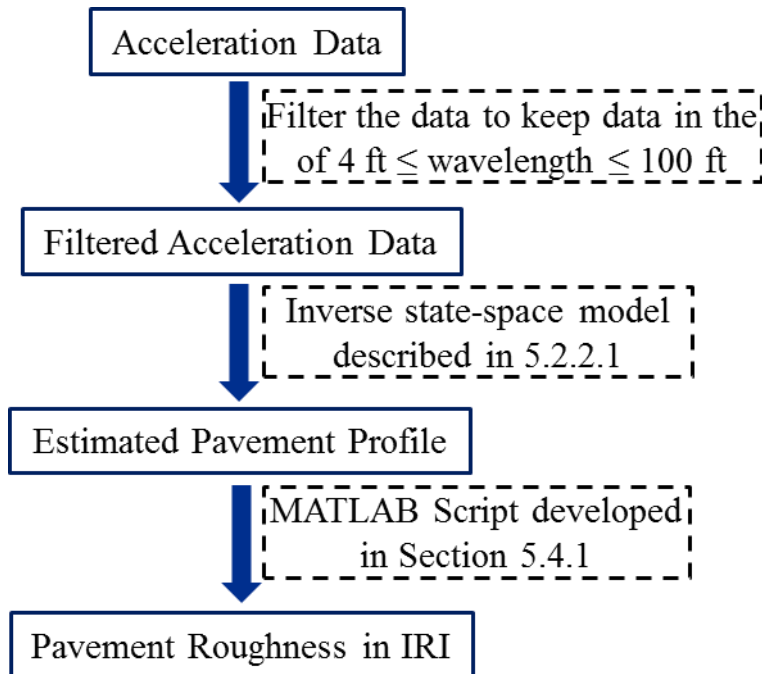


Figure 5.21: IRI Calculation Procedure

Figures 5.22 and 5.23 show the pavement roughness results obtained from county highway 32 for two different sets of data collected from that segment. Smartphone measured IRI values of every 0.1-mile section have been compared with that of the inertial profiler in both figures. In Figure 5.22, it can be seen that IRI of only three 0.1-mile sections are outside of the 10-inch-mile offset lines whereas the IRI of the other seventeen 0.1-mile sections are within the offset lines. This indicates that pavement roughness values measured by smartphone application are predominantly within ± 10 inch/mile of inertial profiler measured IRI.

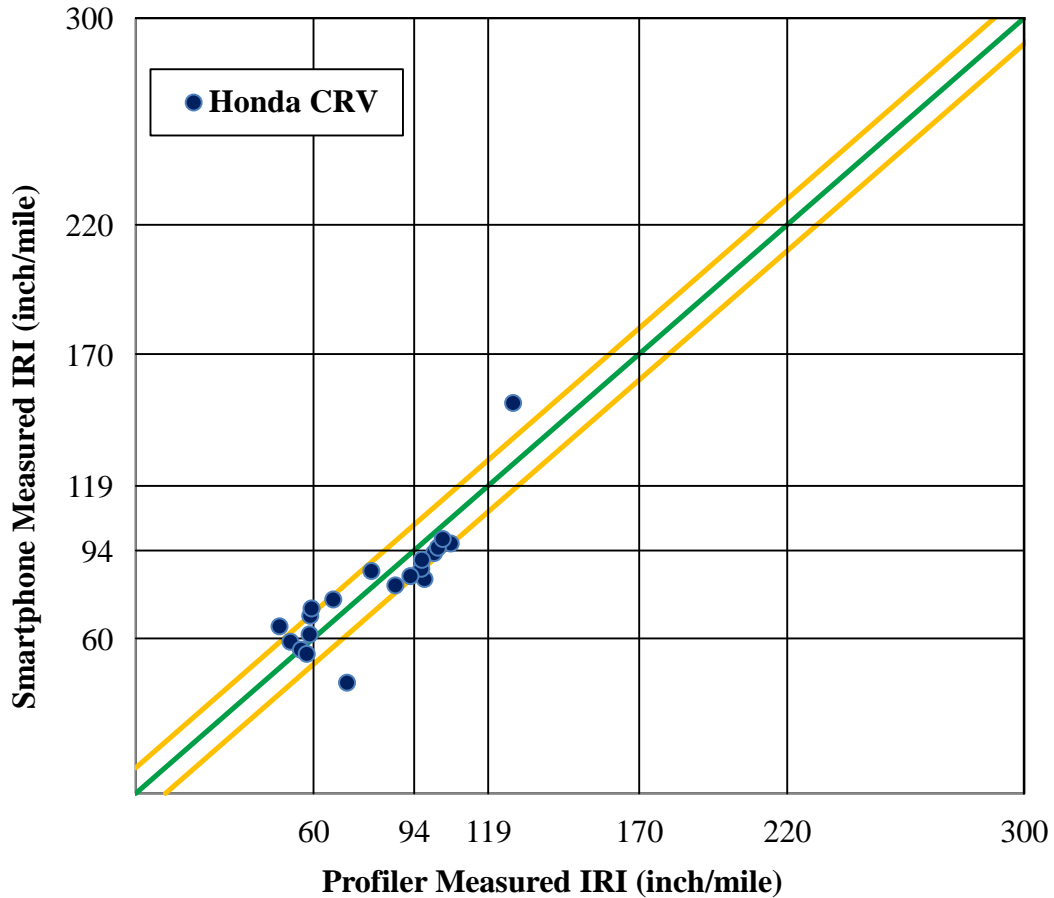


Figure 5.22: Smartphone Measured IRI from County Highway 32 using State Space Model (Run 1)

Figure 5.23 shows IRI results obtained from a different set of acceleration data from county highway 32. It can be noticed that IRI of only four-out-of-twenty 0.1-mile sections are outside the 10 inch/mile offset lines. Moreover, though two of those four values are outside the offset lines, only one of them is significantly different than corresponding inertial profile measured IRI. As a result, it can be summarized that smartphone application measured pavement roughness similar to the inertial profiler.

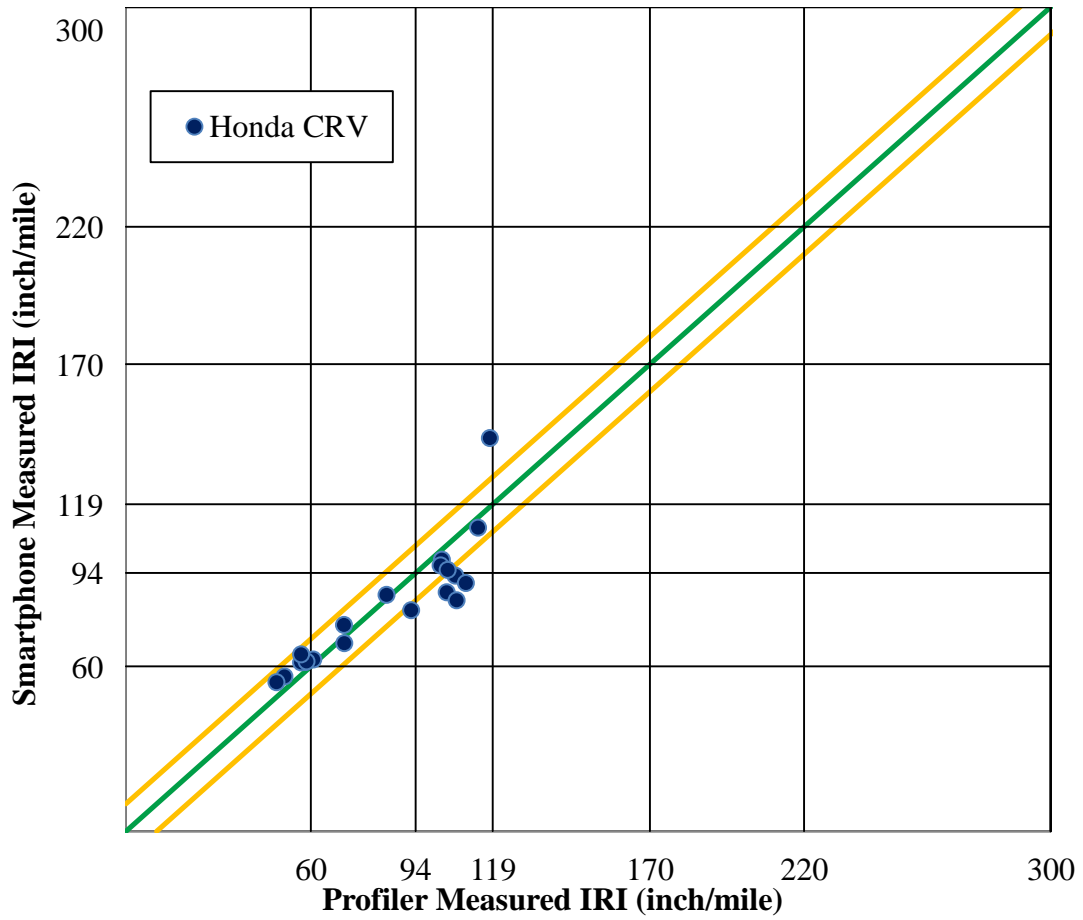


Figure 5.23: Smartphone Measured IRI from County Highway 32 using State Space Model (Run 2)

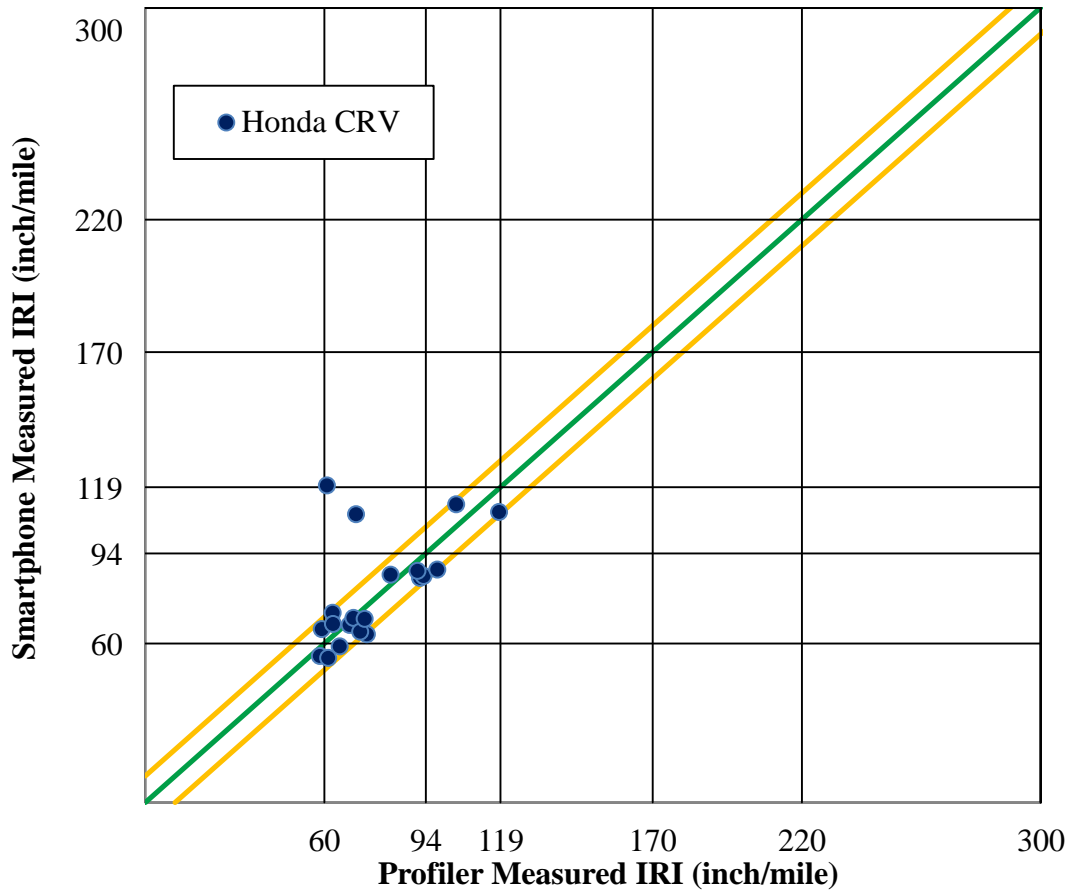


Figure 5.24: Smartphone Measured IRI from County Highway 9 using State Space Model (Run 1)

Similarly, acceleration data was collected from county highway 9, and pavement of this route had minor transverse cracking, longitudinal cracking, and other minor surface distresses. Figure 5.24 and 5.25 show IRI results obtained from county highway 9. From Figure 5.24, it can be observed that IRI values of two pavement sections are significantly different than that of the inertial profiler. However, results obtained from the smartphone application shows that IRI values of most of the sections compare favorably with the inertial profiler IRI.

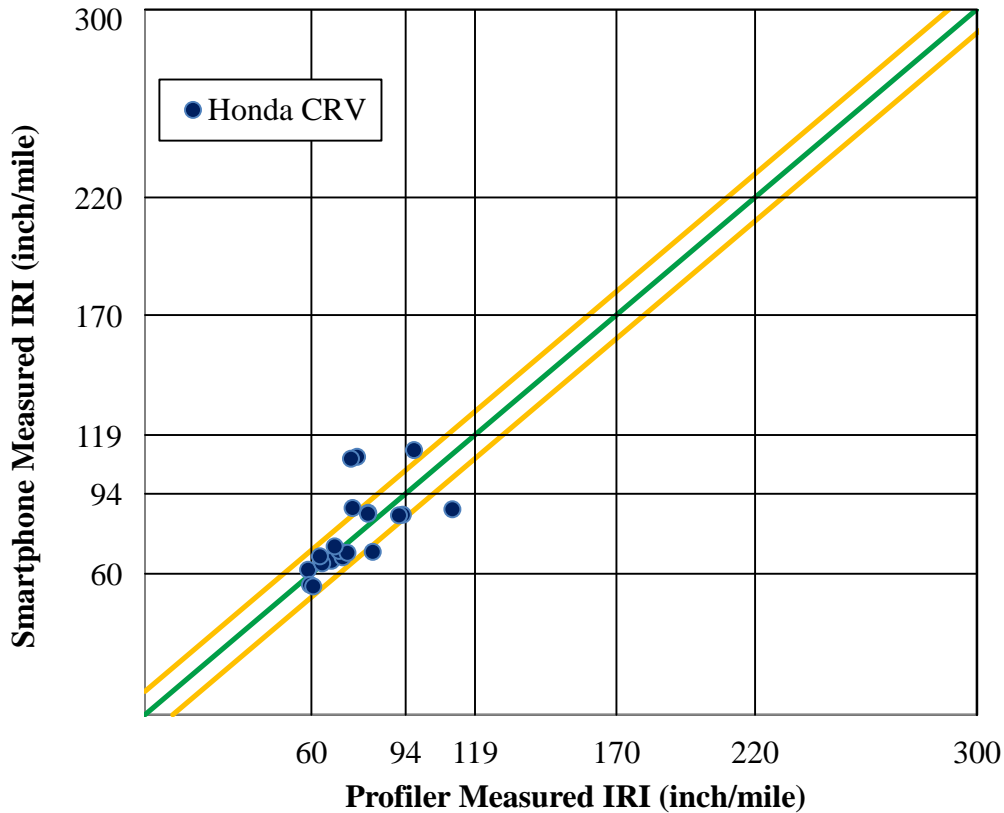


Figure 5.25: Smartphone Measured IRI from County Highway 9 using State Space Model (Run 2)

Figure 5.25 shows a comparison of pavement roughness measured by the smartphone application to that of the inertial profiler at county highway 9 with different set of data collected in different time. From Figure 5.25, it can be seen that the IRI values of five out of twenty 0.1-mile sections are not within the 10 inch/mile offset lines. This indicates that smartphone application measured significantly different (low/high) IRI for these five pavement sections. However, though IRI values of two out of those five sections are outside of the 10 inch/mile offset lines, they are very close (within 15 inch/mile) to the offset lines. Therefore, it can be summarized that smartphone application captured pavement roughness similar to inertial profiler for the most of the pavement section at county highway 9.

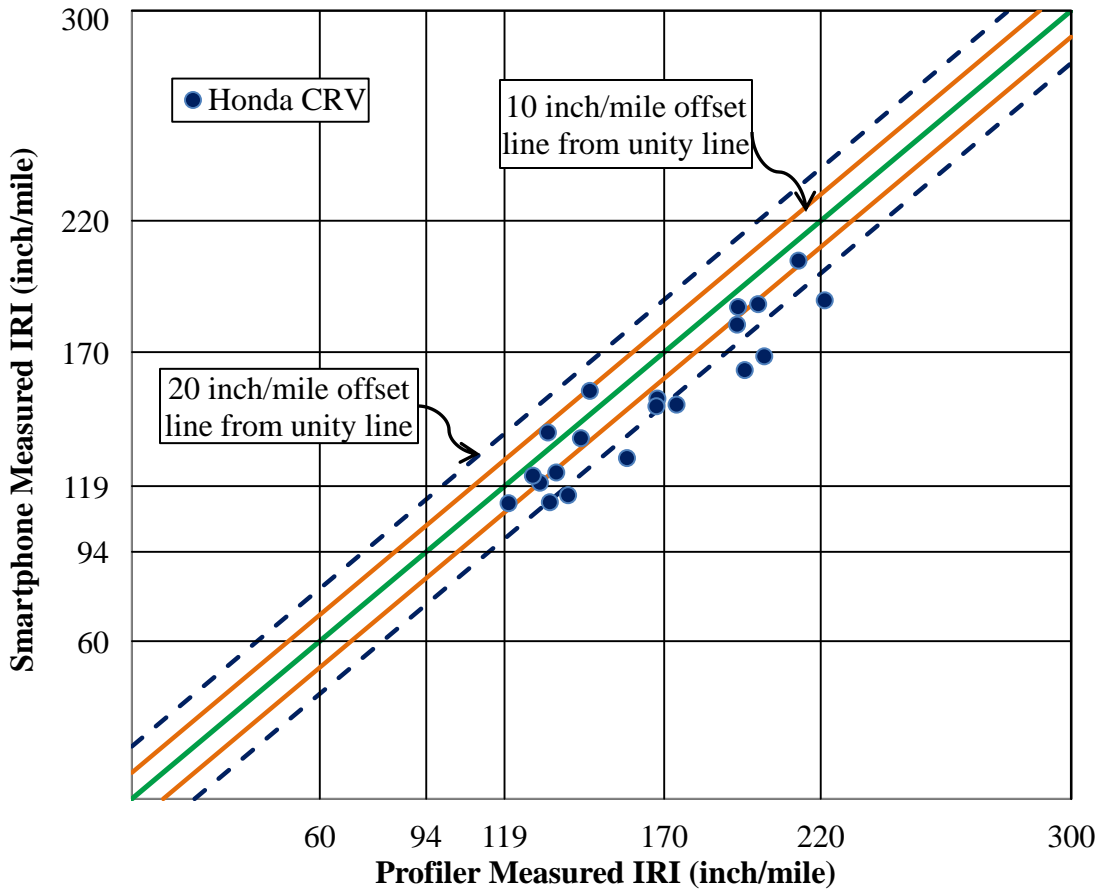


Figure 5.26: Smartphone Measured IRI from County Highway 23 using State-Space Model (Run 1)

Figure 5.26 and 5.27 shows pavement roughness measured using the smartphone application and the inertial profiler for county highway 23. This route had significant transverse and longitudinal cracking, fatigue cracking, and other localized surface distresses; it was a noticeably rough ride. From Figure 5.26, it can be seen that, while the estimated IRI values for most of the pavement sections were not within the 10 inch/mile offset lines, most were within the 20 inch/mile offset lines using the improved scheme. This represents a very significant improvement over the original modeling scheme (Figure 5.17), where an underestimation of nearly 100 inch/mile was observed for one of the data points.

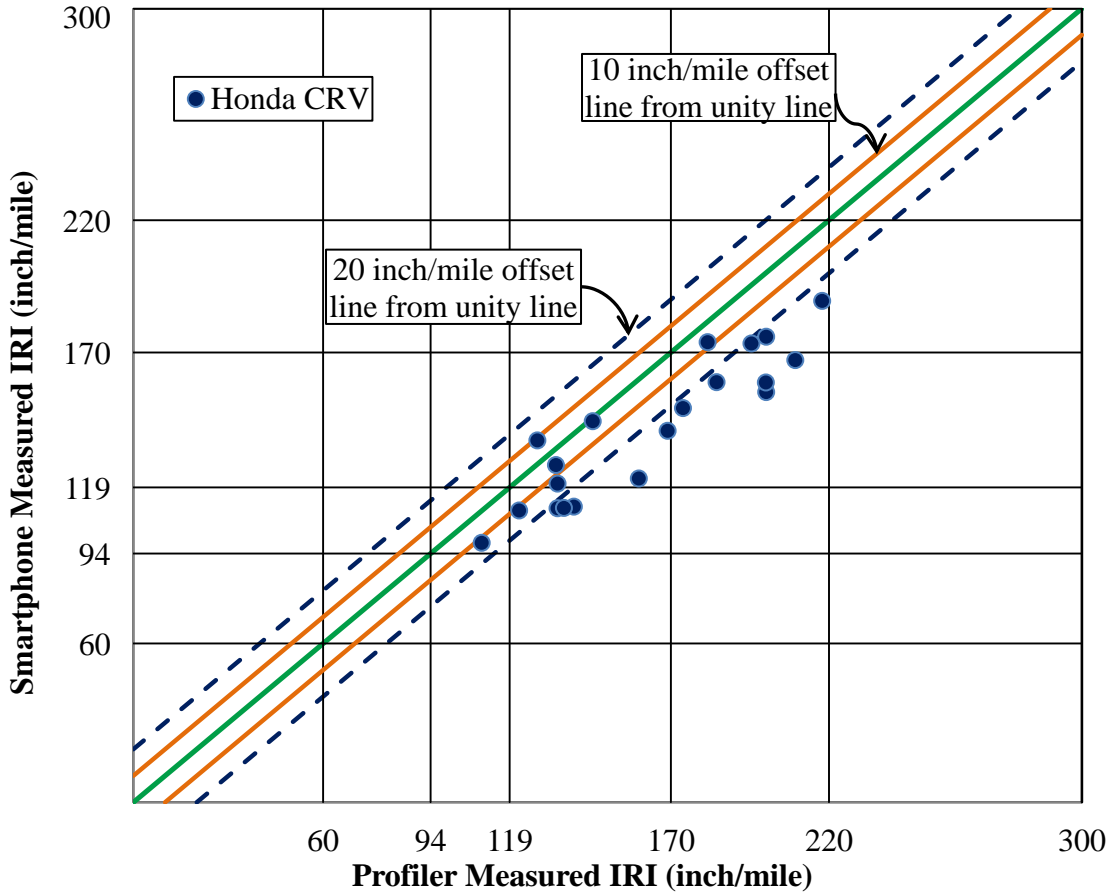


Figure 5.27: Smartphone Measured IRI from County Highway 23 using State-Space Model (Run 1)

Clearly, the improved analysis scheme, which accounts for the effects of vehicle suspension using the state space model solved inversely, led to much improved results. Still, for a very rough pavement section, a slight underprediction of pavement roughness still exists. For practical pavement management purposes, this difference could be simply accounted for via calibration. However, the possibility exists that the tendency for underprediction of IRI for rough pavements will become less pronounced as cellphone technology evolves. Recall that the smartphone application used herein collected 140 acceleration points per second. The vehicle running at 50 miles/hr travels 880 inches per second, resulting in spatial distance between acceleration data points of 6.29 inches. Therefore, the smartphone application may very likely be missing peak accelerations due to the relatively slow data collection rate. On the other hand, the inertial profiler collects data every 0.67 inches traveled, therefore potentially capturing more roughness

creating attributes. This is likely a source of the difference in IRI that exists for rough pavement even when the improved algorithm is used. The good news is that, with the expected advancement of smartphone technology (processor speed, bus throughput, memory, etc.), higher data collection rates will be possible, potentially rendering IRI estimates on rough pavements even more accurate (further reducing the need for system calibration).

The repeatability of the Roughness Capture IRI prediction system was assessed through collection of data from five measurement passes on each test section. Coefficient of variability (COV) was computed as a convenient way to assess variability (normalized by the mean), as shown in Table 5.4. It can be seen that at county highway, 32 COV values are now in the range of 3-17%, compared to 7-22% for the original double integration scheme. For county highway 9, COV's are in the range of 3-16%, as compared to 4-28% with double integration scheme. The COV's at county highway 23 (very rough pavement) are in the range of 4-24% with compared to 4-22% of double integration process. As a result, it was observed that repeatability has also been improved by incorporating the inverse state space model in the estimation of pavement roughness from smartphone captured acceleration data.

Table 5.4: COV's in IRI Estimation by State Space Model

Distance (mile)	COV's at the Test Section		
	CH32	CH9	CH23
0.1	11	10	14
0.2	17	12	9
0.3	15	13	8
0.4	15	10	12
0.5	9	16	5
0.6	8	9	12
0.7	11	16	5
0.8	6	5	9
0.9	19	15	15
1.0	17	4	12
1.1	8	5	9
1.2	3	9	5
1.3	12	13	11
1.4	11	10	9
1.5	4	7	9
1.6	11	3	10
1.7	9	13	5
1.8	13	12	4
1.9	11	16	24
2.0	17	11	16

5.7 CALIBRATION AND VALIDATION OF ROUGHNESS CAPTURE APP

With the improvement of pavement roughness measurement using the inverse state space model, vehicle vertical acceleration data was collected from 14 different pavement sections, having a total length of about 60 miles. The sites were all located in Champaign and Piatt County, IL, and were used to compare the industry standard inertial profiler measured IRI to those of the smartphone application using the improved analysis algorithm. Acceleration data was collected using 4 different vehicles and 6 smartphones.

5.7.1 Data Collection

Table 5.5 shows the list of the pavement sections from where pavement roughness data was collected using both the inertial profiler and smartphone application.

Table 5.5: Name, Location, and Length of the Pavement Sections

Route Name	Start - End	Location	Length (miles)
US-45	Airport Road – 2800N	Champaign County, IL	9.9
County Rd 2500N	County Rd 1300E – 1000E	Champaign County, IL	4.3
County Rd 900E	County Rd 2550N – 3000N	Champaign County, IL	4.53
US-136	County Rd 900E – 700E	Champaign County, IL	2.01
US-136	County Rd 500E – 400E	Champaign County, IL	1.00
IL-47	County Rd 2900N – 2650N	Champaign County, IL	3.2
US-150	County Rd 200E – McKinley St	Champaign/Piatt County, IL	4.01
County Rd 2700N/300E	County Rd 300E – 000E	Champaign County, IL	2.99
County Rd N 1200E	County Rd E 2750N – IL-10E	Piatt County, IL	6.00
IL-10E	County Rd N 1300E – 200E	Piatt County, IL	4.00
County Rd 200E	County Rd 1500N – 1000N	Champaign County, IL	5.04
County Rd 1000N	County Rd 300E – 800E	Champaign County, IL	4.90
County Rd 800E	County Rd 1000N – Curtis Rd	Champaign County, IL	3.00
County Road 9	County 1700E – 1000E	Champaign County, IL	7.00

5.7.2 Vehicle Suspension Parameters Adjustment

As described earlier, the state space model requires vehicle suspension parameters to determine pavement profile from vehicle vertical acceleration data. Although it was possible to find suspension parameters in the literature for a few vehicles, insufficient data existed for the vehicles selected for use in this study. Therefore, suspension parameters were calibrated, by adjusting the parameters to minimize differences between IRI values estimated with the smartphone based system with those obtained using the inertial profiler. For suspension

parameters calibration, acceleration data was collected using four different vehicles from the three test sections. While calculating IRI from the acceleration data, suspension parameters are adjusted so that smartphones measured IRI values are as close as possible to that of inertial profiler but the differences between them are not greater than 10 in/mi in case of smooth pavement (IRI <60 in/mi).

Figure 5.28 shows vehicles and smartphones that were used in the study, while Table 5.6 shows adjusted vehicle suspension parameters.



Figure 5.28: Vehicles and Smartphones Used in the Study

Table 5.6: Adjusted Vehicle Suspension Parameters

	Mazda 3	Honda CR-V	Dodge Avenger	Chevrolet Impala
M1 (kg)	343	420	494	500
M2 (kg)	40	40	40	45
C1 (N*s/m)	1,500	1,400	1,550	1,500
K1 (N/m)	13,500	11,000	12,000	10,000
K2 (N/m)	200,000	198,000	200,000	200,000

5.7.3 Estimation of IRI

Acceleration data collected using smartphones was analyzed using the previously described, improved MATLAB script to estimate pavement roughness. Detailed results are provided in Appendix A, where smartphone measured IRI values are compared to those of the inertial profiler for every 0.1-mile pavement section. Figure 5.29 shows the average IRI values measured using the inertial profiler and smartphone application for all pavement sections. While there is no significant difference between averaged inertial profiler and smartphone application measured IRI values, when viewed at a more granular level, the average difference between smartphone and inertial profiler measured IRI within 0.1-mile sections is in the range of 7.8-24.5 in/mi. From Figure 5.29, it can be seen that the average difference between inertial profiler and smartphone measured IRI for every 0.1-mile section is more than 20 in/mi for US-45, IL-47, and County Rd 2700N where the average IRI is 146, 196, and 149 in/mi, respectively. It has been mentioned earlier that smartphone-collected acceleration data might not include some of the roughness events from a given route, or might underestimate those events due to vehicle suspension dampening effects, which lead to underestimation of IRI measurement. That notwithstanding, very low differences (<10 in/mi) between inertial profile and smartphone application resulted for County Rd 2500N, County Rd N 1200E, and IL-10 using the state space model analysis approach with calibrated vehicle suspension parameters. These three pavement sections are in very good condition with IRI values of 53, 51.8, and 50.9 in/mi, respectively. This trend has also been noticed in a test section which is in very good condition.

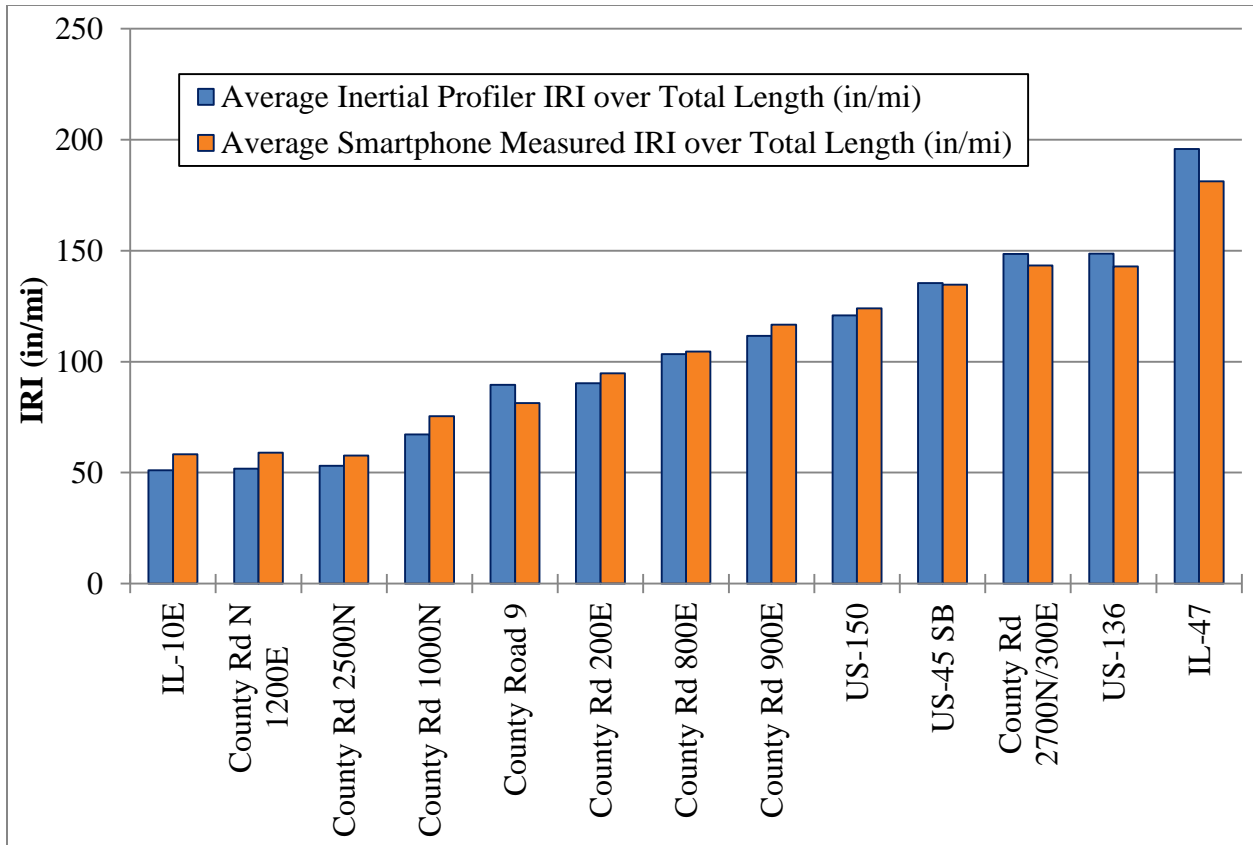


Figure 5.29: Average Difference between Inertial Profiler and Smartphone Measured IRI

The differences in IRI measurement in County Rd 900E, US-150, County Rd 200E, County Road 1000N, and County Road 800E are 14.5, 16.3, 13.7, 10.9, and 12.5 in/mil, respectively where the average IRI's are 111.6, 120.1, 90.2, 67.5, and 103.4 in/mi, respectively.

Although average IRI over the entire pavement sections measured by inertial profiler and smartphone application are very close (Figure 5.29), the average difference over every 0.1-mile pavement section increases with roughness level of the pavement, with few exception. However, it needs to be mentioned that these pavement sections were randomly selected, and smartphone application collected acceleration data was analyzed using state space model with calibrated vehicle suspension parameters. From this limited data, it can be summarized that smartphone application measures similar IRI (difference <10 in/mi) when pavement is in good condition; however, the differences between inertial profiler and smartphone application increase (difference in IRI 11-25 in/mi) when pavement is in poor condition.

5.8 EFFECT OF DIFFERENT SMARTPHONES ON IRI MEASUREMENT

In this section, the variation in pavement roughness caused by the use of different smartphones is investigated. Different smartphones have different accelerometer chips, different overall hardware and software architecture, and different physical characteristics, including location of accelerometer, mass and stiffness of various components, different physical dimensions (which affects phone movement and vibration), and different dashboard mounting characteristics. Thus, it is expected that different smartphones would yield different pavement roughness measurements. To assess the effect of smartphones on IRI measurement, vehicle vertical acceleration data has been collected from county highway 32, county highway 9, and county highway 23 using a 2011 Chevrolet Impala car and six smartphones, where five of them represented different smartphone models. Smartphone-based pavement roughness estimated using the state-space model with calibrated vehicle parameters (as described in the previous section) were compared to those obtained using the inertial profiler. Table 5.7 provides a summary.

Table 5.7: List of Smartphones and Vehicle Used for Data Collection to Assess Effect of Smartphones on IRI Measurement

Vehicle	Smartphone Model
2011 Chevrolet Impala Vehicle parameters: M1 (kg): 500 M2 (kg): 45 C1 (N*s/m): 1,500 K1 (N/m): 10,000 K2 (N/m): 200,000	Samsung Galaxy SII
	Motorola Droid
	Nexus 4
	Samsung SM G900V
	Samsung Galaxy S IV

It should be mention that this 2-mile test section has two different types surface texture, where the first mile had a regular hot mix asphalt surface and the second mile and beyond had a newly placed surface, thin surface treatment (Figure 5.30). An interesting observation was that the inertial profiler produced very high IRI values beyond the second milepost, despite the fact that the segment was observed to have a new, relatively smooth surface-treatment as a surface.



Figure 5.30: Second 1-mile Segment of County Highway 32 (newly placed surface treatment)

Figure 5.31 shows IRI results measured using different smartphones with the 2011 Chevrolet Impala vehicle and inertial profiler on county highway 32. From Figure 5.31, it can be seen that the Motorola Droid phone measures higher IRI than that of the inertial profiler or other smartphones over most of the pavement sections. On the other hand, the Samsung SM G900V, Samsung S2, and Nexus 4 estimated similar IRI values as compared to the inertial profiler. The Motorola Droid is very heavy phone compared to the other phones used in this study, which may have had a significant effect on IRI estimation.

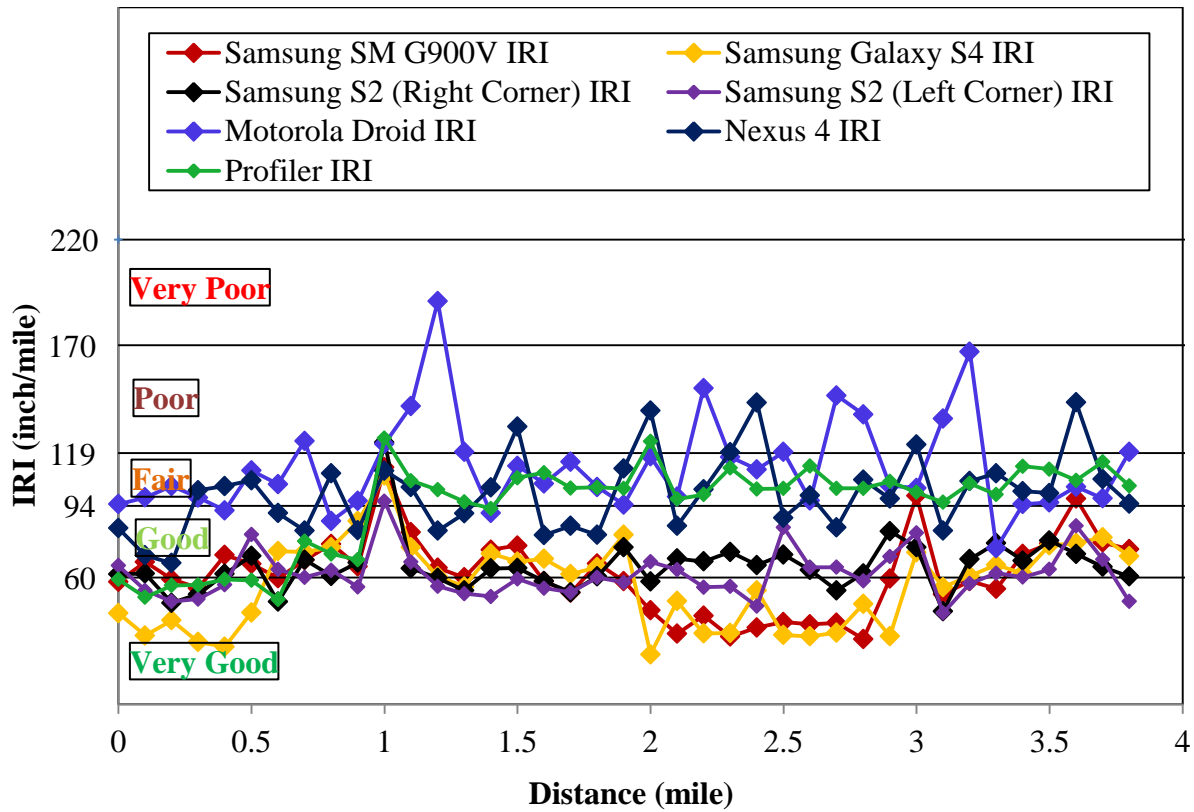


Figure 5.31: Estimation of IRI using Six Smartphones for Chevrolet Impala Vehicle Driven on County Highway 32

Smartphone/Roughness Capture measured IRI values were averaged over every 0.1-mile section and plotted in Figure 5.32. Figure 5.32 shows inertial profiler measured IRI and the average IRI measured by six smartphones mounted in the Chevrolet Impala vehicle. It can be noticed that smartphone measured IRI values averaged over all smartphones were similar to those of the inertial profiler in the first 1-mile segment.

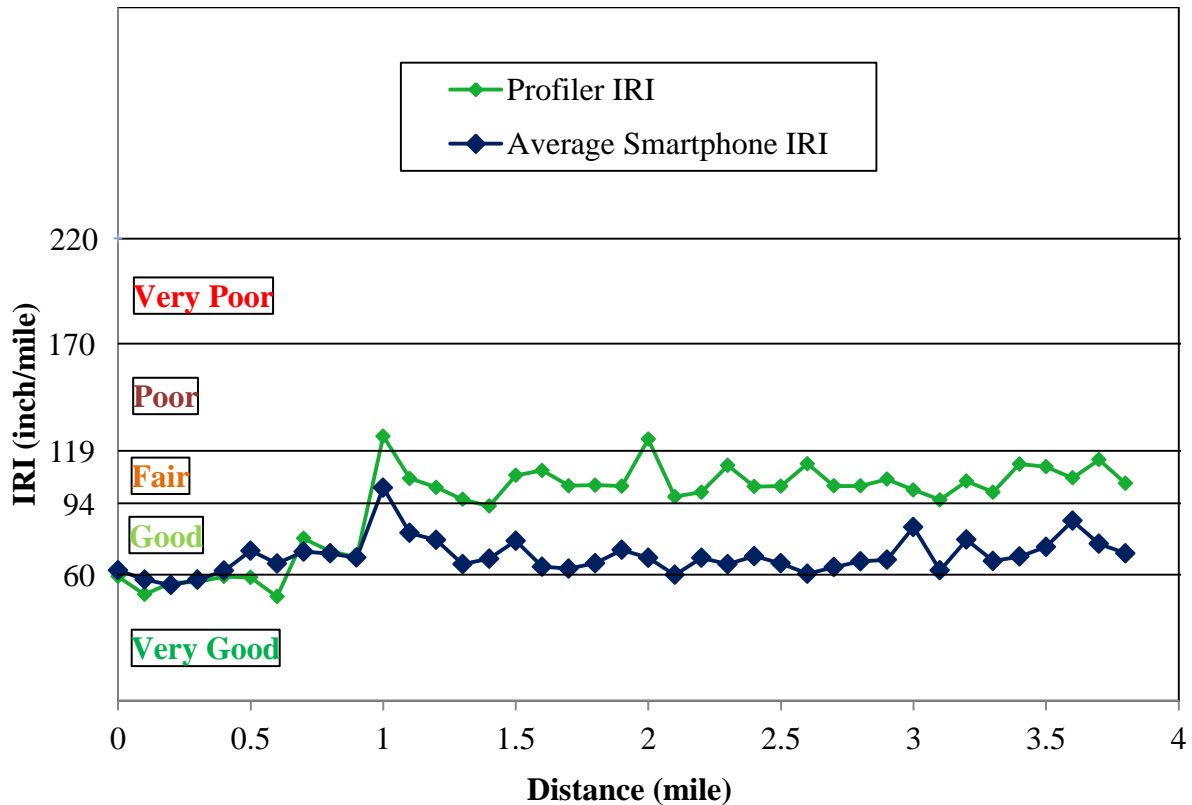


Figure 5.32: Estimation of Average IRI by Smartphones Using Chevrolet Impala Vehicle at County Highway 32

Figure 5.33 shows the inertial profiler and different smartphone measured IRI values collected on county highway 9. The Motorola Droid phone measured significantly higher IRI values, similar to the trend noticed for county highway 32. The other five smartphones produced similar IRI values when compared to the inertial profiler. Figure 5.34 shows the average IRI values as measured by the six smartphones alongside those collected with the inertial profiler. With the exception of the Motorola Droid, good correspondence between smartphone measured IRI values and the inertial profiler for most of the pavement sections was observed.

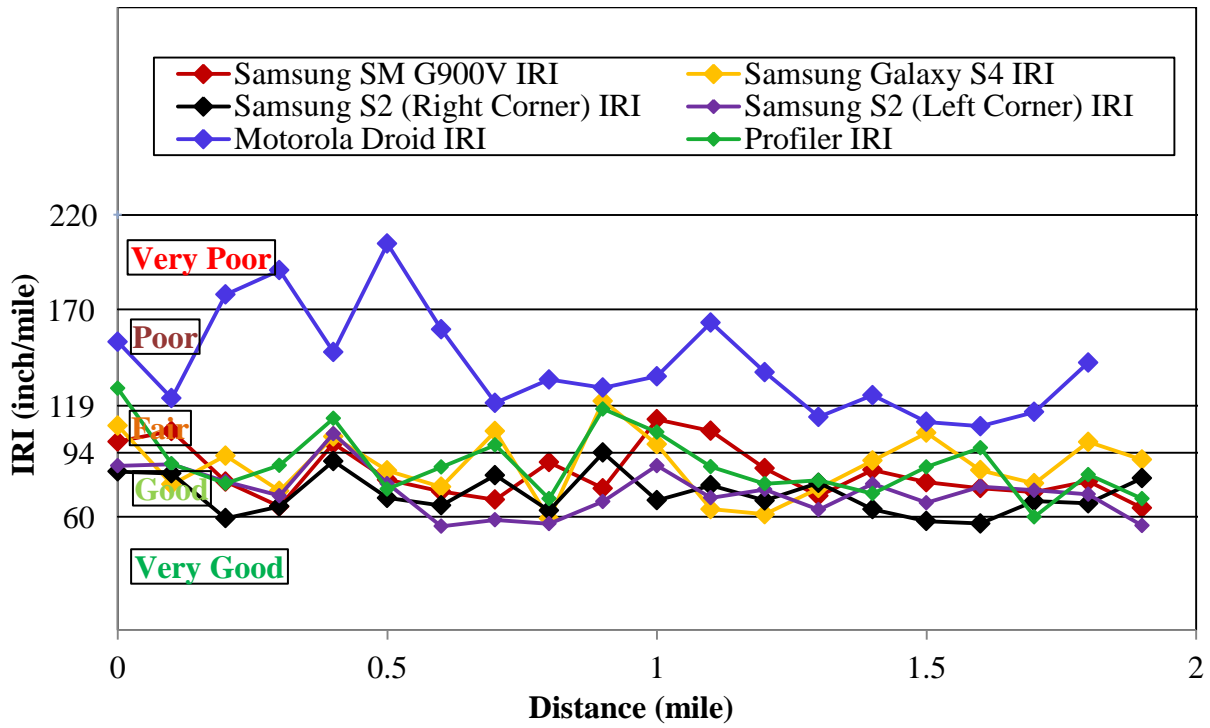


Figure 5.33: Estimation of IRI by Six Smartphones Using Chevrolet Impala Vehicle - County Highway 9

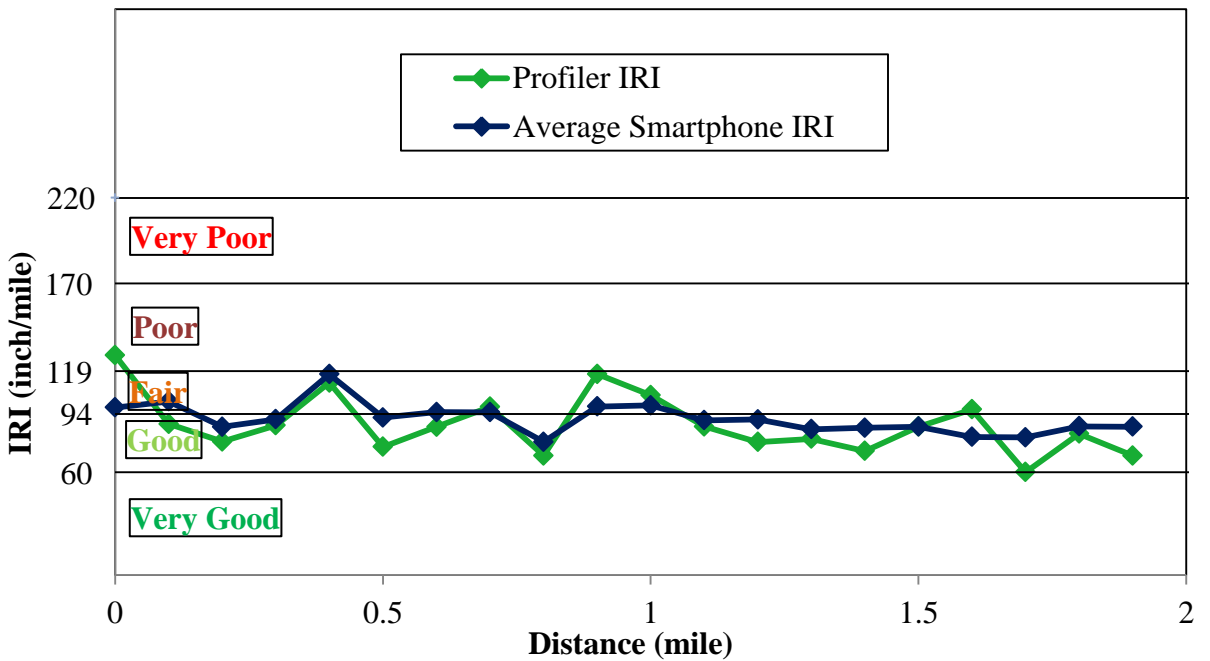


Figure 5.34: Estimation of Average IRI collected from Smartphones Using Chevrolet Impala Vehicle - County Highway 9

In Figure 5.35, IRI values from highway 23 (rough pavement section) as collected by the inertial profiler and six different smartphones are plotted. Similar to county highway 32 and 9, the Motorola Droid phone measured significantly higher IRI values than that of the inertial profiler and five other smartphones. In addition, the 5 other smartphones produced lower IRI values than that of inertial profiler. As explained earlier, although the state space model with calibrated vehicle parameters estimates IRI better than double integration scheme, the smartphone application somewhat underpredicts IRI due to lower sampling rates (140 Hz) as compared to the inertial profiler (1 kHz) on rough pavement.

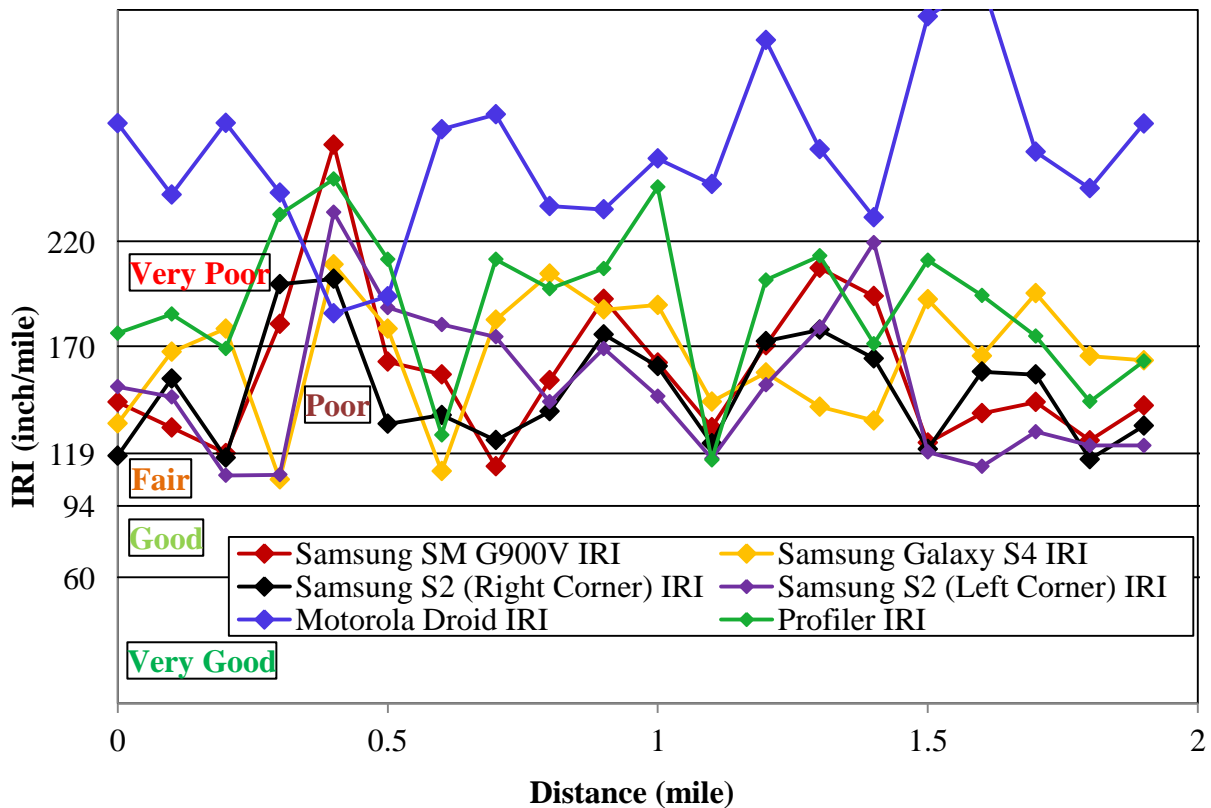


Figure 5.35: Estimation of IRI by Six Smartphones Using Chevrolet Impala Vehicle at County Highway 23

Figure 5.36 shows averaged IRI measured using six different smartphones by using a Chevrolet Impala vehicle at county highway 23 and that of the inertial profiler. Although the smartphone measures somewhat lower IRI for the relatively rough county highway 23 pavement, most of the values are within acceptable limits as shown in Section 5.10.

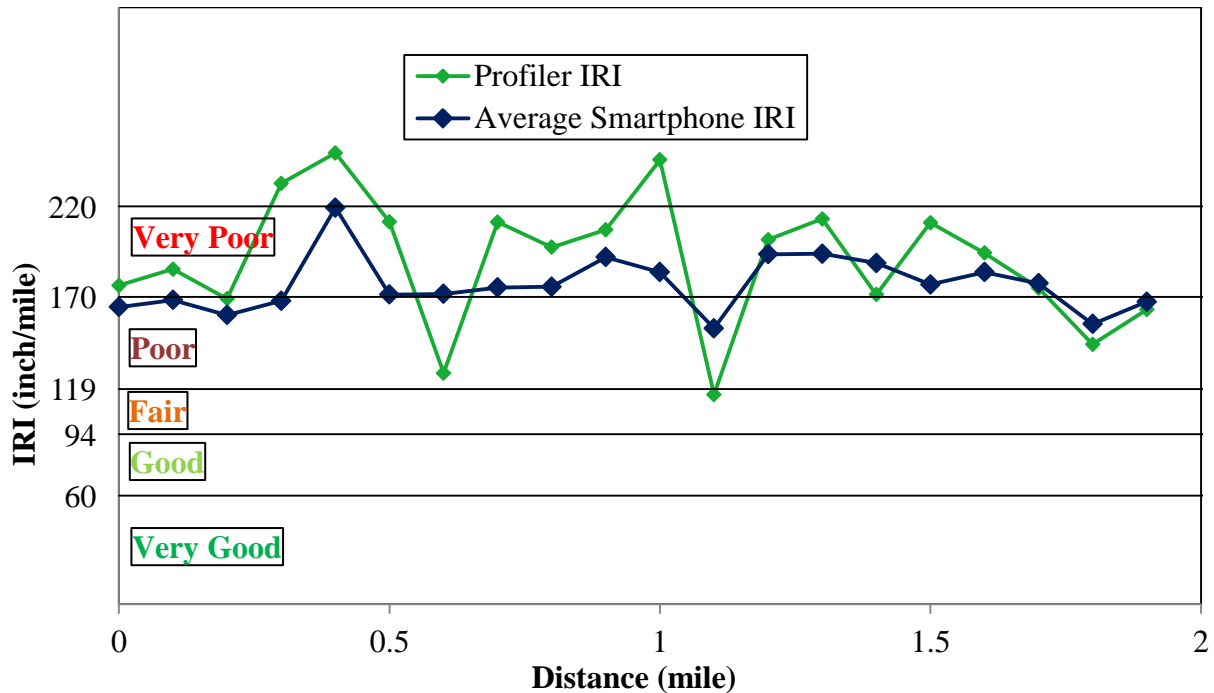


Figure 5.36: Estimation of Average IRI by Smartphones Using Chevrolet Impala Vehicle at County Highway 23

5.9 EFFECT OF DIFFERENT VEHICLES ON IRI

Pavement roughness data has been collected from three different test sections with four different vehicle types, including a 1999 Honda CRV, a 2007 Mazda3, a 2010 Dodge Avenger, and a 2011 Chevrolet Impala. It needs to be mentioned here that roughness data has been collected at different times. Therefore, it is possible that IRI might have changed over time. For instance, a new surface treatment layer has been placed across the second mile of the 2-mile test segment of county highway 32. It has been found that the inertial profiler measured significantly higher IRI than the first mile section irrespective of new smooth surface layer (Figure 5.30).

Figure 5.37 shows pavement roughness data collected by four vehicles from county highway 32. From Figure 5.37, it can be seen that IRI values measured by the smartphone application depends on the vehicle used for data collection. As different vehicles have different mass and suspension system characteristics, these parameters significantly affect the IRI measurement by smartphone application. Among these four types of vehicle, the 2007 Mazda3 measured higher IRI than that of the inertial profiler and other vehicles. The 1999 Honda CRV and 2011

Chevrolet Impala measured similar IRI compared to the inertial profiler across the first mile of this test section.

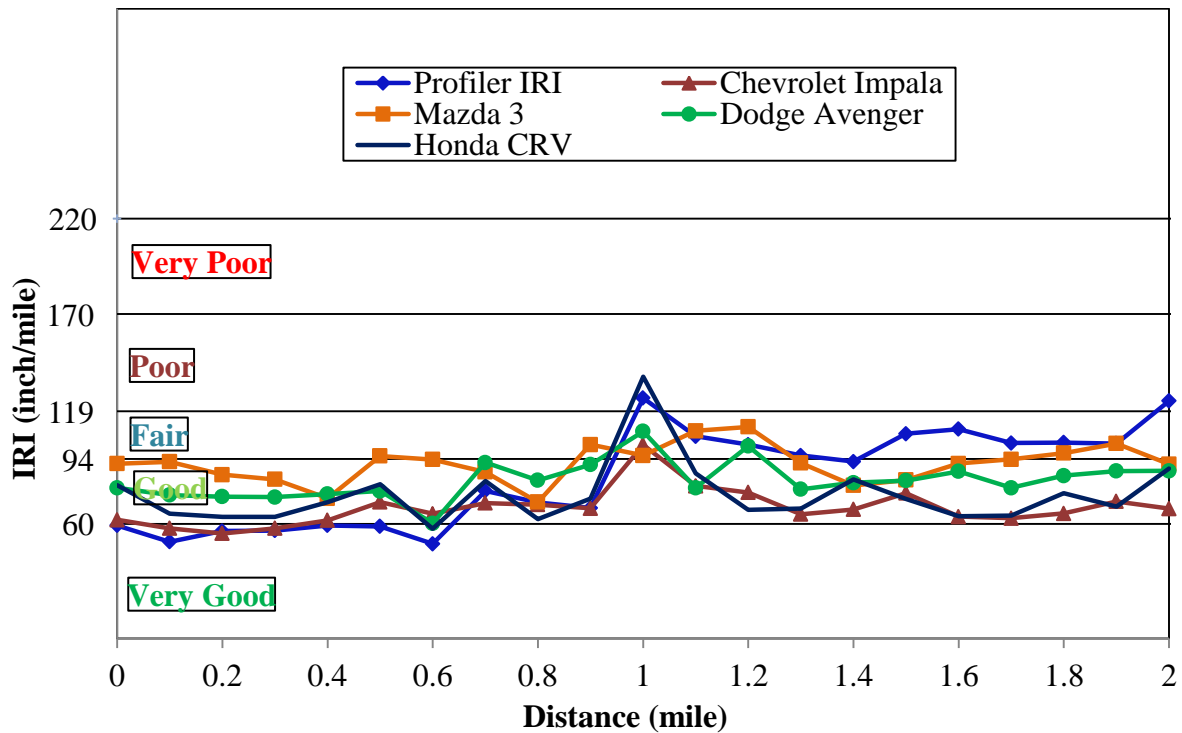


Figure 5.37: Average IRI Measured by Different Smartphones by Different Vehicles at CH32

Figure 5.38 shows the average IRI value measured by the four vehicles used this study. From Figure 5.38, it can be seen that smartphones measured higher for the first mile of the pavement section than that of the inertial profiler IRI. It needs to be mentioned here that four smartphones have been used to collect data, and Motorola Droid measured significantly higher IRI values than other phones. It is possible that IRI measured by the Motorola Droid might have affected the average IRI values.

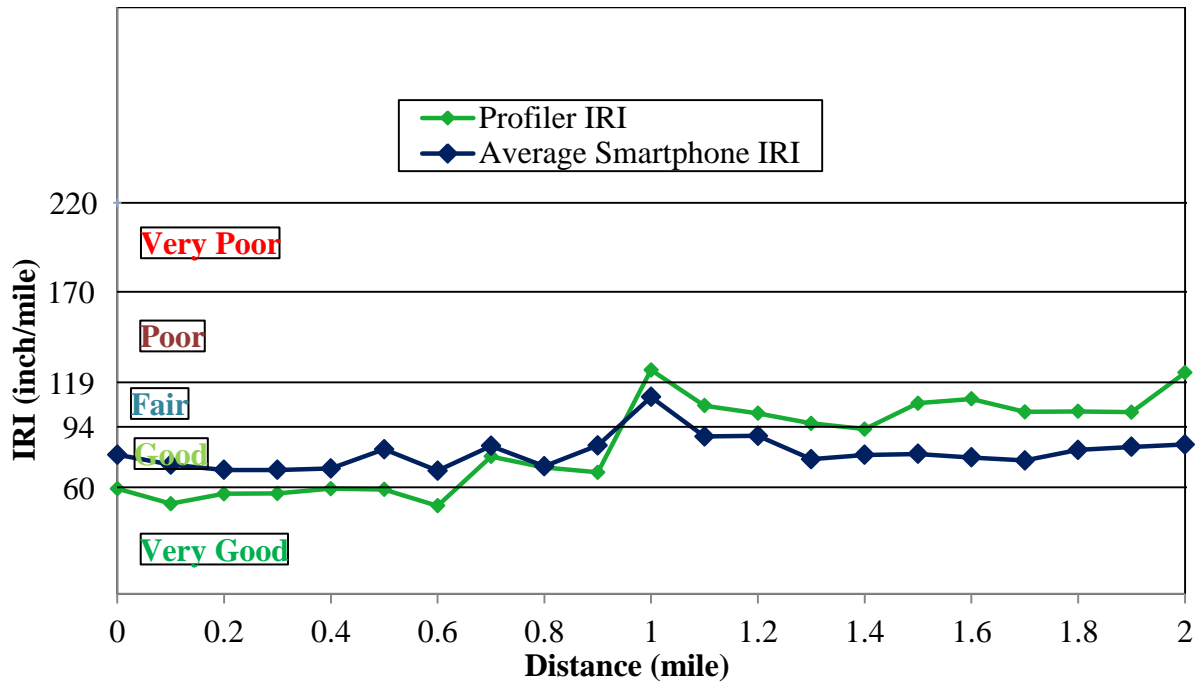


Figure 5.38: Average IRI Measured by All Smartphones and All Vehicles at CH32

Figure 5.39 shows average IRI measured by different vehicles at county highway 9. It can be noticed that both the 2007 Mazda3 and 2010 Dodge Avenger measured higher IRI values than that of the inertial profiler, and this trend has also been observed at county highway 32. Both the 1999 Honda CRV and 2011 Chevrolet impala measured similar IRI compared to the inertial profiler, which was also observed at county highway 32.

Figure 5.40 shows average IRI measured using different smartphones and different vehicles on county highway 9. It can be seen that the average IRI measured by smartphones using different vehicles is similar to those of the inertial profiler over most of the 0.1-mile pavement section.

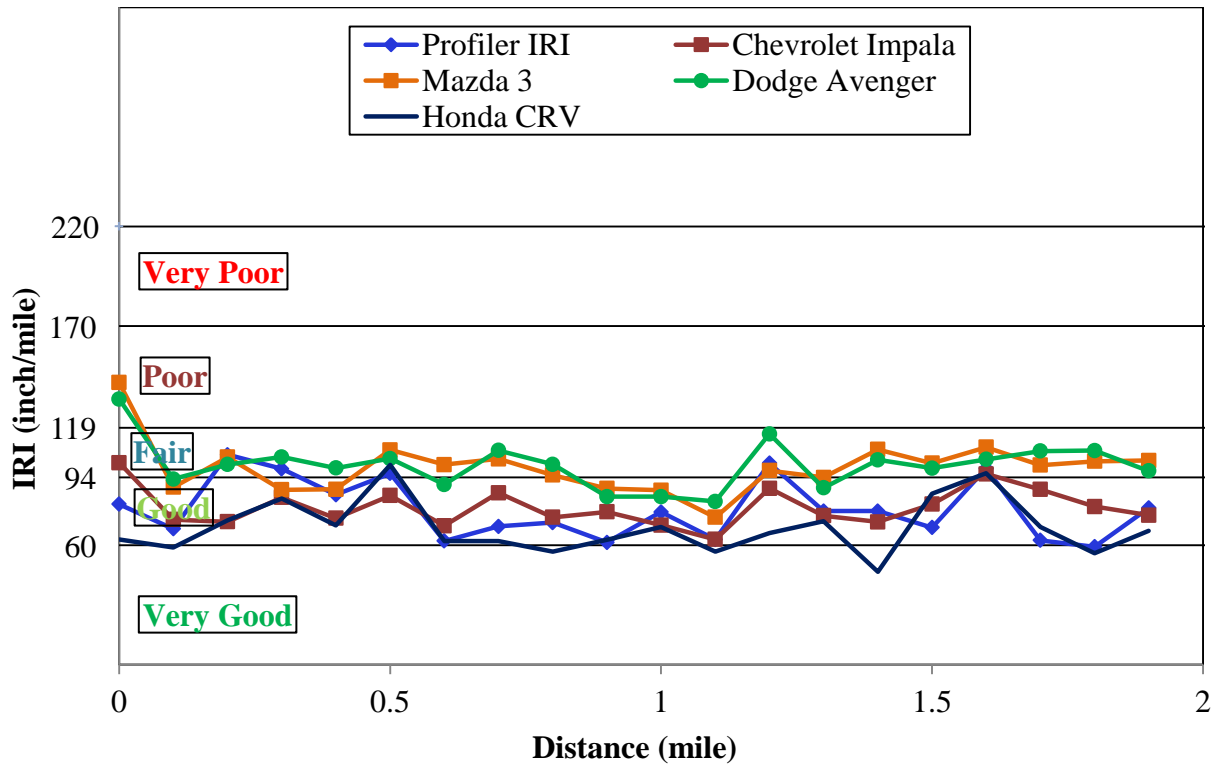


Figure 5.39: Average IRI Measured by Different Smartphones by Different Vehicles at CH 9

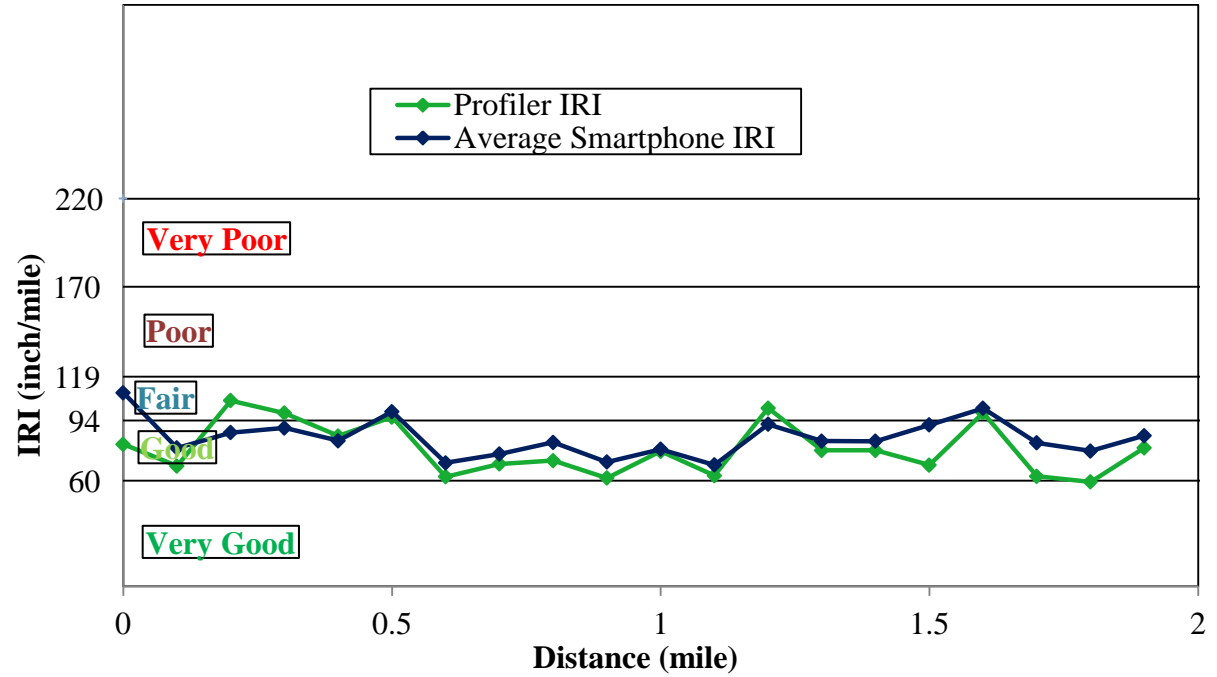


Figure 5.40: Average IRI Measured by All Smartphones and All Vehicles - County Highway 9

Figure 5.41 presents results from county highway 23. It can be seen that IRI values measured by the four test vehicles are lower than that of inertial profiler for the most of the 0.1-mile pavement sections. In this test, there were a lot of significant transvers cracks and longitudinal cracks along the right wheel path. Figure 5.42 shows the averaged IRI results for this section. As before, IRI is somewhat underpredicted by cell phones on rough pavement, even with the improved algorithm and first attempt at calibration. This suggests that additional calibration may be needed.

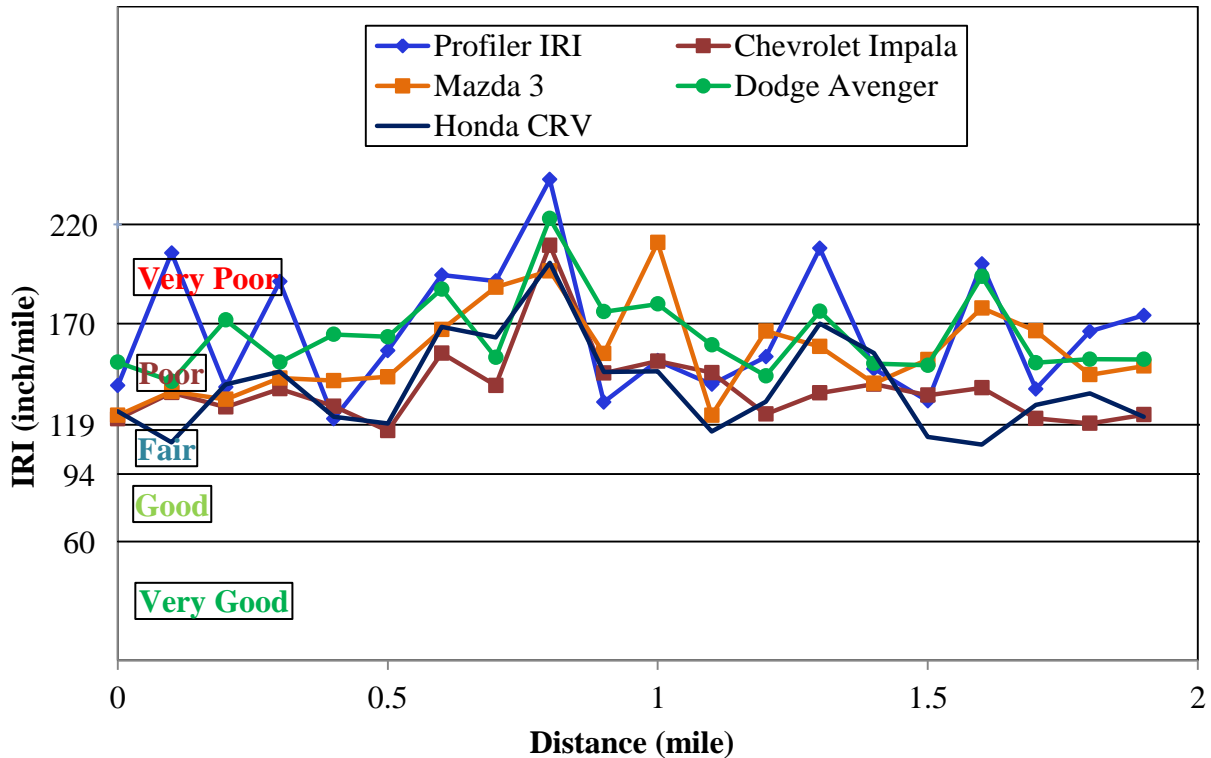


Figure 5.41: Average IRI Measured by All Smartphones and All Vehicles - County Highway 23

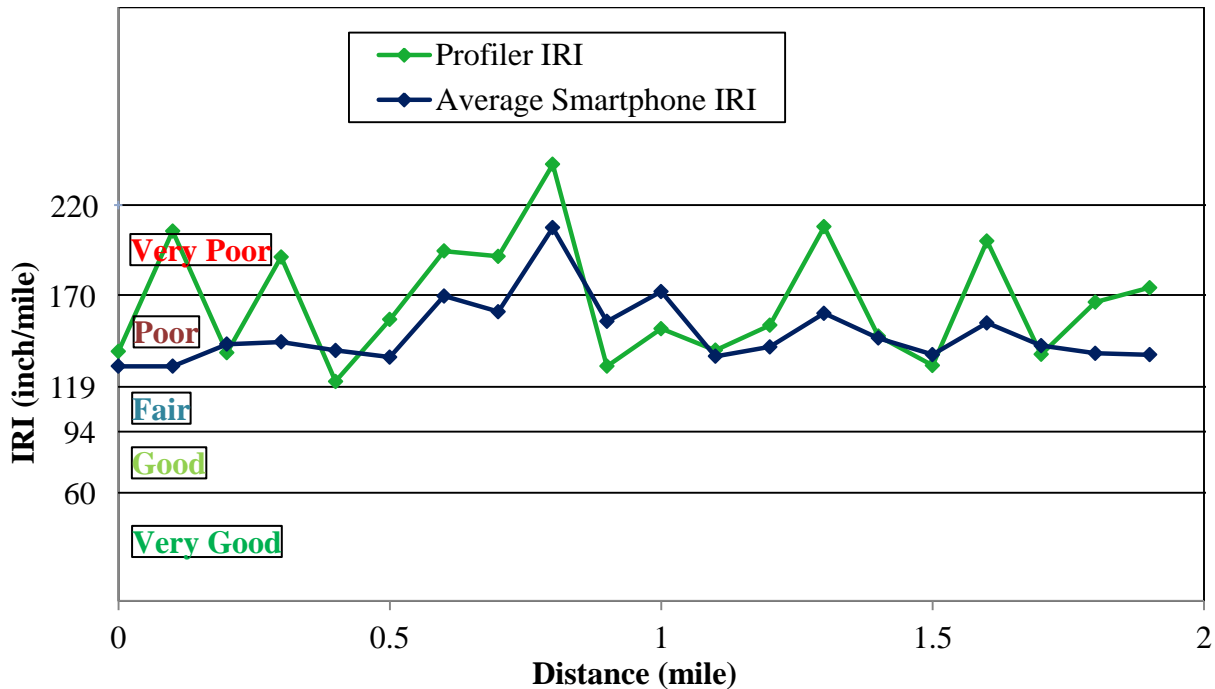


Figure 5.42: Average IRI Measured by All Smartphones and All Vehicles - County Highway 23

Another challenge with rough pavement is the variability in roughness measurements based on the lateral position of the test vehicle from pass to pass if replicate runs are made over a given pavement section. To illustrate this point, pavement roughness data has been collected on county highway 23 (very rough) with two replicate passes of the inertial profiler, as shown in Figure 5.43. Significant differences in IRI values can be observed at a few sections between the two repetition runs. This results from the inability to drive along the exact same wheel path (i.e., lateral trajectory as a function of position along test section); therefore, significant variation in IRI measurement can be observed from run-to-run. Such variations are likewise inherent in smartphone roughness data, which can be combined with the differences in vehicle axle spacing, tire spacing, suspension characteristics, etc.

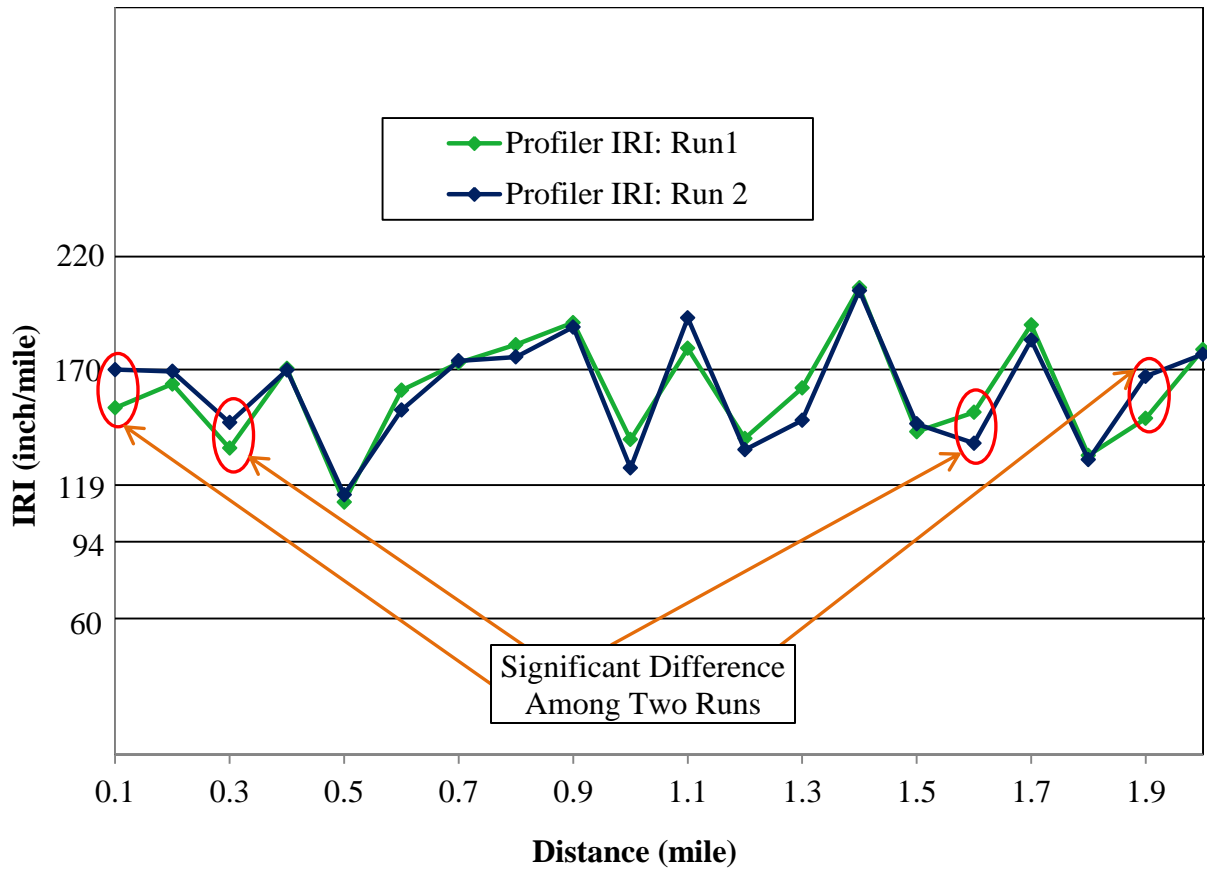


Figure 5.43: Variation of IRI Measurement Using Inertial Profiler

It can thus be presumed that better estimation of IRI might be possible with a large number of smartphones and vehicles. For instance, if a fleet of vehicles and large number of smartphones are used to collect pavement roughness data through crowd sourcing, it might be possible to arrive at a more robust and holistic viewpoint of pavement roughness and its effect on rider comfort and safety, particularly for rough pavements.

5.10 STATISTICAL ANALYSIS OF IRI DATA

As it has been noticed that smartphone application and inertial profiler IRI data are not identical, it is required to check whether they are significantly different or equivalent within a confidence interval. Analysis of variance (ANOVA) has been performed to assess whether inertial profiler and smartphone application measured IRI values are significantly different. ANOVA is used to test the null hypothesis that the means of several populations are all equal.

Null hypothesis: $H_0: \mu_1 = \mu_2$

Alternative hypothesis: H_1 : at least one of the means is different.

If $F < F_{crit}$, we accept the null hypothesis. This is the case here. Therefore, we accept the null hypothesis. The means of the two populations are all equal. Table 5.8 shows ANOVA results of IRI data collected from county highway 32, 9 and 23.

Table 5.8: ANOVA Results of IRI DATA

ANOVA of County Highway 32 Data						
Source of Variation	SS	df	MS	F	P-value	F crit
Between Groups	274.68	1	274.68	0.75753	0.3893	4.08475
Within Groups	14504	40	362.599			
Total	14778.6	41				
ANOVA of County Highway 9 Data						
Source of Variation	SS	df	MS	F	P-value	F crit
Between Groups	381.086	1	381.086	2.28391	0.13899	4.09817
Within Groups	6340.56	38	166.857			
Total	6721.65	39				
ANOVA of County Highway 23 Data						
Source of Variation	SS	df	MS	F	P-value	F crit
Between Groups	1753.07	1	1753.07	2.29956	0.13769	4.09817
Within Groups	28969.3	38	762.349			
Total	30722.3	39				

From Table 5.8, it can be seen that F is less than F crit for county highway 32, 9, and 23. As a result, null hypothesis is accepted which indicates that means of inertial profiler measured IRI are equal to that of smartphone application.

Equivalence test was also performed to three different sections with average IRI of 53.1, 111.6, and 195.9 in/mi. Equivalence provides the idea whether means of inertial profiler and smartphone application measured IRI are close enough to be considered equivalent. In equivalence test, the null hypothesis is that the difference between the means of smartphone application and inertial profiler measured IRI values is greater than a threshold value (d), which

is referred as equivalence interval. If μ_s and μ_i be the mean responses of the smartphones application and inertial profiler measured IRI, the null hypothesis is $|\mu_s - \mu_i| > d$. The threshold value defines a difference that is not large enough to have any effect on measurement. The rejection of null hypothesis will indicate that IRI measurements by smartphone application and inertial profiler are equivalent. Figure 5.43, 5.44, and 5.45 show results of the equivalence test.

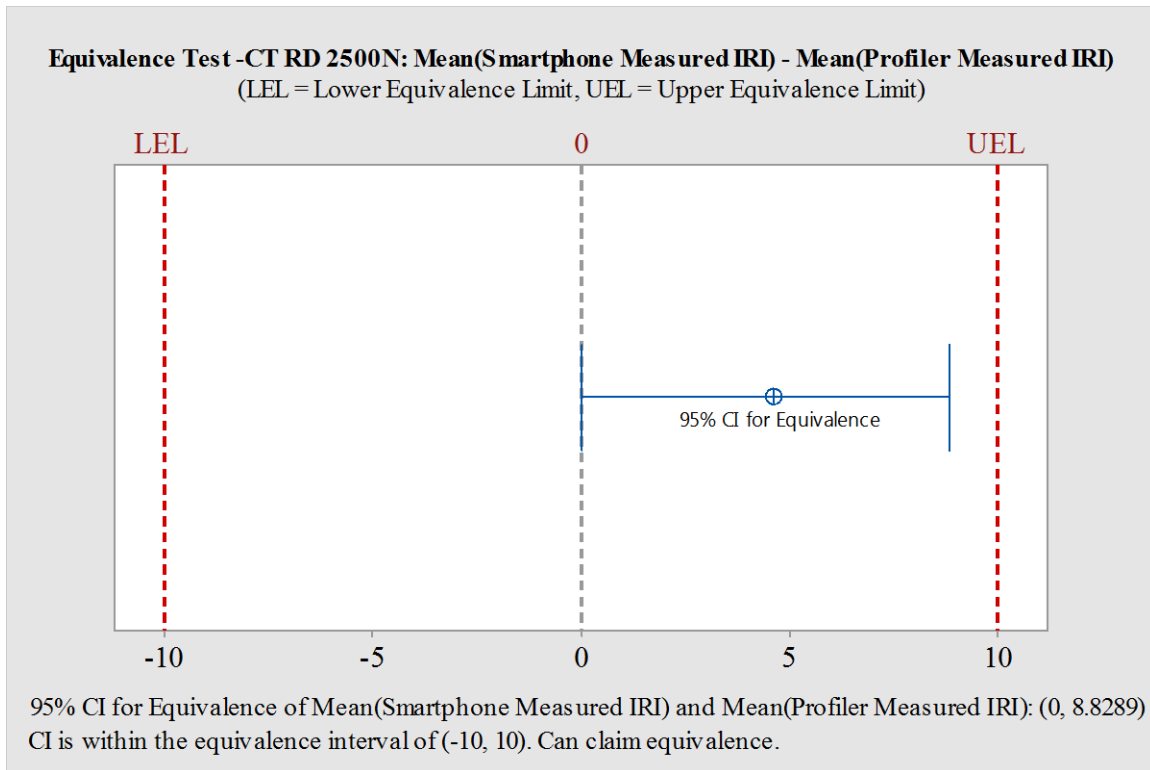


Figure 5.44: Equivalence Test Result of County Road 2500N IRI Data (Smooth Pavement)

In Figure 5.43, the lower and upper equivalence limits represent lower and upper limits of equivalence interval. For smooth pavement (Figure 5.43), it was found that smartphone and profiler measured IRI values are equivalent with 95% confidence level with the equivalence interval of (-10, 10). This implies that if smartphone and inertial profiler measured IRI values are differed by 10 in/mi, they would be considered equivalent.

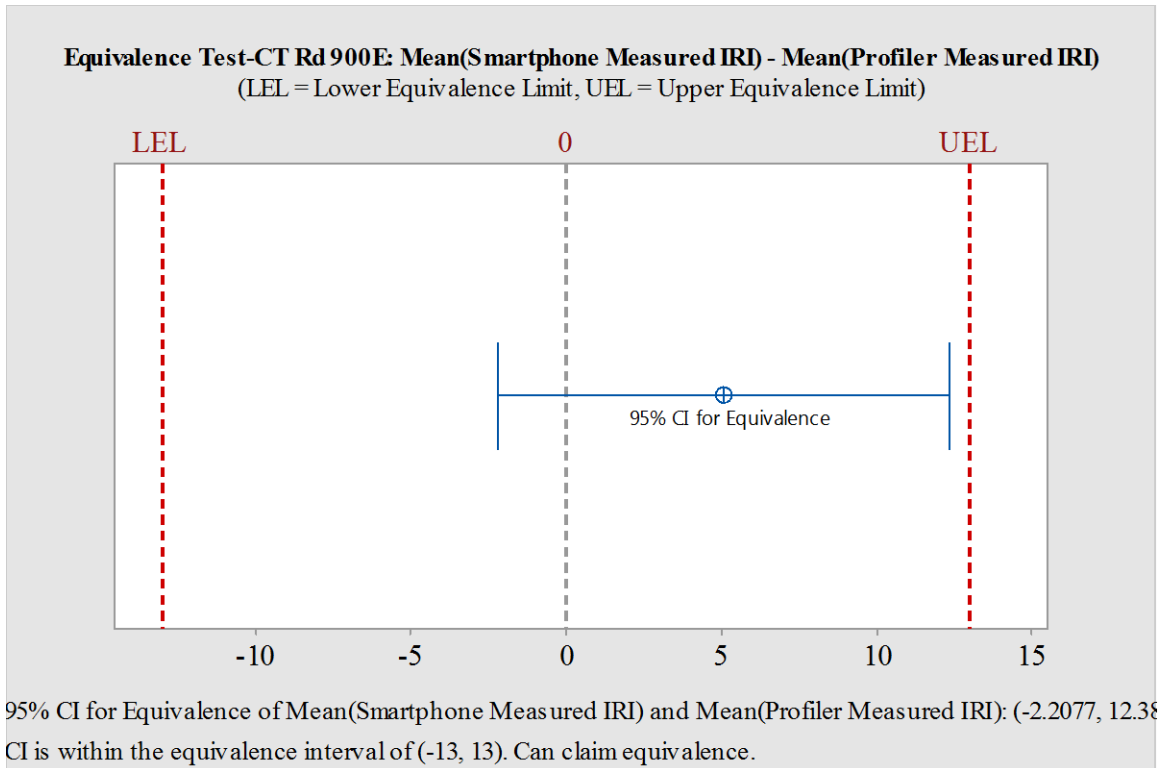


Figure 5.45: Equivalence Test Result of County Road 900E IRI Data (Medium Rough Pavement)

For medium rough pavement a slightly higher equivalence interval (-13, 13) was considered. It was found that means of smartphone application and inertial profiler IRI are equivalent with 95% confidence level if the equivalence interval is (-13, 13). Considering the high IRI values (95-165 in/mi) and lower data collection costs, it is justifiable to increase the equivalence interval to this level.

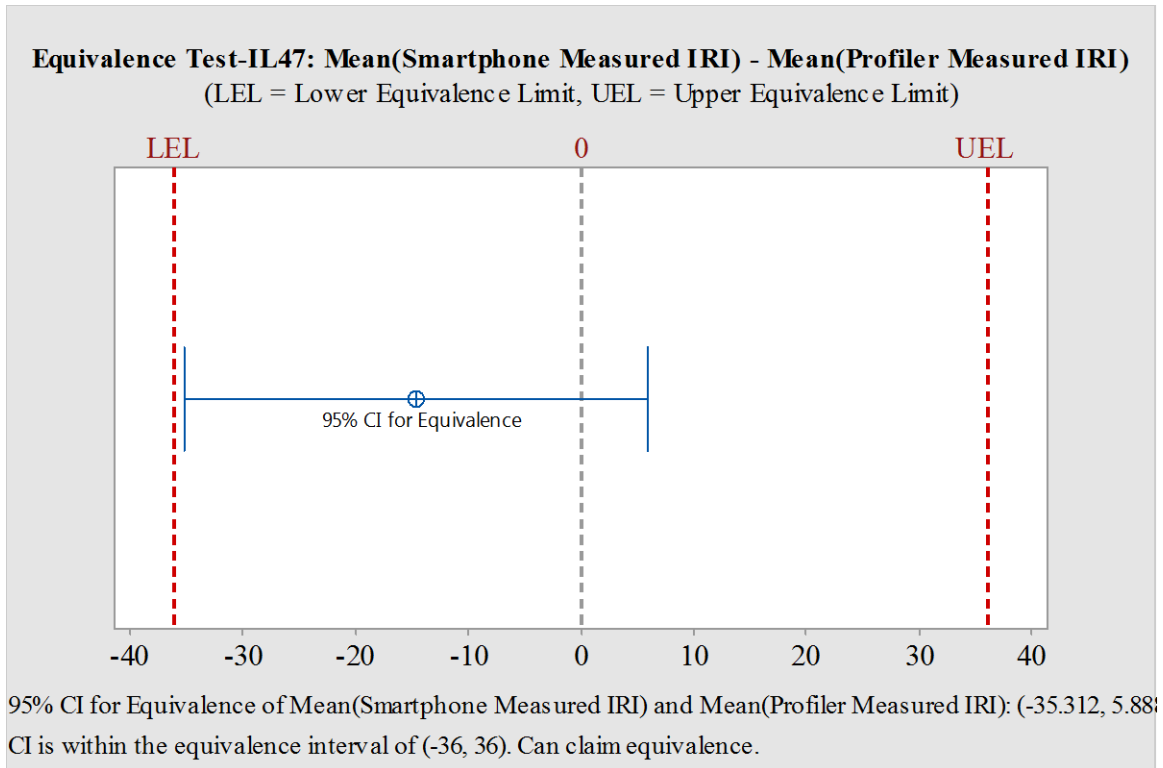


Figure 5.46: Equivalence Test Result of IL-47 IRI Data (Very Rough Pavement)

It was discussed earlier that smartphone application underpredicts pavement IRI for very rough pavement. Therefore, several trials were performed to find the equivalence interval for which smartphone application and inertial profiler measured IRI are equivalent with 95% confidence interval. From Figure 5.45, it can be seen that means of smartphone application and inertial profiler measured IRI values are equivalent if the equivalence interval is (-36, -36).

5.11 MAP-21 ROUGHNESS DATA COLLECTION

The Moving Ahead for Progress in the 21st Century Act (MAP-21) was signed into law P.L. 112-114 on July 6, 2012 [87]. In Section 1203 of the MAP-21 [87], it has been stated that,

“performance management will transform the Federal-aid highway program and refocus it on national transportation goals, increase accountability and transparency of the Federal-aid highway program and improve project decision making through performance-based planning and programming.”

According to MAP-21 legislation, states are now required to [59]:

- Set performance target for pavement condition on Interstate and non-Interstate national highways system roads
- Interstate and non-Interstate pavement condition data are required to submit to Highway Performance Monitoring System (HPMS) annually and biennially, respectively.

According to the recommendation of AASHTO SCOPM MAP-21 Notice of Proposed Rule-Making Taskforce [88], four types of pavement condition information must be reported for every 0.1-mile pavement section, including percentage of pavement sections in good and poor condition based on International Roughness Index (IRI), cracking percentage, rutting, and faulting. In terms of IRI, the attributes shown in Table 5.9 need to be reported for Interstate and non-Interstate national highway system roadways.

Table 5.9: MAP-21 Data Reporting Requirements [87]

Performance Measure	Data
(1) % pavements on the Interstate Systems in Good condition	<ol style="list-style-type: none"> 1. IRI 2. % Cracking 3. Rutting 4. Faulting
(2) % pavements on the Interstate Systems in Poor condition	
(3) % pavements on the NHS in Good condition	
(4) % pavements on the NHS in Poor condition	

This taskforce also recommended classification of pavement smoothness based on the IRI threshold values shown in Table 5.10.

Table 5.10: Pavement Smoothness Category Based on MAP-21 [86]

Surface Type	IRI (inch/mile)	Rating	Area
All Pavements	< 95	Good	
	95 - 170	Fair	Areas with a population <1 million
	95 - 220	Fair	Urbanized areas with population \geq 1 million
	> 170	Poor	Areas with a population <1 million
	> 220	Poor	Urbanized areas with population \geq 1 million

The smartphone-based roughness system developed in this study is now assessed in terms of its ability to classify pavement according to MAP-21 criteria. For this assessment, vehicle vertical acceleration data were collected using four different vehicles and six smartphones, and average IRI values predicted using state space model with calibrated vehicle parameters has been compared with the inertial profiler. Figure 5.46 and 5.47 provides a summary of results. The vertical axis has been labeled according to MAP-21 smoothness criteria threshold values. From Figure 5.46, it can be seen that the smartphone based IRI assessment system developed herein is able to categorize pavement condition based on roughness accurately for most of the pavement sections within the county highway 9 test section.

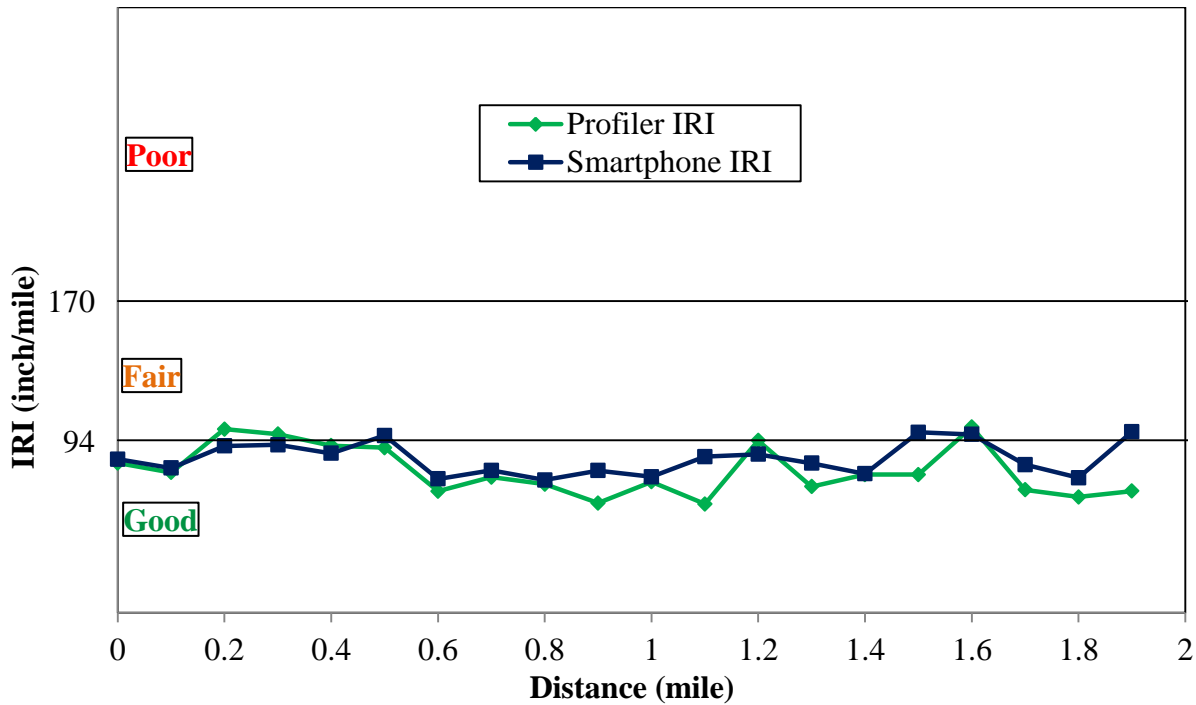


Figure 5.47: County Highway 9 IRI Data with MAP-21 Criteria

Figure 5.47 shows the results obtained using the aforementioned techniques for county highway 23, again plotted alongside the industry standard inertial profiler for reference. It can be seen that smartphone application categorized most of the pavement sections as fair condition as compared to existing the poor condition. Again, it is believed that a higher sampling rate would likely improve the underestimation observed in some of the test segments. Overall; however, it appears that smartphone based, crowdsourced IRI measurements may be a useful, highly cost effective tool for helping states meet MAP-21 data collection requirements, particularly for smooth to moderately rough routes, and as cell phone data collection rates improve.

Future work is still needed to address the effect of vehicle speed on pavement roughness estimation and the demonstration of technology to illustrate benefits of a crowd sourcing approach. Having ‘big roughness data’ should yield improved estimates and possibly real-time roughness assessment. This will be particularly useful for spring thaw conditions and during construction. And with improved smartphone data collection rates, IRI estimates for rough pavements are expected to improve, possibly eliminating the current need for minor calibration.

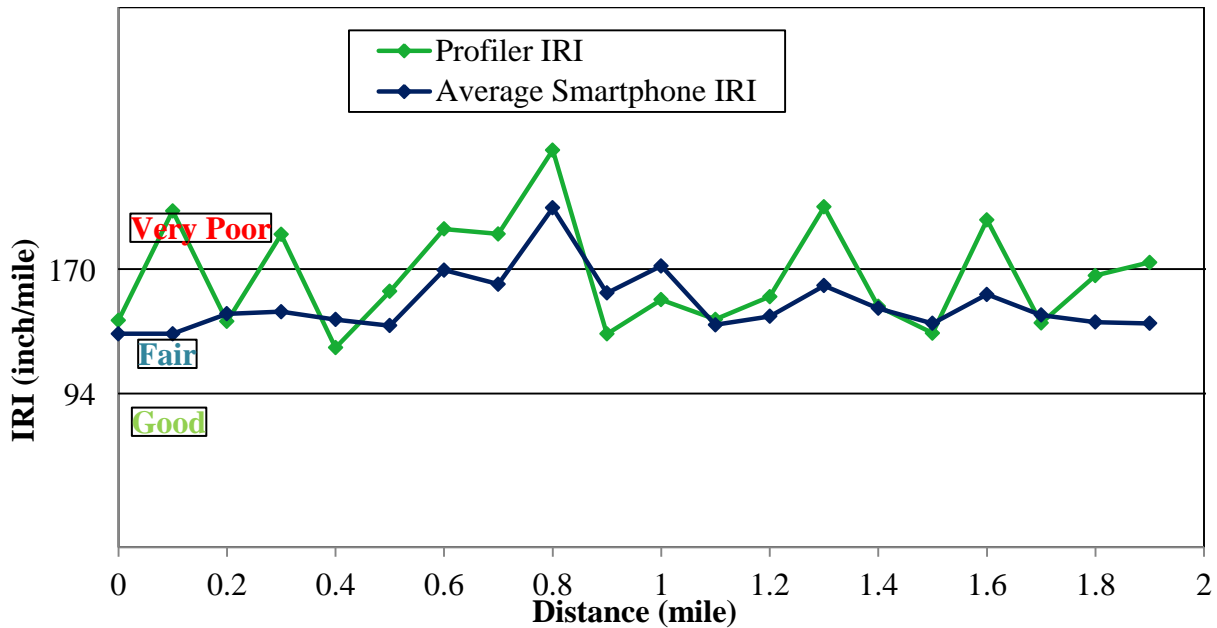


Figure 5.48: County Highway 23 IRI Data with MAP-21 Criteria

5.12 SUMMARY AND CONCLUSIONS

Pavement roughness data is a critical input for maintenance and rehabilitation planning and overall pavement management. Moreover, the assessment of pavement roughness costs state and local agencies over a hundred million dollars to collect annually. A smartphone-based application was developed, called Roughness Capture, which was shown to be capable of measuring IRI data in a very efficient and economical manner, and which has the ability to be scaled up and made even more cost effective through cloud-based, crowd sourcing for data collection on a massive scale. A large experimental study was conducted to compare estimated IRI values against those obtained with an industry standard inertial profiler system. The study evaluated: different phones, different vehicles, pavements with wide range of IRI, a simple double integration and a more sophisticated state space model to analyze acceleration data, and statistical analysis such as ANOVA and equivalence testing.

Two schemes including double integration of acceleration data and inverse state space modeling, which attempts to address vehicle suspension dampening effects on roughness measurement, have been used to determine pavement profile, followed by a computation of pavement roughness. In the double integration scheme, acceleration data was integrated twice to obtain

displacement (relative vertical elevation versus distance). In the inverse state space modeling scheme, acceleration data was used as an input to determine road profile, along with the suspension parameters of the vehicle used for data collection. In addition, as part of this work, a MATLAB script was developed to estimate IRI from the pavement; therefore, it is now possible to conveniently determine IRI directly from acceleration data without using the more cumbersome and commercial ProVAL software. The conclusions drawn in this study were:

(a) With the double integration of acceleration scheme, Roughness Capture application was able to estimate similar IRI as compared to that of the inertial profiler for two test sites where pavements had smooth to medium roughness. However, the app estimated significantly lower IRI than that of the inertial profiler at site 3, where the pavement was much rougher, having significant transverse cracking, longitudinal cracking, and other localized surface distresses. The coefficients of variance (COV) for multiple runs were in the range of 7-22, 4-28, and 4-22 percent for the three test sections.

(b) With the inverse state space model scheme, the Roughness Capture app estimated closer IRI values as compared to the inertial profiler. Although improvements were observed in the IRI estimation at site 3 compared to the double integration scheme, estimated IRI was still lower than that of the inertial profile for most of the pavement sections at this site, even after calibration. It appears that an improved data collection rate and/or the addition of empirical calibration would be needed to arrive at even more accurate results for rougher pavement sections. This scheme also led to improvements in the repeatability of IRI measurement, with COV's ranging from 3-19, 3-16, and 4-24 percent when using this scheme.

(c) As improvements were observed with the inverse state space model, data was collected from 14 different locations with a total length of about 60 miles to validate the results. It was observed that the average difference between inertial profiler and Roughness Capture app measured IRI was in the range of 7.8 in/mi at smooth pavements, and in the range of 24.5 in/mi for very rough pavements.

(d) As different smartphones possess different accelerometers, the effect of smartphone models was explored in this study. It was found that IRI measurement is in fact dependent on the smartphone used to collect acceleration data. It was observed that the Motorola Droid phone

(which was significantly heavier than the other phones used), estimated higher IRI than that of the inertial profiler and other smartphones. Samsung S2, Samsung SM G900V, and Nexus 4 estimated similar IRI values as compared to the inertial profiler.

(e) As the inverse state space model considers vehicle suspension parameters, the effect of different vehicles on IRI measurement using Roughness Capture app was also investigated. It has been found that the pavement roughness measured by the same smartphone depends on the vehicle used to collect acceleration data. Mazda3 (a compact car) measured higher IRI as compared to the inertial profiler and the other vehicles used in the study. A Chevrolet Impala and Honda CRV measured similar IRI values as compared to the industry standard inertial profiler.

(f) MAP-21 requires the States to provide pavement IRI data for every 0.1-mile pavement section for the Interstate and non-Interstate highway systems annually and biennially, respectively. In this study, it was found that the Roughness Capture app measured IRI data classifies most of the test sections with agreement to MAP-21 requirements.

CHAPTER 6

SURFACE IRREGULARITY DETECTION AND VISUALIZATION OF IRI IN ARCGIS

6.1 INTRODUCTION

Localized pavement surface distress detection and maintenance are very important for safety and for the control of further damage to pavements, as repair costs tend to increase exponentially with time when maintenance is delayed [88]. Although IRI provides an average assessment of the condition of existing pavements, it does not provide the location and severity of surface irregularities such as potholes, major crack sites, faults, blowups and other localized distress features. In addition, two different pavement profiles can generate the same IRI values even though the underlying distress types and locations may be completely different. Identifying surface irregularities and their location will help pavement management engineers to maintain those more efficiently, and to avoid more costly repairs, accidents, and can reduce tort liabilities.

6.2 DETECTION METHOD

A surface irregularity detection algorithm has been developed, as shown in Figure 6.1. For the purposes of feature detection, acceleration data collected by the smartphone application Roughness Capture must be filtered to remove non-critical surface irregularities of which there may be hundreds or even thousands per mile. To determine an appropriate threshold value, different sized pavement profile irregularities were experimentally investigated, along with different vehicle speeds. After detecting the localized distresses that cause discomfort to the drivers, location of those distresses will be shown in the google map. To show the location of detected distresses, a MATLAB script has been developed to link up google map and pothole/bump detecting algorithm.

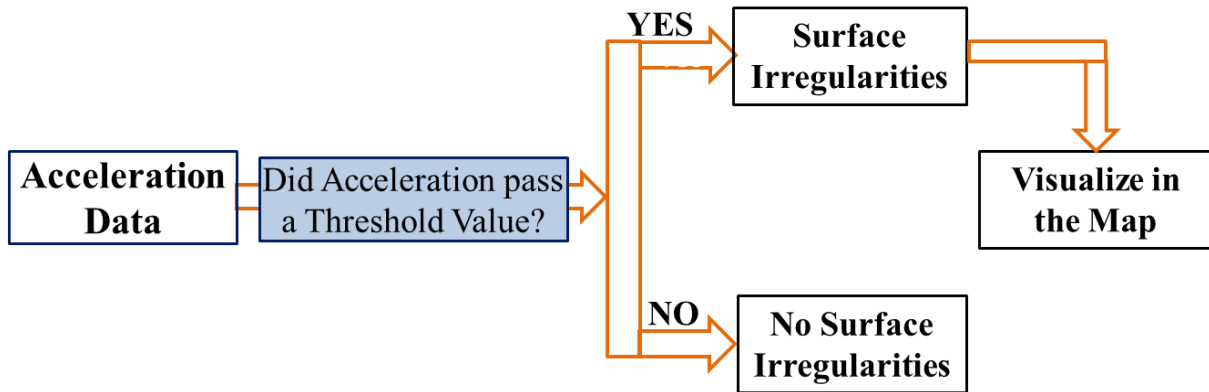


Figure 6.1: Pothole/Bump Detection Algorithm

6.3 DATA COLLECTION

Pavement data was collected using Roughness Capture from two test sections to examine the magnitude and direction of acceleration values generated when a vehicle encounters specific observable bumps and potholes. Bump data was collected on standardized speed bumps, located at a local store parking lot (Blain's Farm & Fleet), and on US 45, just north of Urbana, Illinois. At the parking lot location, four consecutive and identical speed bumps were used for testing, each having a rounded shape and average height of approximately 3 inches. The test vehicle (Mazda 3) was driven at 15 mph while collecting data. Pothole data was collected from the University of Illinois E-14 parking lot near Assembly Hall in south campus, shortly after it was resurfaced. Localized distress data was manually surveyed along US 45.



Figure 6.2: Vehicle Response to Bumps Data Collection at Blain's Farm and Fleet Parking Lot

Figure 6.3 shows vehicle response in terms of vertical acceleration when it encounters speed bumps located at the Blain's Farm and Fleet parking lot. A passenger car was driven at a speed of 15 mph to collect acceleration data. From Figure 6.3, it can be seen that whenever the vehicle hits a speed bump, the vertical acceleration becomes significantly higher (greater than 9 m/sec^2 in excess of gravity) in the positive direction with respect to the smartphone accelerometer axes. It can also be noticed that vertical acceleration values are nearly identical for each speed bump. Extrapolating, it can be deduced that, when a vehicle strikes a pothole, the vertical acceleration data trace from the smartphone would contain a high amplitude, negative acceleration event.

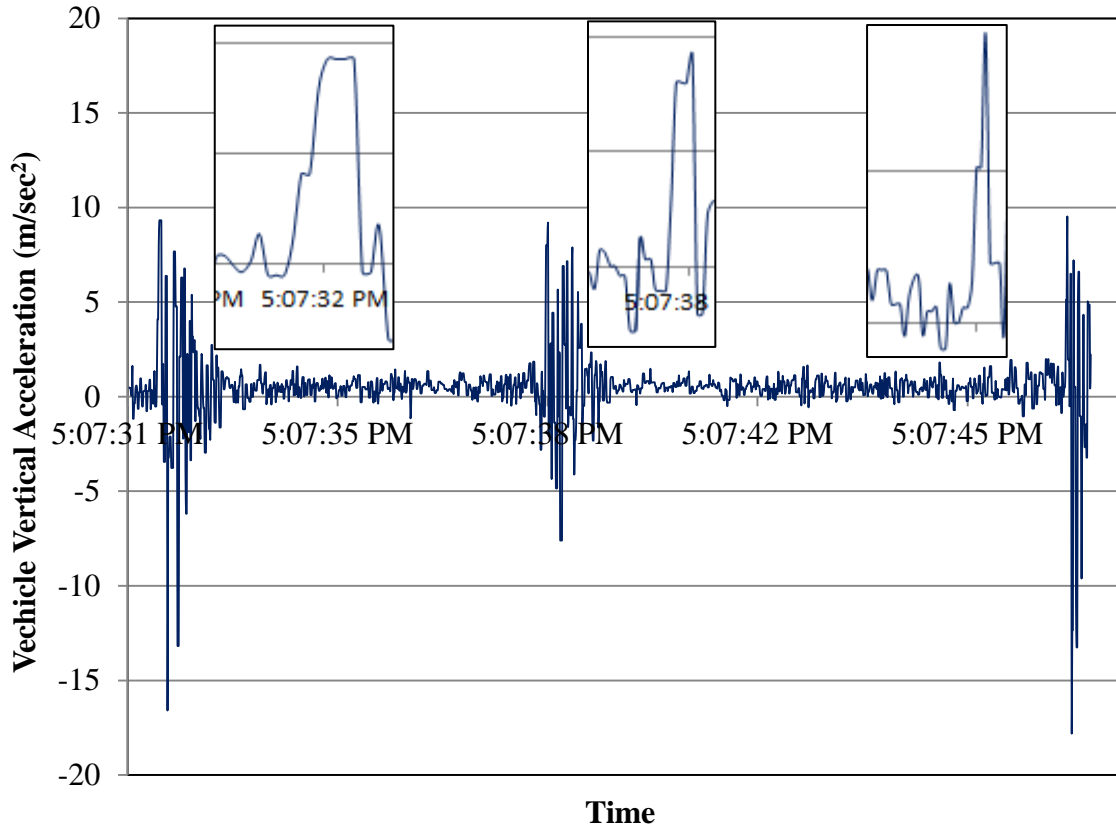


Figure 6.3: Vehicle Vertical Acceleration Collected from Blain’s Fleet and Farm Parking Lot Speed Bumps

6.4 DATA ANALYSIS

To determine an appropriate acceleration threshold value for use with pavement feature detection, data was collected using Roughness Capture and dashboard-mounted cell phones, and significant localized distresses (bump/potholes) were manually surveyed with each of the test sections. Acceleration data was filtered to identify acceleration values greater than 3.2, 3.4, 3.6, 3.8, 4.0 m/sec^2 above or below gravity ($9.81 m/s^2$). As a caveat, note that manually-identified pavement features are considered to be 100% detected; although it acknowledged that a degree of subjectivity is inherent in such an assessment. To reduce anomalies in manual feature detection, localized distress data was collected three times in each of the test sections. Figure 6.4 presents the percentage of significant localized distresses detected by the smartphone application as a function of the acceleration threshold value used. From Figure 6.4, it can be seen that a threshold value in the range of 3.2-3.8 m/sec^2 detected significantly higher localized distresses

than that identified via manual identification. Using a threshold value of 4 m/sec², all smartphones used were found to detect localized distresses in reasonable agreement with those that were manually detected.

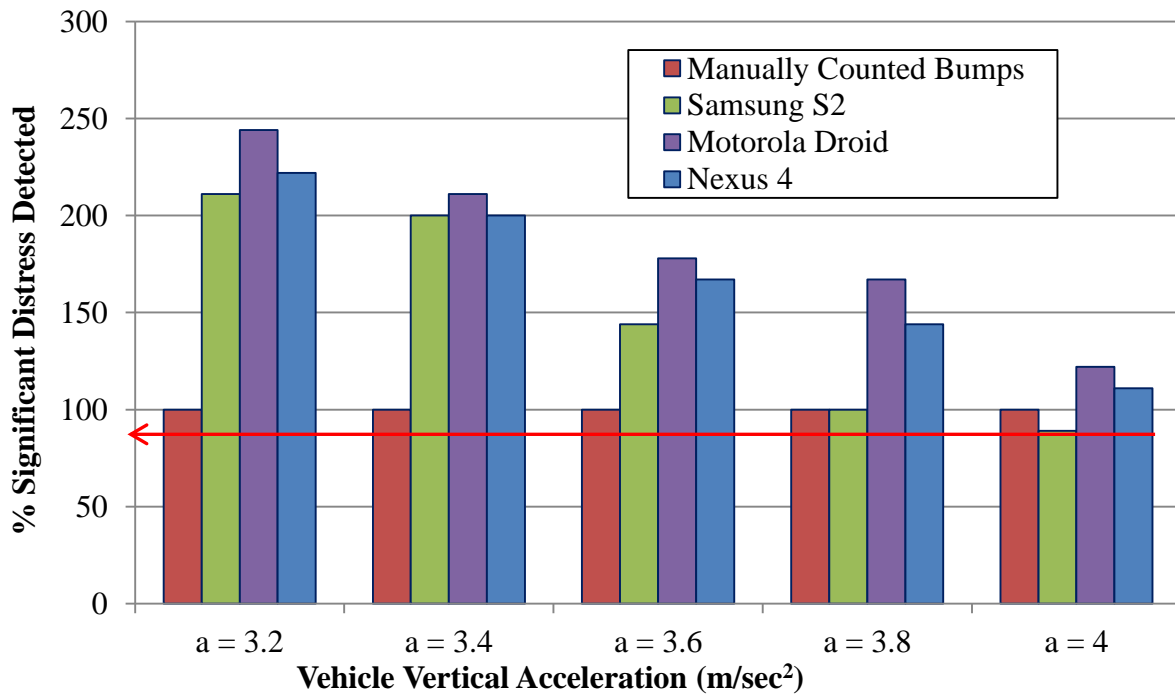


Figure 6.4: Significant Localized Distress Detection at US 45 (Ford Haris St to Lebert St)

Figure 6.5 shows the percentage of potholes/bumps detected from US 45 (from Airport Rd to Olympian Rd) by the smartphone application, with different acceleration threshold values, as compared to the manually-estimated baseline. Again, all smartphones detected a higher number of localized distresses than that from the manual identification baseline when a threshold value of 3.2-3.8 m/sec² was used. The 4.0 m/sec² threshold value, produced reasonable results once again, although in this case, the Nexus 4 and Motorola Droid detected about 125 and 135 percent of localized distresses (some features were picked up by these phones at this analysis threshold which were not deemed as significant distresses by the human evaluator). Very similar results were obtained for US 45 (Lebert St to Ct Rd 2200N), as shown in Figure 6.6). Although phone-dependent, it appears that a relative acceleration event threshold of around 4 m/s² would provide a reasonable start for the identification of significant pavement distresses.

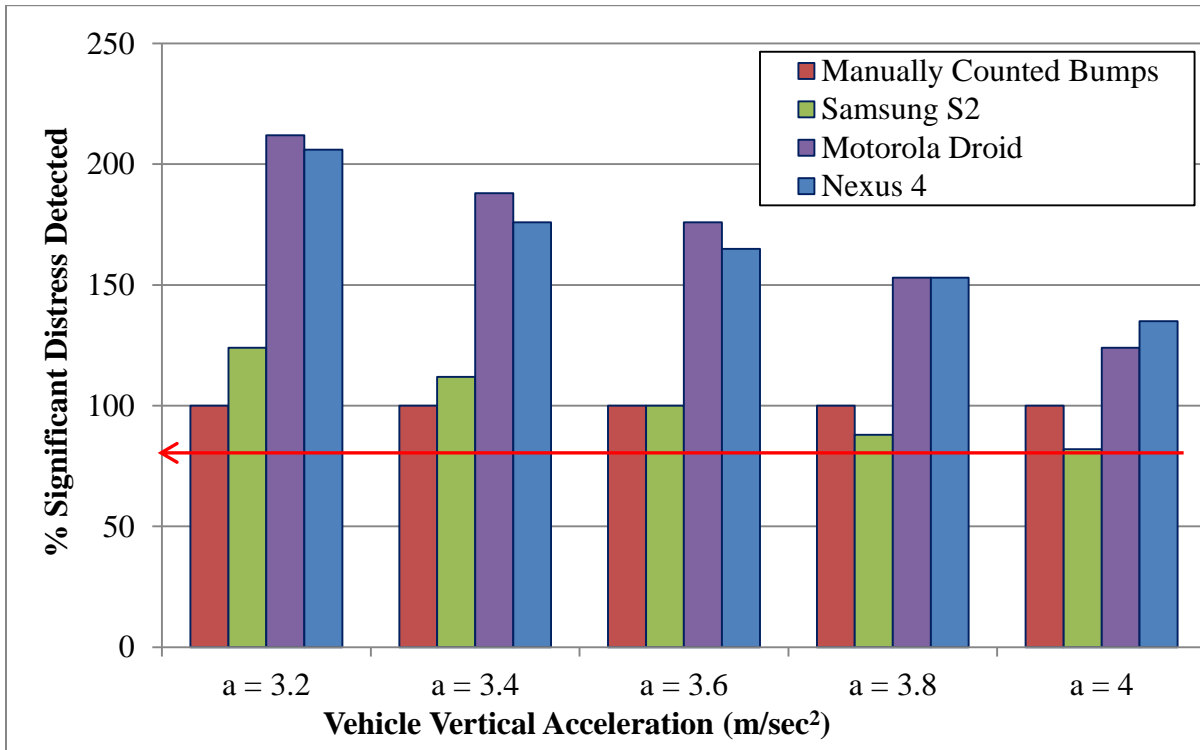


Figure 6.5: Significant Localized Distress Detection at US 45 (Airport Rd to Olympian Rd)

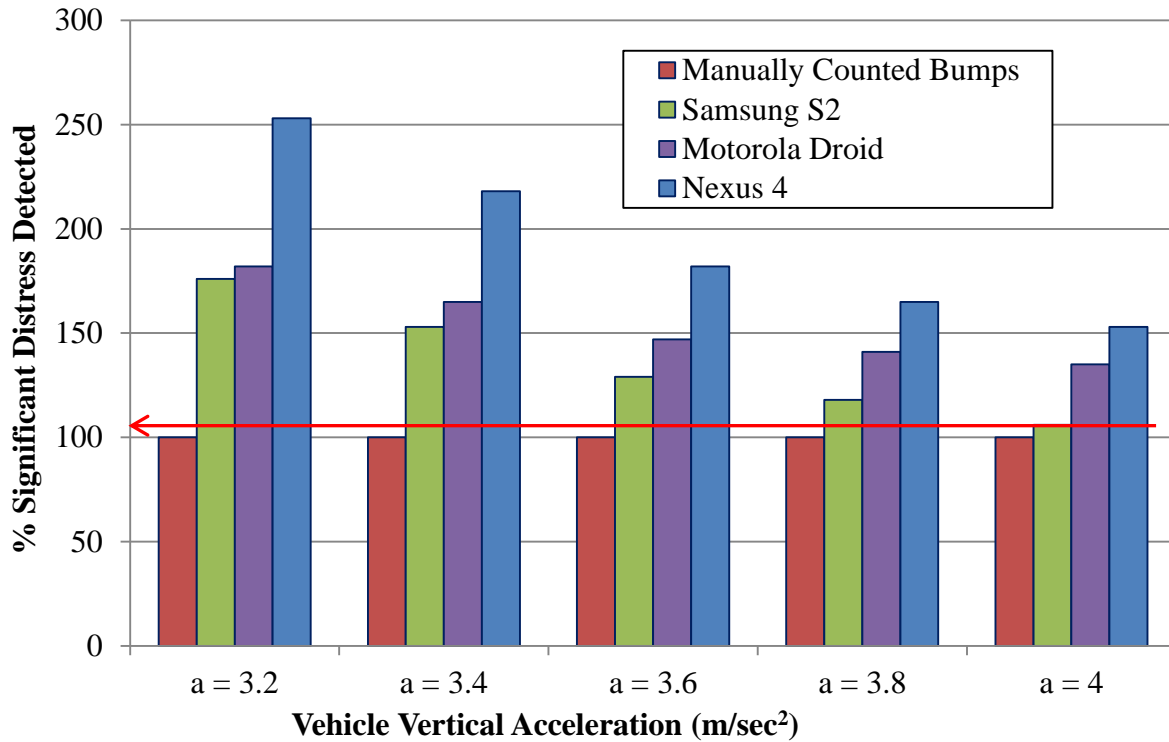


Figure 6.6: Significant Localized Distress Detection at US 45 (Lebert St to Ct Rd 2200N)

It has been noticed from the collected data that most of the smartphone-measured GPS locations are updated on one-second intervals, where a vehicle traveling at 50 miles-per-hour would traverse a distance of 73.33 feet in that time. Since it is quite possible to have multiple, severe distresses occurring within a 73.33 foot span of highway, it was necessary to create a time-space adjustment algorithm in MATLAB script to interpolate GPS coordinates between updates in order to arrive at a more realistic spacing and location identification for significant distresses. This may present a challenge for pavement feature detection using crowd sourcing, although on the other hand, the advantages of having a large number of crowd-sourced measurements would likely outweigh the disadvantages of having ‘noise’ in the location identifier data. Additional artificial intelligence could also be developed to improve location accuracy by finding locations of stopped vehicles at traffic lights, noting bumps at bridges, locating turns in roads via X-Y accelerometers, etc. Figure 6.7 shows location map of detected bumps/potholes at US 45 for a 1-mile section.

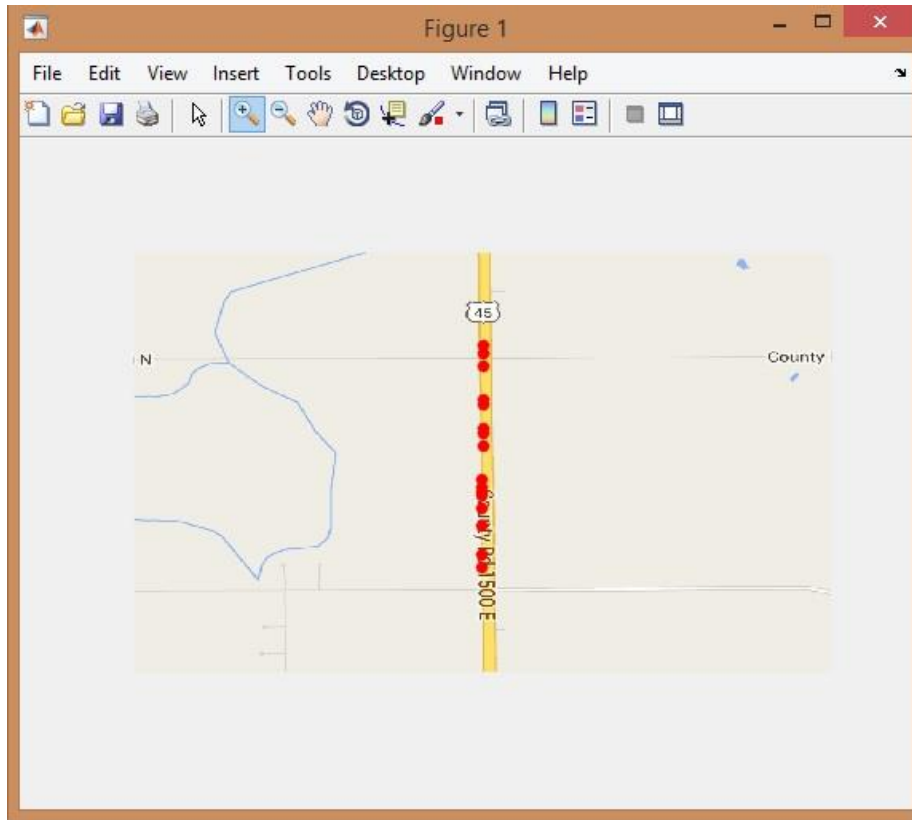


Figure 6.7: Location Map of Detected Severe Pavement Surface Distresses at US 45

6.5 LOCALIZED DISTRESS FROM SELECTED PAVEMENT SECTIONS

Localized distress data was also collected from 12 different pavement sections located in Champaign and Piatt County, Illinois. Figure 6.8 shows bumps and potholes counted manually and by using smartphones from 12 pavement sections. It can be seen that smartphones, in general, counted more bumps/potholes as compared to the human survey results at most of the pavement sections. Again, manual counts are quite subjective, and thus approximate correspondence between measured and observed critical events is deemed acceptable (and conservative in this case).

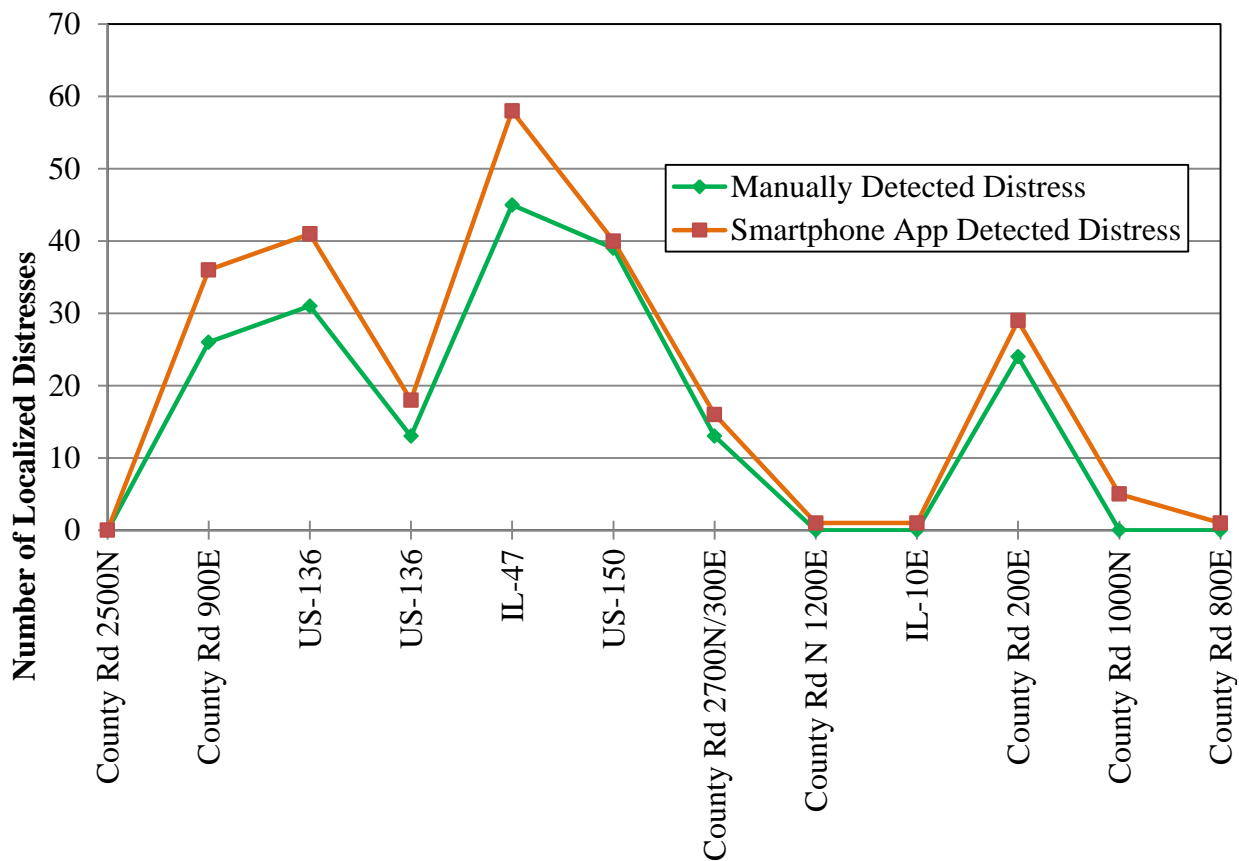


Figure 6.8: Bumps/Pothole Counts by Manually and Smartphone Application

6.6 APPLICATION OF ARCGIS TO VISUALIZE IRI DATA

Incorporation of pavement roughness values in the roadway network map would be helpful to visualize the condition of the overall network. Pavement IRI values measured for every 0.1-mile section can be displaced into a roadway network map using ArcGIS. Roughness Capture application collected GPS coordinate data and estimated IRI data was imported to the highway map in ArcGIS. A few notable challenges were encountered in integrating pavement roughness data into ArcGIS map, including:

- IRI values are required to be shown for every 0.1-mile section; however, pavement sections with varying length ranging from a few feet to few miles exist in GIS map. Therefore, it was required to divide the pavement sections into 0.1-mile sections. The ‘fishnet’ tool was used to create a 0.1-mile by 0.1-mile fishnet, and later, pavement sections were segmented into 0.1-mile sections.

- Location data collected by Roughness Capture were often around 1-50 feet laterally offset from the actual pavement location. Therefore, it was required to shift the GPS coordinates to 'snap' to the known road location. A radius of 200 feet was used to find a nearby road and GPS coordinates were then shifted to correct the lateral offset error.

The average IRI values are displayed in the map with different color as shown in Figure 6.9.

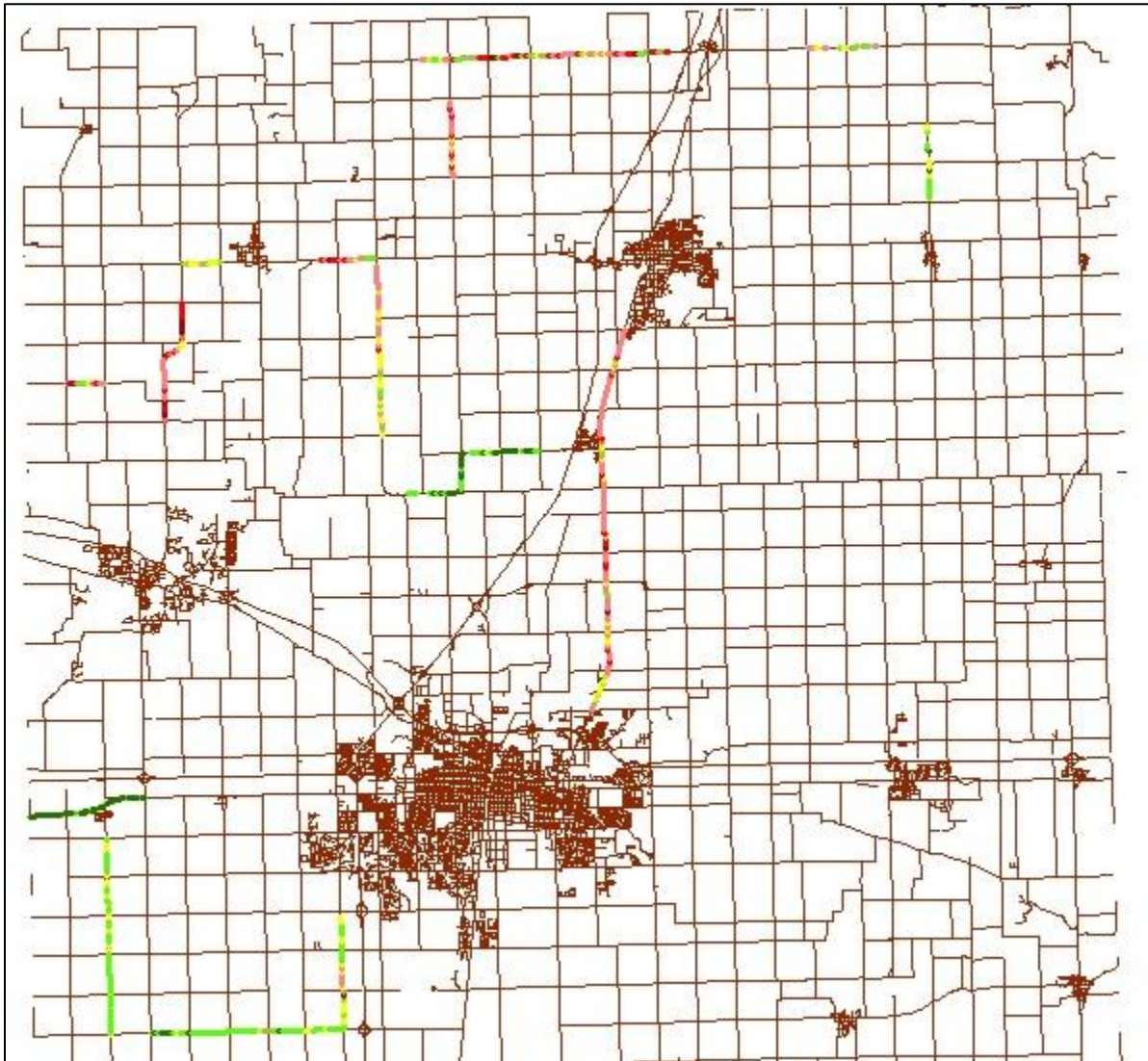


Figure 6.9: Pavement IRI Integrated with Champaign County Map Generated with ArcGIS

CHAPTER 7

CONCLUSION AND RECOMMENDATIONS

7.1 SUMMARY AND FINDINGS

Roadway users judge a pavement to be in good or bad condition based in large part on overall roughness. It is also known that pavement roughness greatly affects user costs. Therefore, roughness (IRI) is important information both for transportation agencies, in maintenance and rehabilitation planning, and for users and navigation systems, to maximize safety and minimize user costs. However, the collection of pavement roughness data is generally only performed by or for owner agencies, and at a great expense to taxpayers. Still, insufficient data exists for robust maintenance decision making, not to mention the lack of data available for private sector use. An improved smartphone application called ‘Roughness Capture’ was presented, as a means to help address current shortcomings in the availability and cost of pavement roughness data. This application is also able to detect significant localized pavement distresses such as bumps and potholes. Finally, Roughness Capture measured pavement roughness data has been integrated into roadway map using ArcGIS. The following findings have resulted from the current research:

(a) Total user costs including fuel consumption, tire, repair and maintenance, and depreciation costs over 35 years of pavement life with AADT of 10,000 for the Interstate and primary road system were estimated. The agency costs were also estimated along with user costs. It has been found that agency costs are in the range of 2.3 to 3.6 percent of the combined costs (agency plus users).

(b) Analysis showed that additional rehabilitation (placing a new overlay every 7 years instead of every 10 years, on average) for 1-mile pavement section would reduce user costs in the range of \$5.1M to \$5.7M (52% to 37%) over a 35-year life cycle depending on the initial pavement roughness. This additional rehabilitation would cost \$108,000 over a 35-year life cycle in terms of present worth.

(c) Agencies expend funds for the construction, maintenance, and rehabilitation of pavements, while users incur costs for extra fuel, tire, repair and maintenance, and depreciation because of

deferred maintenance leading to rougher pavements. It was calculated that keeping pavements in a smoother condition could provide a 50-fold return on investment in terms of reduced user costs as compared to agency expenditure. Besides the economic benefit, users would also derive benefits from safer, more comfortable pavement.

(d) Additional analysis was performed to quantify the cost of environmental effects related to more frequent maintenance to savings in users cost. Life cycle assessment (LCA) was performed along with life cycle analysis to enable this comparison.

(e) Two approaches were investigated in life cycle assessment: a deferred maintenance approach, which allowed the pavement to become rough, and an alternative approach, which required an additional \$108,000 to maintain the pavement in smooth state. For deferred maintenance of 1-mile pavement section, user costs due to roughness were approximately \$9.9 million (94%). For the case of additional maintenance, agency costs, emission costs due to CMR activities, and emission costs due to roughness were about \$545,491 (5%), \$67,151 (1%), and \$31,514 (0.3%), respectively over the 35 year analysis period.

(f) In the alternative approach, which requires an additional \$108,210 investment in M & R over the 35 year analysis period to maintain pavement in a smoother condition, user costs associated with roughness were about \$4.7 million (about 52% less than that associated with the basic approach), whereas agency costs, emissions costs due to CMR, and emissions costs due to roughness were calculated as \$653,701, \$87,686, and \$25,498, respectively.

(g) An additional agency investment of \$108,209 over a 35-year design period for one mile/one lane of roadway can provide a 48-to-1 return on investment in terms of reduced user costs, even when environmental costs are considered. In Chapter 2, a 50-to-1 return on investment was estimated; however, environmental costs associated with additional M & R activities were ignored.

(h) Collecting IRI data using inertial profilers requires significant agency investment, such that transportation agencies cannot afford to collect data every year. Therefore, maintenance and rehabilitation planning are often performed using old data. In this study, a smartphone application 'Roughness Capture' has been developed to capture vehicle vertical acceleration

data. The goal of the research was to determine the feasibility of using smartphones as an inexpensive approach towards achieving more frequent roughness assessment of pavement networks.

(i) Acceleration data from smartphones mounted on vehicle dashboards has been analyzed to determine pavement profile. Two procedures have been used to obtain pavement profile from the acceleration data: double integration of acceleration data and the inverse state space model. A MATLAB script has been developed to estimate IRI from pavement profile; therefore, this standalone script is able to estimate pavement roughness without the need for ProVAL software.

(k) With the double integration process, the Roughness Capture application measured IRI similar to the inertial profiler for two test sections (smooth to medium rough), whereas the app measured lower IRI than that of the inertial profiler over a test section with very rough pavement. The repeatability has also been measured by conducting data collection five times from the test section, where COV's were found to be in the range of 7-22, 4-28, and 4-22%.

(l) Using the inverse state space modeling approach with vehicle suspension parameters obtained through trial-and-error, significant improvements over a simpler double integration process have been achieved. Predictions between smartphone measured IRI values and industry standard inertial profiler results were found to be similar after vehicle suspension parameters were calibrated. Only minor calibration is not required, and only for very rough pavement sections. IRI repeatability has also been improved using new algorithm.

(m) To more fully vet the improved, inverse state space model, acceleration data was collected from 14 pavement sections totaling 60 miles. Once vehicle suspension parameters are calibrated, the new algorithm can be used to accurately obtain IRI estimates on other pavement sections. Averaged IRI values for 14 additional test sections showed a favorable match between the smartphone based estimates and reference values..

(n) Vehicle vertical acceleration was also collected using six smartphones and four vehicles. It was found that both the smartphone model and the vehicle used for data collection will affect the IRI measurement. However, averaged IRI values measured across all smartphones and vehicles

were found to be in good agreement with the inertial profiler measured IRI for most of the pavement sections.

(o) As MAP-21 requires transportation agencies to report IRI values of their roadway network, IRI data measured by the Roughness Capture app has been used to categorize pavement conditions. It has been found that it is possible to categorize pavement conditions accurately for most of the pavement sections using smartphones along with algorithms developed in this study.

(p) As identifying and locating severe localized pavement distresses are very important to the transportation agencies, a preliminary investigation has been conducted in this study. Localized distresses have been detected based on the vehicle vertical acceleration data. A threshold value of 4 m/sec^2 was suggested through experimental trials to identify localized distress. A MATLAB script has been developed mapping the distresses and displaying them in a Google map. An effort has been made to integrate pavement IRI data into roadway network map using ArcGIS. This can help decision makers to see the health of entire roadway network.

7.2 CONCLUSIONS

Based on the findings of this study, the following conclusions can be drawn:

- Pavement roughness incurs significant amount of user costs, and additional agency investment can provide not only safe and smooth ride but also about 48 fold returns in agency investment.
- Smartphone application appears to be a viable option to measure pavement roughness. With this application, it would be possible to get most updated pavement roughness values for a roadway network for maintenance and rehabilitation planning.
- Transportation agencies can report IRI data every year with significantly lower cost compared to the inertial profiler.

7.3 FUTURE EXTENSIONS

The use of smartphones to measure pavement roughness is still in its infancy. There is still plenty of room for additional improvements and new innovations. Based on the findings and conclusions of this study, the following future work is recommended:

- (a) Further validation of Roughness Capture needs to be pursued, particularly for very rough pavement sections, particularly when higher sampling rates become more commonplace in the spectrum of smartphones in service.
- (b) A crowd sourcing feasibility study can be the subject of a later investigation. It is not necessary to rely on a public-facing application to achieve this goal. Rather, taxis, municipal vehicles, certain automobile models, or other fleets could be used to investigate crowd sourcing benefits to roughness data collection.
- (c) In this study, one type of smartphone car mount was used to attach the phone on the dashboard of the vehicle to collect vehicle vertical acceleration data; therefore, it needs to be investigated whether this equipment has any effect on roughness measurement as they vary depending on manufacturer.
- (d) I-phones are somewhat different than other smartphones, and they have not been investigated in this study. This should be investigated in a follow up study.
- (e) A standalone accelerometer with higher data collection frequency can be used, and results can be compared with smartphone acceleration measurements to assess the potential benefits to be realized when smartphone data collection rates are increased.
- (f) In this study, IRI data has been integrated manually into a roadway map using ArcGIS; it would be more beneficial to automate this procedure.
- (g) Effect of vehicle speed on IRI measurement needs to be investigated, as crowdsourcing will lead to variable vehicle speed in collected data sets.

REFERENCES

1. Flintsch, G., and McGhee, K. K. (2009). Quality Management of Pavement Condition Data Collection. National Cooperative Highway Research Program: Transportation Research Board, NCHRP Synthesis 401.
2. Klaubert, E. C. (2001). Highway Effects on Vehicle Performance. FHWA-RD-00-164, Federal Highway Administration, Washington, D.C.
3. McGhee, K. K. (2004). Automated Pavement Distress Collection Techniques. National Cooperative Highway Research Program: Transportation Research Board, Vol. NCHRP Synthesis 334.
4. Sauerwein, P. M., and Smith, B. L. (2011). Investigation of the Implementation of a Probe-Vehicle Based Pavement Roughness Estimation System. Mid-Atlantic Universities Transportation Center, University Park, PA.
5. Papagiannakis, A. T., and Delwar, M. (1999). Methodology to Improve Pavement-Investment Decisions. Final Report to National Cooperative Highway Research Program for Study 1-33, Transportation Research Board, Washington, D.C.
6. Haugodegard, T., Johansen, J., Bertelsen, D., and Gabestad, K. (1994). Norwegian Public Roads Administration: A Complete Pavement Management System in Operation. Proceedings of Third International Conference on Managing Pavements, Volume 2, San Antonio, Texas.
7. ASTM E 876-06 (2006). Terminology Relating to Vehicle-Pavement Systems. ASTM, Philadelphia, PA.
8. Zaniewski, J. P., Butler, B. C., Cunningham, G., Elkins, E., Paggi, M. S., and Machemehl, R. (1982). Vehicle Operating Costs, Fuel Consumption, and Pavement Type and Condition Factors. FHWA-PL-82-001. FHWA, U.S. Department of Transportation.
9. Zaabar, I., and K. Chatti (2010). Calibration of HDM4 Models for Estimating the Effect of Pavement Roughness on Fuel Consumption for US Conditions. In Transportation Research

Record: Journal of the Transportation Research Board, No. 2155, Transportation Research Board of the National Academies, Washington, D.C.

10. Jackson, N. M. (2004). An Evaluation of the Relationship between Fuel Consumption and Pavement Smoothness. University of North Florida, Jacksonville, FL.

11. Walls III, J., and Smith, M. R. (1998). Life-Cycle Cost Analysis in Pavement Design - Interim Technical Bulletin. FHWA-SA-98-079. FHWA, U.S. Department of Transportation.

12. Federal Highway Administration (2011). Our Nation's Highways: 2008. Figure 6-7. Highway Construction Price Trends and Consumer Price Index. U.S. Department of Transportation.

http://www.fhwa.dot.gov/policyinformation/pubs/pl08021/fig6_7.cfm. Accessed July 15, 2011.

13. Sinha, K. C. and Labi, S. (2007). Transportation Decision Making: Principles of Project Evaluation and Programming. John Wiley & Sons, Inc., New York.

14. AAA Association Communication (2011). Your Driving Costs. AAA, Heathrow, Florida, 2011.

<http://www.aaaexchange.com/main/Default.asp?CategoryID=16&SubCategoryID=76&ContentID=353>. DrivingCosts2011.pdf. Accessed July 15, 2011

15. Zaniewski, J. P. (1989). Effect of Pavement Surface Type on Fuel Consumption; Portland Cement Association: Skokie, IL.

16. Lu, X. P. (1985). Effects of Road Roughness on Vehicular Rolling Resistance. Measuring Road Roughness and Its Effects on User Cost and Comfort (T. D. Gillespie and M. Sayers, eds.), ASTM Special Technical Publication 884. American Society for Testing and Materials, Philadelphia, PA.

17. Transportation Research Board Special Report 286 (2006). Tires and Passenger Vehicle Fuel Economy - Informing Consumers, Improving Performance. Transportation Research Board, Washington, D.C.

18. Federal Highway Administration (2011). Highway Finance Data Collection, Our Nation's Highways: 2010. http://www.fhwa.dot.gov/policyinformation/pubs/hf/pl110023/fig5_1.cfm. Accessed July 20, 2011.
19. U.S. Environmental Protection Agency (2011). Fuel Economy Guide – Model Year 2010. Retrieved From: <http://www.fueleconomy.gov/feg/pdfs/guides/FEG2011.pdf>. Accessed April 15, 2011.
20. Bennett, C. R., and Greenwood, I. D. (2003). Volume 7: Modeling Road User and Environmental Effects in HDM-4, Version 3.0. International Study of Highway Development and Management Tools (ISOHDM), World Road Association (PIARC).
21. Hall, K. T., and Correa, C. E. (1999). Estimation of Present Serviceability Index from International Roughness Index. In Transportation Research Record: Journal of the Transportation Research Board, No. 1655, Transportation Research Board of the National Academies, Washington, D.C.
22. Chesher, A., Harrison, R., and Swait, J. D. (1981). Vehicle Depreciation and Interest Costs: Some Evidence from Brazil. Proceedings of the Second World Conference on Transport Research, London, England.
23. Federal Highway Administration (2002). Highway Economic Requirements System Technical Manual, U.S. Department of Transportation, Washington, D.C.
24. Barnes, G., and Langworthy, P. (2004). Per Mile Costs of Operating Automobiles and Trucks. In Transportation Research Record: Journal of the Transportation Research Board, No. 1824, Transportation Research Board of the National Academies, Washington, D.C.
25. Von Quintus, H. L., Eltahan, A., and Yau, A. (2001). Smoothness Models for Hot-Mix Asphalt–Surfaced Pavements Developed from Long-Term Pavement Performance Program Data. In Transportation Research Record 1764, TRB, National Research Council, Washington, D.C.
26. AASHTO (2008). Mechanistic-Empirical Pavement Design Guide. A Manual of Practice, American Association of State Highway Officials, Highway Research Board. Washington, D.C.

27. Perera, R. W., and Kohn, S. D. (2006). Ride Quality Performance of Asphalt Concrete Pavements Subjected to Different Rehabilitation Strategies. ASCE Proceedings of 2006 Airfield and Highway Pavements Specialty Conference, Atlanta, GA.
28. Al-Mansour, A., Sinha, K. C., and Kuczek, T. (1994). Effects of Routine Maintenance on Flexible Pavement Condition. *Journal of Transportation Engineering*, ASCE, Volume 120, Issue 1.
29. Hall, K. T., Correa, C. E., and Simpson, A. L. (2002). LTPP Data Analysis: Effectiveness of Maintenance and Rehabilitation Options. NCHRP Project 20-50[3/4].
30. ASCE (2009). 2009 Report Card for America's Infrastructure. American Society of Civil Engineers, Reston, VA.
31. Hansen, K., and Newcomb, D. (2007). RAP Usage Survey. National Asphalt Pavement Association, Lanham, MD.
32. Harrington, J. (2005). Recycled Roadways. *Public Roads*, Vol. 68, No. 4, FHWA-HRT-05-003.
33. ISO (2006). Environmental Management — Life Cycle Assessment — Principles and Framework. ISO 14040:2006(E), International Organization for Standardization, Geneva.
34. Matthews, H., Hendrickson, C., and Horvath, A. (2001). External Costs of Air Emissions from Transportation. *Journal of Infrastructure Systems*, Vol. 7, No. 1, pp. 13-17.
35. Harvey, J. T., Kim, C., and Lee, E. (2011). Selection of Pavement for Highway Rehabilitation Based on Life-Cycle Cost Analysis Transportation Research Record: Journal of the Transportation Research Board, Vol. 2227, pp. 23-32.
36. Brillet, F., Jullien, A., and Sayagh, S. (2006). Assessment of Consumptions and Emissions during Pavement Lifetime. In *Transport Research Arena Europe 2006*, TRA, Gotenborg, Sweden.

37. Kucukvar, M., and Tatari, O. (2012). Ecologically Based Hybrid Life Cycle Analysis of Continuously Reinforced Concrete and Hot-Mix Asphalt Pavements. *Transportation Research Part D: Transport and Environment*, Vol. 17, No. 1, pp. 86-90.
38. Cass, D., and Mukherjee, A. (2011). Calculation of Greenhouse Gas Emissions for Highway Construction Operations by using a Hybrid Life-Cycle Assessment Approach: Case Study for Pavement Operations. *Journal of Construction Engineering and Management*, Vol. 137, No. 11, pp. 1015-1025.
39. Horvath, A. (2004). Life-Cycle Analysis Model and Decision-Support Tool for Selecting Recycled Versus Virgin Materials for Highway Applications. RMRC Research Project No. 23, Recycled Materials Resource Center, Durham, NH.
40. Hendrickson, C., Horvath, A., Joshi, S., and Lave, L. (1998). Peer Reviewed: Economic Input-Output Models for Environmental Life-Cycle Assessment. *Environmental Science & Technology*, Vol. 32, No. 7, pp. 184A-191A.
41. Environmental Protection Agency (2012). Motor Vehicle Emission Simulator (MOVES). , Vol. MOVES2010b.
42. AASHTO (2008). Mechanistic-Empirical Pavement Design Guide (M-E PDG). A Manual of Practice, 2008.
43. Mallela, J., and Sadasivam, S. (2011). Work Zone Road User Costs. FHWA-DTFH61-06-D-00004, Federal Highway Administration, Washington, D.C.
44. Tol, R. S. J. (2005). The Marginal Damage Costs of Carbon Dioxide Emissions: An Assessment of the Uncertainties. *Energy Policy*, Vol. 33, No. 16, pp. 2064-2074.
45. Tol, R. S. J., Downing, T. E., Fankhauser, S., Richels, R. G., and Smith, J. B. (2001). Progress in Estimating the Marginal Costs of Greenhouse Gas Emissions. Research unit Sustainability and Global Change, Hamburg University.
46. Tol, R. S. J. (2003). Is the Uncertainty about Climate Change Too Large for Expected Cost-Benefit Analysis? *Climatic Change*, Vol. 56, pp. 265-289.

47. Kendall, A., Keoleian, G. A., and Helfand, G. E. (2008). Integrated Life-Cycle Assessment and Life-Cycle Cost Analysis Model for Concrete Bridge Deck Applications. *Journal of Infrastructure Systems*, Vol. 14, No. 3, pp. 214-222.
48. Unruh, B. (2002). Delivered Energy Consumption Projections by Industry in the Annual Energy Outlook 2002. <http://www.eia.gov/oiaf/analysispaper/industry/consumption.html>, Accessed July 20, 2012.
49. Stripple, H. (2001). Life Cycle Assessment of Road: A Pilot Study for Inventory Analysis. B1210E, IVL Swedish Environmental Research Institute, Gothenburg, Sweden.
50. Zapata, P., and Gambatese, J. (2005). Energy Consumption of Asphalt and Reinforced Concrete Pavement Materials and Construction. *Journal of Infrastructure Systems*, Vol. 11, No. 1, pp. 9-20.
51. Chatti, K., and Zaabar, I. (2011). New Mechanistic-Empirical Approach for Estimating the Effect of Roughness on Vehicle Durability Transportation Research Record: *Journal of the Transportation Research Board*, Vol. 2227, pp. 180-188.
52. Hughes, C. S., Moulthrop, J. S., Tayabji, S., Weed, R. W., and Burati, J. L. (2011). Guidelines for Quality related Pay Adjustment Factors for Pavements. National Cooperative Highway Research Program, NCHRP Project No. 10-79.
53. Perera, R. W., and Kohn, S. D. (2002). Issues in Pavement Smoothness. NCHRP Web Document 42 (Project 20-51[1]), National Research Council, Washington, D.C.
54. Perera, R. W., S. D. Kohn, and S. Tayabji. (2005). Achieving a High Level of Smoothness in Concrete Pavements without Sacrificing Long-Term Performance. FHWA-HRT-05-068, Washington, D.C.
55. Carey, W. N., and Irick, P. E. (1960). The Serviceability-Performance Concept. *Highway Research Board Bulletin* 250.

56. Wilde, W. James, (2007). Implementation of an International Roughness Index for Mn/DOT Pavement Construction and Rehabilitation, Report No. MN/RC-2007-09, Minnesota Department of Transportation.
57. Janoff, M. S., Nick, J. B., Davit, P. S., and Hayhoe, G.F. (1985). Pavement Roughness and Rideability. NCHRP Report 275, National Research Council, Washington, D.C.
58. Janoff, M. S. (1988). Pavement Roughness and Rideability Field Evaluation. NCHRP Report 308, National Research Council, Washington, D.C.
59. FHWA (2015). Moving Ahead for Progress in the 21st Century. Washington, D.C. <http://www.fhwa.dot.gov/map21/>.
60. Sayers, M. W., and Karamihas, S. M. (1998). The Little Book of Profiling, University of Michigan.
61. Nemmers, C. J., Gagarin, N., and Mekemson, J. R. (2006). Assessing IRI vs. PI as a Measurement of Pavement Smoothness. Report No. RI06-003, Missouri Department of Transportation.
62. Sarabi-Jamab, A., and Araabi, B. N. (2006). PiLiMoT: A Modified Combination of LoLiMoT and PLN Learning Algorithms for Local Linear Neurofuzzy Modeling. Journal of Control Science and Engineering, Vol. 2011, Article ID 121320.
63. U.S. Department of Transportation (2000). 1999 Status of the Nation's Highways, Bridges and Transit: Conditions and Performance. U.S. Department of Transportation, Federal Highway Administration, Washington, D.C.
64. Woodstrom, J. H. (1990). Measurements, Specifications, and Achievement of Smoothness for Pavement Construction. National Cooperative Highway Research Program: Transportation Research Board, Vol. NCHRP Synthesis 167, pp. 4, Washington, D.C.
65. McGhee, K. K. (2002). A New Approach to Measuring the Ride Quality of Highway Bridges. Report No. VTRC 02-R10. Virginia Transportation Research Council, Charlottesville.

66. Smith, K. L., Titus-Glover, L., and Evans, L. D. (2002). Pavement Smoothness Index Relationships. FHWA-RD-02-057. Washington, D. C.
67. Spangler, E. B. and Kelley, W. J. (1964). GMR Road Profilometer - A Method for Measuring Road Profile. Research Publication GMR - 452, General Motor Research Laboratory, Warren, Michigan.
68. American Society of Testing and Materials (1999). Annual Book of ASTM Standards, Volume 4.03, Road and Paving Materials, Philadelphia.
69. <https://pavemaintenance.wikispaces.com/CVEEN+7570-+Spring+2011>.
70. Donnelly, D. E., Hutter, W., Kiljan, J. P. (1988). Pavement Profile Measurement. Seminar Proceedings, Volume II, Report FHWA DP-88-072-004, Washington, D.C.
71. Perera, R. W., and Kohn, S. D. (2005). Quantification of Smoothness Index Differences Related to LTPP Equipment Type. FHWA-HRT-05-054, Washington, D. C.
72. Haas, R., Hudson, W. R., and Zaniewski, J. (1994). Modern Pavement Management. Krieger Publishing Company, Malabar, FL.
73. <http://data-informed.com/crowdsourced-app-analyzes-smartphone-data-to-identify-potholes/>
74. Sensors and Cell Phones. <http://www.stanford.edu/class/cs75n/Sensors.pdf>.
75. Gajic, Z. (2015). State Space Approach. <http://www.ece.rutgers.edu/~gajic/psfiles/chap3.pdf>
76. Fairman, F. W. (1998). Linear Control Theory – The State Space Approach. John Wiley & Sons, Inc., New York.
77. Rath, J. J., Veluvolu, K. C., and Defoort, M. (2014). Estimation of Road Profile for Suspension Systems Using Adaptive Super-Twisting Observer. Control Conference (ECC), 2014 European , pp.1675.
78. Roy, S., and Liu, Z. (2008). Road Vehicle Suspension and Performance Evaluation Using a Two-Dimensional Vehicle Model.

79. Gillespie, T. D. (1992). *Fundamentals of Vehicle Dynamics*. Society of Automotive Engineers, Warrendale, PA.
80. Martinez, M. (2014). *The Rideability of a Deflected Bridge Approach Slab*. FHWA/LA.14/531, Springfield, VA.
81. Emmanuel, J. H., Das, S., Perrig, A., and Zhang, J. (2012). *ACCessory: password inference using accelerometers on smartphones*, Proceedings of the Twelfth Workshop on Mobile Computing Systems & Applications, San Diego, California.
82. <http://www.engadget.com/2012/05/22/the-engineer-guy-shows-how-a-smartphone-accelerometer-works/>.
83. <http://www.sensormag.com/sensors/acceleration-vibration/noise-measurement-8166>.
84. Sayers, M. W. (1995). *On The Calculation of International Roughness Index from Longitudinal Road Profile*. Transportation Research Record, (1501), pp.1-12.
85. The Transtec Group, Inc. (2013). *Profile Viewing and Analysis (ProVAL 3.4)*. Austin, Texas. <http://www.roadprofile.com/node/50>.
86. ASTM Standard E1926-08 (2008). *Standard Practice for Computing International Roughness Index of Roads from Longitudinal Profile Measurements*. ASTM International, West Conshohocken, PA.
87. AASHTO (2013). *SCOPM MAP-21 Notice of Proposed Rule-Making Checklist*. Standing Committee on Performance Management, Washington, D.C.
88. Burningham, S., and Stankevich, N. (2005). *Why Road Maintenance is Important and How to Get it done*. Transportation Note No. TRN-4, The World Bank, Washington, D.C.

APPENDIX A

Table A.1: Smartphone and Inertial Profiler Measured IRI at County Rd 2500N (From 1300E to 1000E)

County Rd 2500N (From 1300E to 1000E)			
Distance (mile)	Profiler Measure IRI (in/mi)	Smartphone App Measured IRI (in/mi)	Difference in IRI (in/mi)
0.1	53.4	53.5	0.1
0.2	55.5	51.4	4.1
0.3	41.9	38.9	3.0
0.4	48.5	46.7	1.8
0.5	56.2	60.1	3.9
0.6	62	66.7	4.7
0.7	55.1	68.7	13.6
0.8	43.8	56.1	12.3
0.9	95	101.3	6.3
1	59.2	81.4	22.2
1.1	49.3	58.7	9.4
1.2	43	45.0	2.0
1.3	41.2	53.9	12.7
1.4	48.6	58.0	9.4
1.5	46.3	57.4	11.1
1.6	44.8	50.2	5.4
1.7	44.2	42.4	1.8
1.8	46	60.8	14.8
1.9	47	49.7	2.7
2	51.2	50.0	1.2
2.1	76.8	75.6	1.2
2.2	51.1	53.4	2.3
2.3	50.9	52.3	1.4
2.4	63.1	61.0	2.1
2.5	50	51.5	1.5
2.6	45.7	55.4	9.7
2.7	48	58.9	10.9
2.8	46.3	48.1	1.8
2.9	53.7	66.6	12.9
3	69.9	78.7	8.8
3.1	65	82.4	17.4
3.2	52.2	63.1	10.9
3.3	51.8	45.7	6.1
3.4	46.6	33.8	12.8
3.5	53.1	45.7	7.4
3.6	53.8	62.8	9.0
3.7	46.5	55.8	9.3
3.8	48.3	60.8	12.5
3.9	50.8	59.0	8.2
4	78.6	65.4	13.2
4.1	46.4	55.4	9.0
4.2	47.4	58.6	11.2
4.3	54.6	41.1	13.5
Average Difference between Profile and Smartphone Measured IRI =			7.8

Table A.2: Smartphone and Inertial Profiler Measured IRI at County Rd 900E (From 2550N to US-136)

County Rd 900E (From 2550N to US-136)			
Distance (mile)	Profiler Measure IRI (in/mi)	Smartphone App Measured IRI (in/mi)	Difference in IRI (in/mi)
0.1	93.9	109.6	15.7
0.2	111.9	94.3	17.6
0.3	83.8	85.6	1.8
0.4	103	126.5	23.5
0.5	100.2	105.2	5.0
0.6	90	106.2	16.2
0.7	110.8	137.6	26.8
0.8	106.7	117.9	11.2
0.9	100.6	79.5	21.1
1	94.9	113.7	18.8
1.1	103.8	128.5	24.7
1.2	106.4	88.3	18.1
1.3	93.6	93.9	0.3
1.4	97.7	100.0	2.3
1.5	102.1	97.7	4.4
1.6	94.2	99.5	5.3
1.7	114.5	90.3	24.2
1.8	107	131.4	24.4
1.9	105	118.9	13.9
2	105	109.6	4.6
2.1	94	97.6	3.6
2.2	127.7	102.4	25.3
2.3	134.8	172.2	37.4
2.4	154.1	164.1	10.0
2.5	101.9	108.0	6.1
2.6	97.8	107.0	9.2
2.7	130.8	140.1	9.3
2.8	106.1	120.0	13.9
2.9	165.2	134.5	30.7
3	103.5	108.8	5.3
3.1	112.8	121.0	8.2
3.2	119.5	111.9	7.6
3.3	97.8	118.3	20.5
3.4	162.7	136.7	26.0
3.5	125.1	157.5	32.4
3.6	123	129.3	6.3
3.7	125.2	136.3	11.1
3.8	97.2	107.3	10.1
3.9	138.6	129.4	9.2
4	103.6	126.9	23.3
4.1	128.1	120.0	8.1
Average Difference between Profile and Smartphone Measured IRI =			14.5

Table A.3: Smartphone and Inertial Profiler Measured IRI at US-136 (From 500E to 400E)

US-136 (From 500E to 400E)			
Distance (mile)	Profiler Measure IRI (in/mi)	Smartphone App Measured IRI (in/mi)	Difference in IRI (in/mi)
0.1	220.3	184.3	36.0
0.2	163.7	148.2	15.5
0.3	182.8	188.5	5.7
0.4	168.6	165.3	3.3
0.5	303.4	235.9	67.5
0.6	163.6	185.4	21.8
0.7	247.2	217.2	30.0
0.8	167.9	165.1	2.8
0.9	205.8	201.2	4.6
1	203.6	168.4	35.2
1.1	93.8	120.4	26.6
1.2	99.5	110.3	10.8
1.3	111.4	125.7	14.3
1.4	149.5	135.9	13.6
1.5	106.2	77.3	28.9
1.6	77.9	87.4	9.5
1.7	94.2	107.4	13.2
1.8	91.3	86.9	4.4
1.9	108	98.4	9.6
2	91.3	115.9	24.6
2.1	113.8	98.3	15.5
2.2	107.4	120.1	12.7
Average Difference between Profile and Smartphone Measured IRI =			18.5

Table A.4: Smartphone and Inertial Profiler Measured IRI at IL-47 (From 2900N to 2650N)

IL-47 (From 2900N to 2650N)			
Distance (mile)	Profiler Measure IRI (in/mi)	Smartphone App Measured IRI (in/mi)	Difference in IRI (in/mi)
0.1	241.2	202.4	38.8
0.2	230.2	212.4	17.8
0.3	151.9	143.7	8.2
0.4	321.9	253.5	68.4
0.5	249	245.9	3.1
0.6	308.5	248.3	60.2
0.7	285.5	238.5	47.0
0.8	220.1	202.4	17.7
0.9	218.8	198.4	20.4
1	171.5	178.1	6.6
1.1	229.6	203.4	26.2
1.2	225.9	231.2	5.3
1.3	175.6	210.2	34.6
1.4	182.3	163.4	18.9
1.5	161.1	170.1	9.0
1.6	117.5	119.0	1.5
1.7	88.3	127.4	39.1
1.8	125.8	119.0	6.8
1.9	156.1	178.0	21.9
2	124.2	123.4	0.8
2.1	262.6	234.6	28.0
2.2	222.5	187.5	35.0
2.3	198.1	178.6	19.5
2.4	193.4	221.4	28.0
2.5	117.6	128.1	10.5
2.6	181.3	153.5	27.8
2.7	221.4	195.3	26.1
2.8	173.3	143.9	29.4
2.9	195.5	163.9	31.6
3	138.9	119.5	19.4
3.1	195.8	164.9	30.9
3.2	182.8	137.5	45.3
Average Difference between Profile and Smartphone Measured IRI =			24.5

Table A.5: Smartphone and Inertial Profiler Measured IRI at County Rd 2700N/300E (From 300E to 000E)

County Rd 2700N/300E (From 300E to 000E)			
Distance (mile)	Profiler Measure IRI (in/mi)	Smartphone App Measured IRI (in/mi)	Difference in IRI (in/mi)
0.1	168.7	161.8	6.9
0.2	167.4	192.7	25.3
0.3	235	221.3	13.7
0.4	169	153.9	15.1
0.5	86.1	83.6	2.5
0.6	71.8	64.0	7.8
0.7	123.5	115.0	8.5
0.8	124.2	163.8	39.6
0.9	163.9	208.8	44.9
1	191.3	156.5	34.8
1.1	88.9	70.7	18.2
1.2	191.9	128.3	63.6
Average Difference between Profile and Smartphone Measured IRI =			23.4

Table A.6: Smartphone and Inertial Profiler Measured IRI at US-150 (From 200E to Mckinley)

US 150 (From 200E to Mckinley St)			
Distance (mile)	Profiler Measure IRI (in/mi)	Smartphone App Measured IRI (in/mi)	Difference in IRI (in/mi)
0.1	102.7	87.7	15.0
0.2	93.8	90.4	3.4
0.3	86.9	102.8	15.9
0.4	114.2	161.0	46.8
0.5	150.1	143.4	6.7
0.6	101.6	114.3	12.7
0.7	121.5	118.2	3.3
0.8	186.8	165.8	21.0
0.9	131.6	129.7	1.9
1	126.5	89.7	36.8
1.1	91.7	132.1	40.4
1.2	156.6	162.1	5.5
1.3	111.8	98.5	13.3
1.4	107.3	113.1	5.8
1.5	101.4	96.3	5.1
1.6	130.5	163.1	32.6
1.7	136.4	140.8	4.4
1.8	112.3	117.3	5.0
1.9	119.2	118.4	0.8
2	113.9	111.2	2.7
2.1	156.7	150.6	6.1
2.2	124	82.9	41.1
2.3	100.9	90.0	10.9
2.4	113.2	105.9	7.3
2.5	78.6	66.0	12.6
2.6	135.7	139.1	3.4
2.7	79.3	89.0	9.7
2.8	68.2	119.0	50.8
2.9	178.7	242.2	63.5
3	204.9	188.6	16.3
3.1	108.3	114.2	5.9
Average Difference between Profile and Smartphone Measured IRI =			16.3

Table A.7: Smartphone and Inertial Profiler Measured IRI at County Rd 1200E (From 2750N to IL-10 E)

County Rd N 1200E (From 2750N to IL-10E)			
Distance (mile)	Profiler Measure IRI (in/mi)	Smartphone App Measured IRI (in/mi)	Difference in IRI (in/mi)
0.1	48.5	56.4	7.9
0.2	45.3	48.7	3.4
0.3	52.9	55.3	2.4
0.4	46.5	53.2	6.7
0.5	46.2	50.7	4.5
0.6	47.4	51.7	4.3
0.7	47.9	55.3	7.4
0.8	49.8	60.8	11.0
0.9	54.8	65.1	10.3
1	62.2	72.7	10.5
1.1	53.7	71.9	18.2
1.2	173.7	148.1	25.6
1.3	52.9	51.0	1.9
1.4	42.2	42.2	0.0
1.5	43.2	48.1	4.9
1.6	44.4	53.8	9.4
1.7	48.5	62.2	13.7
1.8	39.4	57.6	18.2
1.9	43.2	58.9	15.7
2	40.6	57.1	16.5
2.1	42.5	58.5	16.0
2.2	51.3	64.9	13.6
2.3	62.8	58.7	4.1
2.4	56.5	59.4	2.9
2.5	53.5	62.2	8.7
2.6	37.6	45.8	8.2
2.7	42.9	55.4	12.5
2.8	49.5	61.9	12.4
2.9	56.1	59.3	3.2
3	51.3	48.9	2.4
3.1	51.1	51.4	0.3
3.2	54.9	53.6	1.3
3.3	53.9	58.2	4.3
3.4	63.8	61.1	2.7
3.5	62.4	50.2	12.2
3.6	48.2	62.6	14.4
3.7	59	61.4	2.4
3.8	56.4	59.5	3.1
3.9	40	61.3	21.3
4	39.9	55.2	15.3
4.1	41	54.6	13.6
4.2	41.9	62.9	21.0
4.3	44.7	46.0	1.3
4.4	40	56.6	16.6
4.5	41.5	45.9	4.4
4.6	42.5	56.7	14.2

Table A.7 (cont.)

4.7	43.7	48.3	4.6
4.8	54.8	58.3	3.5
4.9	51.7	55.6	3.9
5	68.4	72.9	4.5
5.1	56	66.4	10.4
5.2	47.4	57.9	10.5
5.3	50.7	58.8	8.1
5.4	58.3	63.0	4.7
5.5	49	61.8	12.8
5.6	54	62.4	8.4
Average Difference between Profile and Smartphone Measured IRI =			8.9

Table A.8: Smartphone and Inertial Profiler Measured IRI at IL-10 (From 1300E to 200E)

IL-10 (From 1300E to 200E)			
Distance (mile)	Profiler Measure IRI (in/mi)	Smartphone App Measured IRI (in/mi)	Difference in IRI (in/mi)
0.1	46.6	52.4	5.8
0.2	42.3	48.9	6.6
0.3	43.7	51.8	8.1
0.4	42.7	48.6	5.9
0.5	45	58.9	13.9
0.6	53.1	46.9	6.2
0.7	47	57.4	10.4
0.8	51.9	58.2	6.3
0.9	48.5	61.2	12.7
1	51	58.3	7.3
1.1	51.4	51.8	0.4
1.2	54.3	73.3	19.0
1.3	109.6	95.1	14.5
1.4	50.1	57.2	7.1
1.5	43	54.7	11.7
1.6	46.1	65.3	19.2
1.7	47.6	58.3	10.7
1.8	68	69.9	1.9
1.9	54.9	58.8	3.9
2	47.5	49.2	1.7
2.1	48.9	61.2	12.3
2.2	46.9	58.0	11.1
2.3	55.9	61.8	5.9
2.4	44.1	46.7	2.6
2.5	42.4	54.6	12.2
2.6	41.7	62.2	20.5
2.7	48.5	51.2	2.7
2.8	49.2	57.3	8.1
2.9	55.9	62.3	6.4
Average Difference between Profile and Smartphone Measured IRI =			8.8

Table A.9: Smartphone and Inertial Profiler Measured IRI at County Rd 200E (From 1500N to 1000N)

County Rd 200E (From 1500N to 1000N)			
Distance (mile)	Profiler Measure IRI (in/mi)	Smartphone App Measured IRI (in/mi)	Difference in IRI (in/mi)
0.1	106.7	100.6	6.1
0.2	80.6	93.6	13.0
0.3	72.7	76.9	4.2
0.4	63.9	81.4	17.5
0.5	68.5	64.1	4.4
0.6	86.3	75.5	10.8
0.7	73.4	64.6	8.8
0.8	73.5	96.8	23.3
0.9	80.5	85.5	5.0
1	82.7	75.0	7.7
1.1	81.9	96.8	14.9
1.2	76.7	89.3	12.6
1.3	94.3	87.2	7.1
1.4	74.7	90.3	15.6
1.5	77.5	87.2	9.7
1.6	73.1	87.2	14.1
1.7	66.4	83.9	17.5
1.8	86.5	71.6	14.9
1.9	77.7	69.0	8.7
2	83.9	89.8	5.9
2.1	95.3	79.8	15.5
2.2	102.4	109.3	6.9
2.3	90	119.8	29.8
2.4	106.8	109.7	2.9
2.5	99.4	85.9	13.5
2.6	102.6	93.5	9.1
2.7	91.9	113.1	21.2
2.8	83.7	113.7	30.0
2.9	87.7	77.4	10.3
3	114.4	125.1	10.7
3.1	102.6	104.6	2.0
3.2	88.1	103.1	15.0
3.3	83.9	84.9	1.0
3.4	91.2	110.4	19.2
3.5	100.5	85.5	15.0
3.6	105.7	97.8	7.9
3.7	97.1	103.7	6.6
3.8	94.8	81.8	13.0
3.9	109.6	94.1	15.5
4	122.4	103.4	19.0
4.1	147.8	260.0	112.2
4.2	89.8	103.9	14.1
4.3	95.3	81.9	13.4

Table A.9 (cont.)

4.4	91.2	93.8	2.6
4.5	83.8	73.2	10.6
4.6	81.5	79.2	2.3
4.7	90.3	81.7	8.6
4.8	91.1	94.4	3.3
4.9	95.3	114.5	19.2
Average Difference between Profile and Smartphone Measured IRI =			13.7

Table A.10: Smartphone and Inertial Profiler Measured IRI at County Rd 1000N (From 300E to 800E)

County Rd 1000N (From 300E to 800E)			
Distance (mile)	Profiler Measure IRI (in/mi)	Smartphone App Measured IRI (in/mi)	Difference in IRI (in/mi)
0.1	82	78.2	3.8
0.2	52.2	63.2	11.0
0.3	43.2	53.4	10.2
0.4	63.3	62.1	1.2
0.5	42.6	55.6	13.0
0.6	50.4	49.2	1.2
0.7	47.7	57.4	9.7
0.8	61.8	72.3	10.5
0.9	72.1	100.8	28.7
1	70.9	63.3	7.6
1.1	48.8	66.7	17.9
1.2	49.7	58.9	9.2
1.3	52.5	69.8	17.3
1.4	62.6	68.2	5.6
1.5	50.2	60.4	10.2
1.6	50.3	74.7	24.4
1.7	78.4	92.8	14.4
1.8	47.8	65.3	17.5
1.9	68.9	77.0	8.1
2	65.3	65.2	0.1
2.1	79.2	94.0	14.8
2.2	71	67.7	3.3
2.3	75.2	78.8	3.6
2.4	64.5	71.9	7.4
2.5	66.2	82.7	16.5
2.6	66.3	72.6	6.3
2.7	64.8	76.2	11.4
2.8	60.2	62.3	2.1
2.9	76.8	67.0	9.8
3	88.8	116.0	27.2
3.1	75.2	83.6	8.4
3.2	109.1	125.7	16.6
3.3	67.2	76.3	9.1
3.4	60.8	86.8	26.0
3.5	63.9	57.4	6.5
3.6	69.4	65.9	3.5
3.7	55.3	65.8	10.5
3.8	66	70.7	4.7
3.9	73.1	75.0	1.9
4	67.2	61.0	6.2
4.1	62.7	72.4	9.7
4.2	81.3	96.7	15.4
4.3	79.2	102.1	22.9

Table A.10 (cont.)

4.4	86.5	82.8	3.7
4.5	85.4	68.7	16.7
4.6	88.3	84.7	3.6
4.7	74.2	102.5	28.3
4.8	72.7	82.7	10.0
4.9	81.3	89.1	7.8
Average Difference between Profile and Smartphone Measured IRI =			10.9

Table A.11: Smartphone and Inertial Profiler Measured IRI at County Rd 800E (From 1000N to Curtis Rd)

County Rd 800E (From 1000N to Curtis Rd)			
Distance (mile)	Profiler Measure IRI (in/mi)	Smartphone App Measured IRI (in/mi)	Difference in IRI (in/mi)
0.1	68.7	79.1	10.4
0.2	80.6	74.9	5.7
0.3	111.8	97.4	14.4
0.4	91.1	99.0	7.9
0.5	109.7	93.3	16.4
0.6	115.6	98.4	17.2
0.7	122.2	107.3	14.9
0.8	104.1	118.8	14.7
0.9	94.1	85.9	8.2
1	181.3	230.5	49.2
1.1	125.1	128.3	3.2
1.2	108	109.0	1.0
1.3	138.2	124.5	13.7
1.4	152	126.5	25.5
1.5	122.6	123.1	0.5
1.6	138.2	110.4	27.8
1.7	121.1	122.2	1.1
1.8	99.3	112.0	12.7
1.9	94.3	78.5	15.8
2	88	94.0	6.0
2.1	72.9	75.5	2.6
2.2	72.6	92.6	20.0
2.3	79.2	89.4	10.2
2.4	81.2	101.2	20.0
2.5	89	99.4	10.4
2.6	83.9	84.3	0.4
2.7	74.5	86.9	12.4
2.8	76.2	83.4	7.2
Average Difference between Profile and Smartphone Measured IRI =			12.5

Table A.12: Smartphone and Inertial Profiler Measured IRI at County Rd 9 (From 1700E to 1000E)

County Rd 9 (From 1700E to 1000E)			
Distance (mile)	Profiler Measure IRI (in/mi)	Smartphone App Measured IRI (in/mi)	Difference in IRI (in/mi)
0.1	85.8	88.2	2.4
0.2	97.1	85.0	12.1
0.3	88.2	89.2	1.0
0.4	83.2	88.4	5.2
0.5	95.7	74.0	21.7
0.6	75.8	88.8	13.0
0.7	74.6	68.0	6.6
0.8	85.4	80.1	5.3
0.9	59.7	70.1	10.4
1	60.4	74.4	14.0
1.1	76.6	68.8	7.8
1.2	63.8	70.7	6.9
1.3	79.4	77.7	1.7
1.4	79.5	68.8	10.7
1.5	65.5	67.5	2.0
1.6	69	69.2	0.2
1.7	86.6	76.8	9.8
1.8	74.7	71.4	3.3
1.9	61.4	68.3	6.9
2	63.2	84.4	21.2
2.1	78.1	76.3	1.8
2.2	101	74.7	26.3
2.3	76.5	80.4	3.9
2.4	77.7	80.8	3.1
2.5	68.1	74.4	6.3
2.6	101.9	78.9	23.0
2.7	69.8	71.8	2.0
2.8	89.9	94.7	4.8
2.9	92.4	78.1	14.3
3	83.9	76.4	7.5
3.1	65.1	67.2	2.1
3.2	88.4	69.8	18.6
3.3	71.4	64.5	6.9
3.4	82.7	71.9	10.8
3.5	76.9	62.1	14.8
3.6	71.5	62.4	9.1
3.7	84.4	72.2	12.2
3.8	70.4	68.5	1.9
3.9	78.7	75.3	3.4
4	78.5	70.6	7.9
4.1	78	84.1	6.1
4.2	90.2	85.5	4.7
4.3	101.3	83.1	18.2
4.4	89.4	73.1	16.3

Table A.12 (cont.)

4.5	92.5	84.8	7.7
4.6	134.9	97.0	37.9
4.7	104.5	94.5	10.0
4.8	101.4	105.7	4.3
4.9	86.3	123.9	37.6
5	205.4	113.3	92.1
5.1	139.4	113.4	26.0
5.2	182.8	114.5	68.3
5.3	130.5	93.4	37.1
5.4	106.1	94.6	11.5
5.5	111.6	83.1	28.5
5.6	101.2	93.4	7.8
5.7	99.9	81.3	18.6
5.8	79.3	80.0	0.7
5.9	90.2	82.0	8.2
6.0	98.0	88.9	9.1
6.1	104.7	83.8	20.9
6.2	88.1	77.0	11.1
6.3	88.1	81.9	6.2
6.4	86.9	80.0	6.9
6.5	93.9	82.0	11.9
6.6	86.3	85.4	0.9
6.7	90.5	87.0	3.5
Average Difference between Profile and Smartphone Measured IRI =			12.8

Table A.13: Smartphone and Inertial Profiler Measured IRI at US-45S (From 2800N to Airport Rd)

US-45 (From 2800N to Airport Rd)			
Distance (mile)	Profiler Measure IRI (in/mi)	Smartphone App Measured IRI (in/mi)	Difference in IRI (in/mi)
0.1	128.4	114.3	14.1
0.2	157.5	134.7	22.8
0.3	206.1	129.5	76.6
0.4	194.8	159.3	35.5
0.5	141.3	126.0	15.3
0.6	149	163.2	14.2
0.7	164.1	128.4	35.7
0.8	145.4	135.9	9.5
0.9	132.7	125.2	7.5
1	134.5	115.3	19.2
1.1	196.5	160.7	35.8
1.2	152	135.6	16.4
1.3	133.5	171.4	37.9
1.4	132.3	136.6	4.3
1.5	119.2	115.0	4.2
1.6	133.5	121.6	11.9
1.7	135.3	139.9	4.6
1.8	132.6	147.9	15.3
1.9	161.1	162.3	1.2
2	122.9	139.0	16.1
2.1	131.1	122.3	8.8
2.2	102.2	125.4	23.2
2.3	120.4	115.8	4.6
2.4	137.4	124.5	12.9
2.5	124	146.7	22.7
2.6	126.8	127.8	1.0
2.7	127	136.1	9.1
2.8	120.3	162.1	41.8
2.9	171.8	113.4	58.4
3	129.2	143.2	14.0
3.1	139.9	154.9	15.0
3.2	178.9	172.4	6.5
3.3	230.6	134.7	95.9
3.4	150.4	156.2	5.8
3.5	140.6	184.3	43.7
3.6	185.7	136.8	48.9
3.7	135.9	141.9	6.0
3.8	127.9	162.7	34.8
3.9	135.6	134.1	1.5
4	159.7	119.6	40.1
4.1	134.9	147.1	12.2
4.2	122.9	141.4	18.5
4.3	164.1	134.9	29.2
4.4	135.9	147.4	11.5
4.5	151.3	177.9	26.6

Table A.13 (cont.)

4.6	161.4	169.0	7.6
4.7	171	179.3	8.3
4.8	143.6	171.9	28.3
4.9	178.1	202.6	24.5
5	137.1	224.6	87.5
5.1	191.4	134.1	57.3
5.2	172.8	184.7	11.9
5.3	128	133.8	5.8
5.4	140.9	111.3	29.6
5.5	133.8	126.1	7.7
5.6	122.8	128.0	5.2
5.7	135.7	131.8	3.9
5.8	151.2	134.5	16.7
5.9	126.5	130.2	3.7
6	128.4	129.2	0.8
6.1	127.0	134.8	7.8
6.2	105.2	136.1	30.9
6.3	142.7	162.1	19.4
6.4	168.4	143.2	25.2
6.5	165.7	130.8	34.9
6.6	109.8	130.3	20.5
6.7	99.2	131.2	32.0
6.8	110.1	106.9	3.2
6.9	108.2	122.1	13.9
7.0	112.7	109.6	3.1
7.1	107.5	120.8	13.3
7.2	121.8	136.9	15.1
7.3	93.3	113.7	20.4
7.4	128.7	116.9	11.8
7.5	143.1	105.0	38.1
7.6	120.1	126.3	6.2
7.7	92.2	108.0	15.8
7.8	107.9	115.0	7.1
7.9	128.9	108.8	20.1
8.0	102.2	105.1	2.9
8.1	88.2	115.4	27.2
8.2	84.9	116.3	31.4
8.3	94.3	94.9	0.6
8.4	91.2	112.1	20.9
8.5	105.5	110.5	5.0
8.6	96.4	101.7	5.3
8.7	87.1	101.3	14.2
8.8	151.8	96.9	54.9
8.9	84.5	96.0	11.5
9.0	130.5	101.7	28.8
Average Difference between Profile and Smartphone Measured IRI =			20.3